DYNAMIC KILL OF UNDERGROUND BLOWOUTS

ALVARO F. NEGRÃO, PETROBRAS

VICTOR GERARDO VALLEJO-ARRIETA, PEMEX

ADAM T. BOURGOYNE, JR. LSU

JOHN ROGERS SMITH, LSU

Table of Contents

Chapter 1

Executive Summary

This LSU study was funded by the Minerals Management Services, U. S. Department of the Interior, Washington, D.C., under Contract Number 14-35-001-30749. This report has not been reviewed by the Minerals Management Service and approved for publication. Approval does not signify that the contents necessarily reflect the views and policy of the Service, nor does mention of trade names or commercial products constitute endorsement or recommendation for use.

This report describes the work performed for Task 8 - Requirements for Dynamic Kill of Underground Blowouts. This task was part of the 1994 –1999 LSU/MMS well control research project focused on underground blowouts. Dynamic kills have been successfully used to control both surface and underground blowouts. Therefore this task related to improved modeling of dynamic kills for underground blowouts.

The original goals of Task 8 were to modify a dynamic kill simulator that was developed in a previous project to include a hydraulic fracture model, to design and conduct an experimental test of the fracture model, and to initiate technology transfer activities for dynamic kills. These goals were met and are described in Chapter 3. A program listing for the dynamic kill simulator is included as Appendix A. The primary conclusions from conducting this work are that the new model predicts a lower minimum mud flow rate to control an underground blowout than the current models, is significantly more difficult to use and maintain than previous time-dependent and steady-state models, and provides a more exact prediction of pressure versus time during a kill than current models.

Steady-state models have also been widely used as a basis for design and analysis of dynamic kills. Given the difficulty in using and maintaining the new time-dependent simulator, steady-state methods are described in Chapter 4. A steady-state method was implemented in Excel™ spreadsheets to design and analyze dynamic kills for both surface and underground blowouts. Application of the spreadsheets to actual examples of surface and underground blowouts are described in Chapter 5. The resulting conclusions are that the spreadsheets provide reasonable estimates of steady-state pressures and flows to be expected during kill operations and that the quality of the estimates could be improved by implementing a power-law rheology model and by accounting for the measured depth in directional wells. The spreadsheets are included as Appendices B and C to this report.

Chapter 2

Introduction

The Minerals Management Service is concerned about reducing the potential for surface and underground blowouts because Congress has mandated that MMS is responsible for worker safety and environmental protection.

The 1994 –1999 LSU/MMS well control research project was proposed by Bourgoyne and Kelly[1] to focus on the development of improved procedures for detecting and handling underground blowouts in marine environments. Task 8 of the project was proposed to consider dynamic kills of underground blowouts.

The original proposal stated that "the current model used for contingency planning of dynamic kill operations often does not perform satisfactorily for a case involving an underground blowout because it is necessary to assume that the pressure in the fracture is independent of kill rate. Subtask 8a would involve the modification of a dynamic kill computer simulator that was developed in a previous project to include a representative hydraulic fracture model and the design of an experimental test for verifying the model in our research well. Subtask 8b would involve conducting the experimental test and initiating technology transfer activities.[1]" The work performed for these tasks is described in Chapter 3. Chapter 4 describes additional work on a simplified dynamic kill calculation method implemented in an Excel™ spreadsheet. While this method does not include the hydraulic fracture model, it is more practical to run and maintain than the simulator. Chapter 5 compares results from the spreadsheet method to other published methods used in analyzing a surface blowout and to data recorded during kills of both surface and underground blowouts.

Concept

The dynamic kill is a relatively new technique. It was formalized by Mobil Oil Corporation and was first reported by Blount and Soeiinah[7]. The method was designed to control an Arun field surface blowout in Indonesia. The well caught fire in June 1978, destroying the drilling rig and burning for 89 days at an approximate rate of 400 MMscfd. Due to the well's high deliverability and potential, it was expected to be an extremely difficult well to kill. However, the engineering basis for the dynamic kill procedure was sound, and the kill was so successful that the well was controlled one hour and 50 minutes after the kill started.

The dynamic kill is a procedure that can be used to regain control of a surface or underground blowout. It involves pumping kill fluid through either a relief well or an injection string into a well that is blowing out. The pump rate used must create enough back pressure due to the frictional

pressure losses and increases in hydrostatic pressure due to the multiphase flow of formation and kill fluid to exceed the shut in formation pressure and stop the gas flow. Dynamic kills have proven successful in both on - bottom and off – bottom, surface and underground blowouts[7,8,15,16,17,18,21].

This concept can be better explained with Figure 1, which illustrates a well and its pressure gradient. Section (a) shows the well with mud in static conditions, with a hydrostatic pressure value at the bottom. In section (b), the drilling mud is pumped through the injection string, and as shown by the shaded area, the frictional pressure losses due to flow is used to increase the bottom hole pressure. In a kill operation, that pressure increment will help to stop the flow from the reservoir.

The main objective of the dynamic kill calculation technique is to determine the minimum injection rate of available kill fluid that is necessary to stop reservoir fluid flow into the wellbore. The method is designed to kill the well by exceeding the natural flow capacity of the wellbore.

The simplest application of this technique is based on the steady state system analysis approach, which consists of a study involving both the reservoir inflow performance and the wellbore performance. System analysis, also known as NODAL™ analysis, has been used in production wells and has received widespread acceptance in the oil industry. Another successful application is in blowout control studies, since a well under blowout conditions is very similar to a production well, with the difference that the producing well is flowing under control and the reservoir fluids flow to the production facilities rather than to the atmosphere.

Figure 2 illustrates a blowout scenario. It can be seen that the reservoir and the wellbore can act as a single hydraulic system and that the whole system is affected by several factors such as reservoir pressure and properties, formation fluid characteristics, and wellbore and drillstring geometry.

Figure 2 shows that the system can be considered as having two important components: the reservoir and the wellbore. The flow from the reservoir into the well has been called "inflow performance," and a plot of producing rate versus flowing bottomhole pressure is called an "inflow performance relationship," shown as IPR on the plot. On the other hand, the "wellbore hydraulics performance" is given by the flow behavior from the bottom of the well to the surface. It is shown by WHP on the plot representing the bottom pressure versus flowrate relationship for the wellbore. Both inflow and wellbore performance can be mathematically represented, and the simultaneous solution of those analytical representations defines the steady-state formation flow rate for that system at the intersect of the two curves on the plot. For a blowout, this defines the steady-state rate at which the well is blowing out.

This style of system analysis can also be applied to determine the pump rate required to achieve a dynamic kill. In this case, the analysis of pressures in the wellbore must account for the combined flow of the kill fluid and reservoir fluids. Figure 3 is an example of a plot including WHP curves for three different pump rates as well as the initial blowout conditions with only gas flowing. Note that the combination of any gas flowrate with a pump rate shown as injection rate #3 results in a bottomhole pressure that always exceeds the bottomhole pressure on the IPR curve. Therefore there is no steady-state solution that results in a formation flow with injection rate #3. This rate is the minimum dynamic kill rate.

The system analysis of an underground blowout utilizes these same concepts. The difference is that the downstream end of the wellbore is defined as the location of the loss zone where flow exits the

wellbore and goes into subsurface formations. Therefore the injection or fracture pressure at this depth defines the downstream pressure for the wellbore hydraulics performance instead of surface pressure. Likewise the flow path is from bottomhole to this depth rather than to the surface. The determination of the steady-state flowrate during the blowout and the minimum pump rate for a dynamic kill uses the same logic as a for a surface blowout.

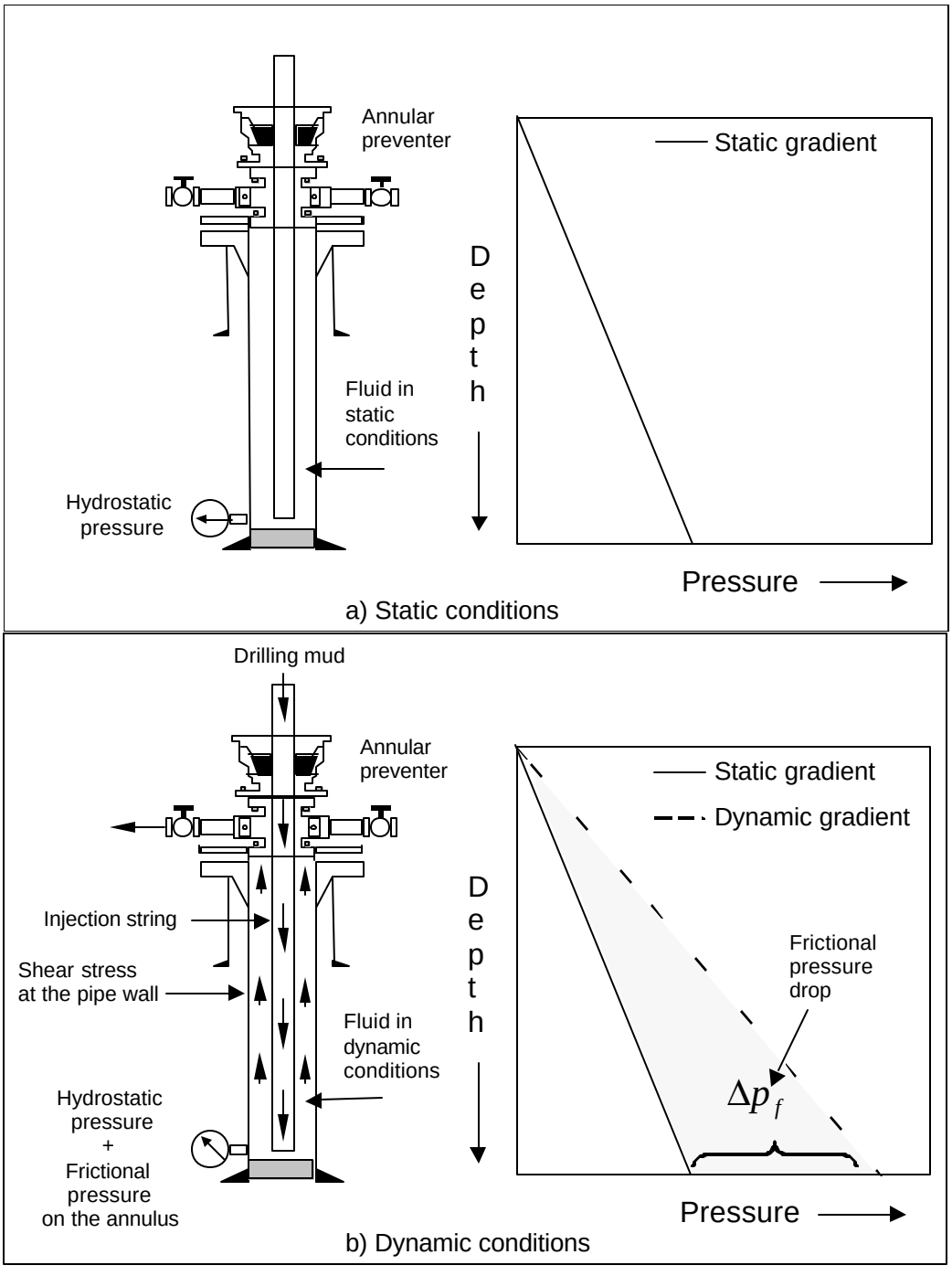

Figure 1 Effect of hydrostatic and frictional pressure losses on bottom hole pressure

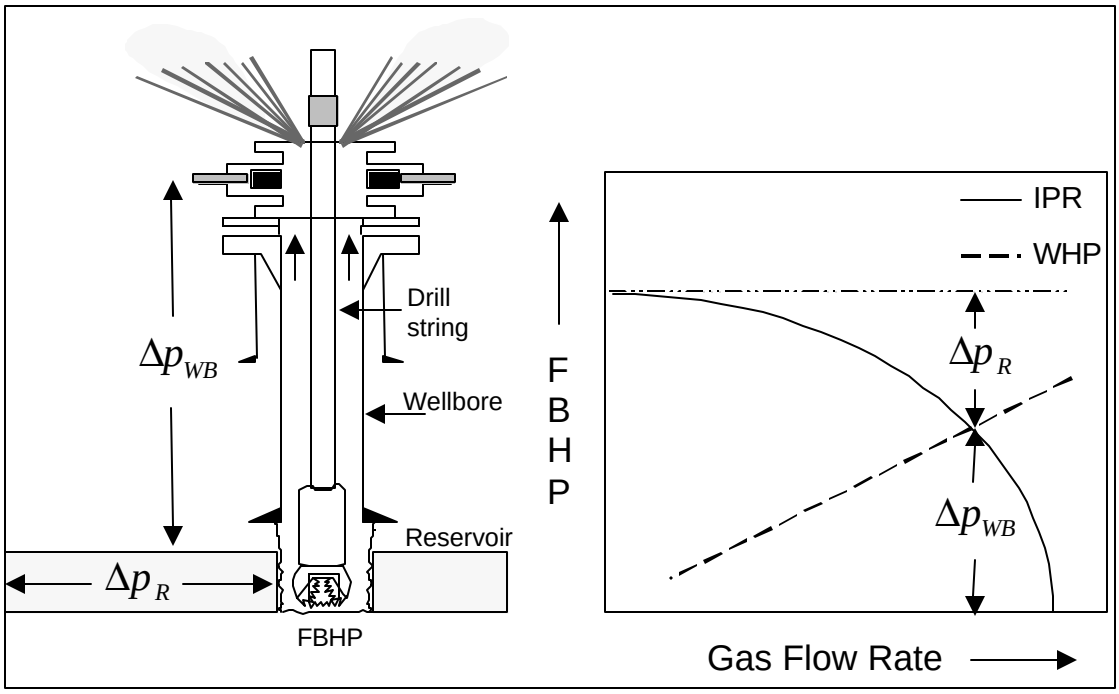

Figure 2 Reservoir and wellbore as a single hydraulic system

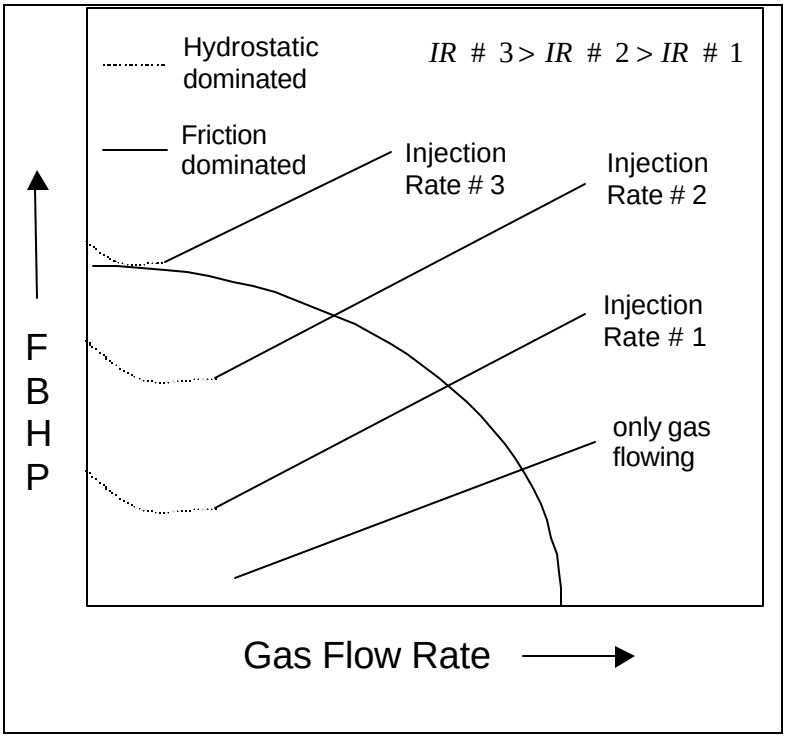

Figure 3 System analysis for a dynamic kill

A complete hydrostatic kill of either a surface or underground blowout requires that the hydrostatic pressure provided by filling the well with kill fluid exceeds the formation pressure. If the fluid density used during the dynamic kill is less than required for hydrostatic control, the fluid must be replaced with a kill density fluid while pumping so that bottomhole pressure is maintained by the combination of fluid density and friction until the kill density fluid is in place.

Summary

The dynamic kill concept has been successfully applied to control of both surface and underground blowouts. The concept requires pumping a fluid into the well during the blowout such that the combination of fluid density and friction loss effects raises the bottomhole pressure to a value greater than the formation pressure. Systems analysis can be used to determine the combination of fluid density and rate that will achieve a dynamic kill.

Chapter 3

Computer Model for Dynamic Kill of an Underground Blowout Considering Fracture Propagation

The primary task originally envisioned for this project was to account for fracture extension pressure when simulating a dynamic kill of an underground blowout. This chapter describes the work and the resultant model to do so.

Introduction

The planning of well control operations involving an induced fracture is potentially a very complex operation and its success depends on the knowledge of reservoir and fracture characteristics, wellbore dimensions, and fluid properties.

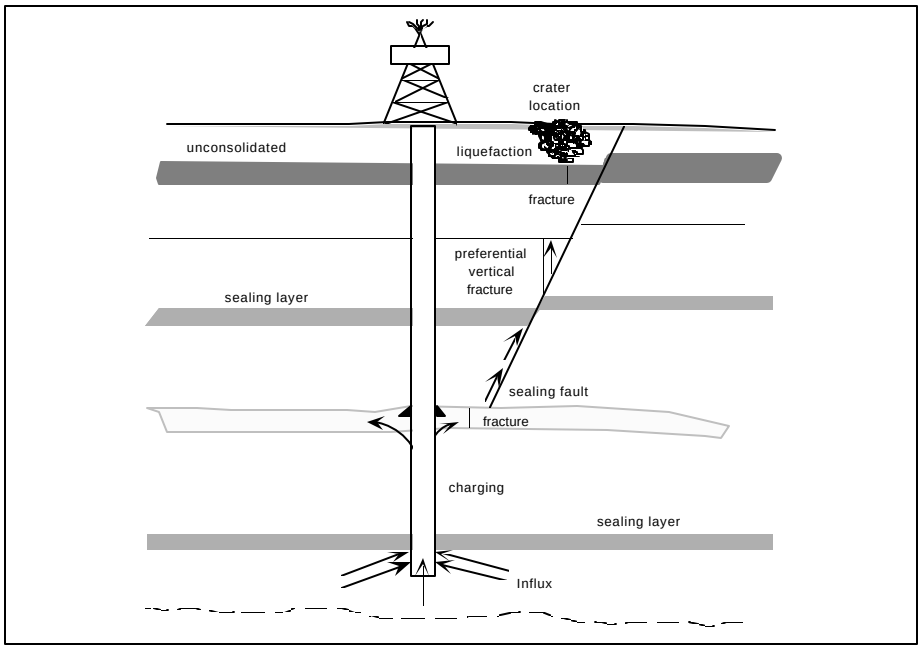

Figure 4 Principal Mechanisms Following an Underground Blowout (after Walters, 1991)

Figure 4 shows the principal mechanisms that can take place following a well control operation involving an induced fracture. This chapter focuses on the case that the fracture propagates the entire time the gas reservoir produces fluid into the wellbore, as shown in the left wing of the fracture in Figure 4.

Although there are many potential ways (the use of barite plugs, cementing, packers, etc.) to control underground blowouts, this report will focus on the dynamic kill as a means to regain the control of the well. The dynamic kill method is a well control procedure that calls for pumping down the drill pipe with a flow rate that causes the bottom hole pressure to exceed the formation pressure, thus displacing the fluids out of the annulus.

Previously published procedures for planning a dynamic kill have modeled the fracture by assuming a constant pressure in the wellbore at the depth of fracture. This assumption is unrealistic because this pressure will change with time as the fracture propagates and as the flow rate is increased. This change has been shown by two-dimensional models (PKN and GdK), by fracture treatment data, and by three-dimensional models. Thus, assuming a constant fracture injection pressure can lead to an inappropriate estimate of the mud flow rate needed to regain control of the well.

The main objective of this study is to evaluate when the assumption of a constant fracture injection pressure will lead to unacceptable errors in the design of a dynamic kill procedure. The evaluation is accomplished using a new computer model that couples a hydraulic fracture model with conventional reservoir and wellbore models using a system analysis approach. A more comprehensive description of this study is available in the Ph.D. Dissertation entitled Model for Planning Well Control Operations Involving an Induced Fracture by Alvaro F. Negrao[4].

Gas Reservoir Model

The gas reservoir model is based on Al-Hussainy and Ramey's (1966) expressions modified to account for changes in flow rate and pressure. To calculate the wellbore pressure in an infinite gas reservoir produced at a constant flow rate, including skin and the non-Darcy effects, the following expression is used:

$$\frac{\left[m(P_{RES}) - m(P_{BHP})\right] khT_{SC}}{0.367 P_{SC} T} = Q\left[\log(2.245 t_D) + 0.87(S + DQ)\right] \ldots\ldots\ldots\ldots\ldots (1)$$

where the real gas pseudo pressure is defined as:

$$m(P) = 2\int_0^P \frac{P}{z\mu_g} dP \ldots\ldots\ldots\ldots\ldots\ldots\ldots\ldots\ldots\ldots (2)$$

and the dimensionless time by:

$$t_D = \frac{kt}{\phi(\mu_g c_t)_i r_w^2} \ldots\ldots\ldots\ldots\ldots\ldots\ldots\ldots\ldots\ldots (3)$$

where the total compressibility is approximated as:

$$c_t = c_g\left(1 - S_{wi}\right).....(4)$$

The non-Darcy factor is calculated with:

$$D = 0.159\frac{\beta_g M P_{sc} k}{R\mu h r_w T_{sc}}.....(5)$$

where the velocity coefficient for consolidated sandstone was determined by Geertsma (1974) as:

$$\beta_g = \frac{0.005}{\phi^{5.5}\sqrt{k}}.....(6)$$

The gas compressibility and the gas viscosity in these equations are evaluated at the reservoir pressure.

The bottom hole pressure and gas flow rate vary with time in a case of underground blowout. Due to this fact, the solution for the wellbore pressure can be found by applying the principle of the super-position for different flow rates in equation (1). The result after that is:

$$\frac{\left[m(P_{RES}) - m(P_{BHP})\right]khT_{SC}}{0.367 P_{SC} T} = \sum_{j=1}^{n}\left(Q_j - Q_{j-1}\right)\log\left[2.245\left(t_D - t_{Dj-1}\right)\right] + 0.87 Q_n\left(S + DQ_n\right).....(7)$$

After algebraic manipulation the solution for the flow rate can be obtained from the following quadratic equation:

$$Q_n^2 + \frac{0.87S + \log\left(2.245\left(t_D - t_{Dn-1}\right)\right)}{0.87D} Q_n + + \frac{B - A - Q_{n-1}\log\left(2.245\left(t_D - t_{Dn-1}\right)\right)}{0.87D} = 0.....(8)$$

where:

$$A = \frac{\left[m(P_{RES}) - m(P_{BHP})\right]khT_{sc}}{0.367 P_{sc} T}.....(9)$$

and

$$B = \sum_{j=1}^{n-1}\left[\left(Q_j - Q_{j-1}\right) log\left(2.2454\left(t_D - t_{Dj-1}\right)\right)\right]..(10)$$

The flow rate for each time step in the computer model is calculated through equation (8) using the value of the bottom hole pressure in that time step.

Wellbore Model

The wellbore model is an unsteady state numerical procedure based on Santos' model[5]. This model accounts for unsteady state flow effects by preserving all terms of the equation of continuity and equation of momentum for a two-phase mixture.

The program must be able to account for the two different flow conditions occurring in a well from a time just after a kick is taken until an underground blowout occurs. In the early time after a kick is taken, two distinct regions exist within the wellbore. In the lowermost section, a two-phase flow region occurs due to the mixing of kick fluid with the drilling mud in the annulus. The second region exists above the two-phase leading edge (boundary) and consists of drilling mud not yet contacted by the kick influx.

Once the kick has migrated up the annulus and induced a fracture in a shallower formation, an underground blowout is in progress. During the blowout, two-phase flow is occurring within the entire section of the borehole being modeled. The model for two-phase flow in the annulus was based on Nickens' methodology with some modifications due to the new configuration of the problem.

The solution for unsteady state flow of two-phase mixture is based on a simultaneous solution of the continuity equations for gas and liquid phases, a momentum balance equation for two-phase mixture, an equation of state for gas and a semi-empirical relationship between the gas and liquid in-situ velocities.

The continuity equation for the liquid phase is given by:

$$\frac{\partial H}{\partial t} + \frac{\partial (v_l H)}{\partial x} = 0 \qquad \ldots\ldots\ldots\ldots\ldots\ldots\ldots\ldots\ldots\ldots (12)$$

and for the gas phase by:

$$\frac{\partial \left[\rho_g (1-H)\right]}{\partial t} + \frac{\partial \left[v_g \rho_g (1-H)\right]}{\partial x} = 0 \qquad \ldots\ldots\ldots\ldots (13)$$

The momentum balance equation for two phase mixture is written as:

$$\frac{\partial \left[\left(v_l F_c \rho_l H\right) + \left(v_g F_c \rho_g (1-H)\right)\right]}{\partial t} + \frac{\partial}{\partial x}\left[\left(v_l^2 F_c \rho_l H\right) + \right.$$

$$\left.\left(v_g^2 F_c r_g (1-H)\right)\right] + \left(\frac{\P P}{\P x}\right) + \left(\frac{\P P}{\P x}\right)_{elev} + \left(\frac{\P P}{\P x}\right)_{fric} = 0 \qquad \ldots\ldots\ldots\ldots\ldots\ldots (14)$$

The elevation term for two-phase flow is calculated with:

$$\left(\frac{\partial P}{\partial x}\right)_{elev} = g\left(F_c \rho_l H + F_c \rho_g (1-H)\right) \qquad \ldots\ldots\ldots\ldots\ldots (15)$$

The friction term is computed using the Beggs and Brill correlation which was modified to account for the non-Newtonian fluid used in drilling operations:

$$\left(\frac{\partial p}{\partial x}\right)_{fric} = \frac{f_{tf} F_c \rho_{ns} v_{mix}^2}{25.8d} \ldots\ldots\ldots\ldots\ldots\ldots\ldots\ldots\ldots\ldots(16)$$

where the two-phase mixture velocity is calculated by:

$$v_{mix} = v_l H + v_g (1-H) \ldots\ldots\ldots\ldots\ldots\ldots\ldots\ldots\ldots\ldots(17)$$

and the mixture no-slip density by:

$$\rho_{ns} = \rho_l \lambda + \rho_g (1-\lambda) \ldots\ldots\ldots\ldots\ldots\ldots\ldots\ldots\ldots\ldots(18)$$

The two-phase flow friction factor in this case can be calculated through:

$$f_{tf} = e^s f \ldots\ldots\ldots\ldots\ldots\ldots\ldots\ldots\ldots\ldots\ldots\ldots\ldots\ldots(19)$$

where f is the Fanning friction factor which is dependent on the pipe relative roughness and the two-phase Reynolds number which is given by:

$$(N_{Re})_{tf} = \frac{F_c \rho_{ns} v_{mix} d}{\mu_{ns}} \ldots\ldots\ldots\ldots\ldots\ldots\ldots\ldots\ldots\ldots(20)$$

and the non-slip viscosity is defined as:

$$\mu_{ns} = \mu_l \lambda + \mu_g (1-\lambda) \ldots\ldots\ldots\ldots\ldots\ldots\ldots\ldots\ldots\ldots(21)$$

where the liquid viscosity is the drilling fluid plastic viscosity.

The exponent (s) in equation (19) is defined as:

$$s = \frac{\ln y}{-0.052 + \ln y\left(3.182 + \ln y\left(-0.873 + 0.0185(\ln y)^2\right)\right)} \ldots\ldots\ldots\ldots(22)$$

where

$$y = \frac{l}{H^2} \ldots\ldots\ldots\ldots\ldots\ldots\ldots\ldots\ldots\ldots\ldots\ldots\ldots\ldots(23)$$

If y is greater than 1.2 or less than 1.0, the exponent (s) is calculated as:

$$s = ln(2.2y - 1.2) \ldots\ldots\ldots\ldots\ldots\ldots\ldots\ldots\ldots\ldots\ldots\ldots(24)$$

The fluid density of the liquid phase is considered constant and the density of the gaseous phase is related to pressure and temperature by the real gas equation:

$$\rho_g = \frac{PM}{zRT} \quad \text{.....(25)}$$

In this wellbore model, the gas in situ velocity is related to the liquid in situ velocity through the equation:

$$v_s = v_g - C_{fr} v_{mix} = v_g - C_{fr}\left(v_l H + v_g (1-H)\right) \quad \text{.....(26)}$$

or in terms of gas velocity:

$$v_g = \frac{C_{fr} v_l H + v_s}{1 - C_{fr} + C_{fr} H} \quad \text{.....(27)}$$

where the factors C_{fr} and v_s depend on flow regime. The liquid hold up defines the flow regime boundary in this study. This definition is based on Caetano Filho (1986). He verified that the bubble flow occurs when the liquid hold up is between 1.0 and 0.85, slug flow between 0.75 and 0.45 and annular flow for liquid hold up less than 0.1. For the range of values of liquid hold up not covered in the definition of the regime (H between 0.85 and 0.75, and H between 0.45 and 0.1), a transition regime is adopted with the same procedure as Santos[5] where the in situ gas velocity is calculated through a linear interpolation between the regimes. This procedure avoids numerical inconsistencies in the solution when changing flow regimes. The equations for gas in situ velocity and the values for the factor C_{fr} were the same used by Santos[5]. They are written as:

(a) Bubble Flow:

$$v_s = 1.53 H^{0.5} \sqrt[0.25]{\frac{g_c\left(\rho_l - \rho_g\right) g \sigma_{st}}{\rho_l^2}} \quad \text{.....(28)}$$

with C_{fr} equal to 1.1.

(b) Slug Flow

$$v_s = 0.289 K_1 \sqrt{\frac{\left(\rho_l - \rho_g\right) D g}{\rho_l}} \quad \text{.....(29)}$$

where D is the outside diameter of the annulus,

$$K_1 = 0.345 - 0.037 R - 0.235 R^2 - 0.134 R^3 \quad \text{.....(30)}$$

and R is the ratio of the inner to outer diameters in the annulus. The value of coefficient C_{fr} is adopted equal to 1.1.

(c) Annular Flow

In this regime there is almost no slippage between phases. Therefore, the slip velocity is assumed equal to zero and the gas and liquid velocities are the same.

The solution of the differential equation is achieved numerically by using a Finite Difference Method. This method consists of segmenting the annulus into equal finite cells where finite difference approximations of flow equations are solved. The finite difference approximation used is centered in distance and backward in time. Figure 5 shows a cell for two different time steps. The current time step is determined by the length of the cell divided by the mixture leading velocity of the previous time step.

Point 1 represents the flow properties at the previous time step and at the lower boundary and point 2 at the upper boundary. Points 5 and 6 represent the same as points 1 and 2, respectively, at the present time. Points 3 and 4 represent arithmetic averaging of the properties at the center of the grid at previous and present times, respectively. The flow properties are known at points 1, 2, and 5. The finite difference approximation estimates the flow properties at point 6.

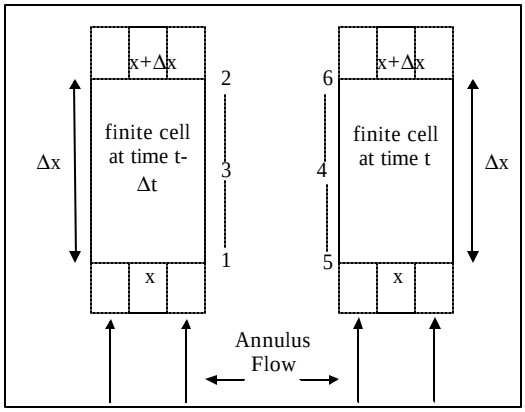

Figure 5 Finite Difference for Annulus Cell (after Santos, 1989)

The approximation for the space derivative in the continuity equation is calculated as:

$$\frac{\partial f}{\partial x} = \frac{f_6 - f_5}{\Delta x} \quad \ldots\ldots\ldots\ldots\ldots\ldots\ldots\ldots\ldots\ldots\ldots\ldots (31)$$

where f is some function of x and t. Substituting this approximation in the continuity equations for the liquid phase leads to:

$$\frac{\left(v_l \rho_l H\right)_6 - \left(v_l \rho_l H\right)_5}{\Delta x} + \frac{\left(\rho_l H\right)_6 + \left(\rho_l H\right)_5}{2\Delta t} -$$

$$- \frac{\left(\rho_l H\right)_2 + \left(\rho_l H\right)_1}{2\Delta t} = 0 \ldots\ldots\ldots\ldots\ldots\ldots\ldots\ldots\ldots\ldots (32)$$

and for the gas phase to:

$$\frac{\left(v_g \rho_g (1-H)\right)_6 - \left(v_g \rho_g (1-H)\right)_5}{\Delta x} +$$

$$+\frac{\left(\rho_g(1-H)\right)_6+\left(\rho_g(1-H)\right)_5}{2\Delta t}-$$

$$-\frac{\left(\rho_g(1-H)\right)_2+\left(\rho_g(1-H)\right)_1}{2\Delta t}=0\ldots\ldots\ldots\ldots(33)$$

The momentum balance equation is approximated by using a centered-in-distance and centered-in-time finite difference scheme. The approach for time derivative is the same, but the spatial derivative becomes:

$$\frac{\partial f}{\partial x}=\frac{f_6+f_2-f_5-f_1}{2\Delta x}\ldots\ldots\ldots\ldots\ldots\ldots\ldots(34)$$

Substituting the momentum equation into Equation 34 gives:

$$\frac{F_c}{2\Delta x}\left[\left(v_g^2\rho_g(1-H)\right)_2+\left(v_g^2\rho_g(1-H)\right)_6-\right.$$

$$-\left(v_g^2\rho_g(1-H)\right)_1-\left(v_g^2\rho_g(1-H)\right)_5+\left(v_l^2\rho_l H\right)_2+$$

$$\left.+\left(v_l^2\rho_l H\right)_6-\left(v_l^2\rho_l H\right)_1-\left(v_l^2\rho_l H\right)_5\right]+$$

$$+\frac{F_c}{2\Delta t}\left[\left(v_g\rho_g(1-H)\right)_5+\left(v_g\rho_g(1-H)\right)_6-\right.$$

$$-\left(v_g\rho_g(1-H)\right)_1-\left(v_g\rho_g(1-H)\right)_2+\left(v_l\rho_l H\right)_5+$$

$$\left.+\left(v_l\rho_l H\right)_6-\left(v_l\rho_l H\right)_1-\left(v_l\rho_l H\right)_2\right]-\frac{p_5-p_6}{\Delta x}+$$

$$+0.25\left[\left(\frac{\Delta p}{\Delta x}\right)_1+\left(\frac{\Delta p}{\Delta x}\right)_2+\left(\frac{\Delta p}{\Delta x}\right)_5+\left(\frac{\Delta p}{\Delta x}\right)_6\right]_{fric}-$$

$$-0.25\left[\left(\frac{\Delta p}{\Delta x}\right)_1+\left(\frac{\Delta p}{\Delta x}\right)_2+\left(\frac{\Delta p}{\Delta x}\right)_5+\left(\frac{\Delta p}{\Delta x}\right)_6\right]_{elev}=0.....(35)$$

The calculation of the flow properties at point 6 requires an iterative process which uses the known flow properties at points 1, 2 and 5. The process consists of the following steps:

a) Assume an initial in-situ liquid velocity at point 6.

b) Calculate the liquid hold up through Equation (32) and deter-mine the flow regime.

c) Calculate the in situ gas velocity.

d) Calculate the gas density at point 6 using Equation (33).

e) Calculate the pressure at point 6 using Equation (25). Use the Z value calculated for pressure at point 5.

f) With the flow properties calculated at point 6 and the assumed in situ liquid velocity, calculate the pressure at point 6 using Equation (35).

g) Compare the pressures calculated in (e) and (f). If they are within an acceptable range of tolerance, the process is over and the properties at point 6 are deter-mined. If not, assume another in situ liquid velocity and repeat the process.

If there is more than one grid, the process is repeated for the adjacent down-stream grid with the properties at point 6 of the previous cell becoming the flow properties at point 5.

The Induced Fracture Model

The induced fracture model used in the computer model is based on the assumption of an infinite plate with a circular hole in it. Poisson's ratio, Biot's constant, horizontal matrix stresses and vertical matrix stresses may be estimated from field data or correlated from a particular field.

In this work, compression is represented as positive and tension as negative. Therefore, tensile strength of the formation (S_t) is then a negative number.

The computer model only considers the extension for vertical fracture because this occurs in almost all cases in depths greater than 500 meters. The cases of formations shallower than 500 meters will not be studied here. Therefore, the program does not analyze cases where a horizontal fracture occurs.

Vertical Fracture Initiation

Vertical fracture starts when the maximum effective tangential stress S_t exceeds the tensile strength of the formation. Thus at fracture initiation:

$$S_t = \left(\frac{2\nu}{1-\nu}\right)\sigma_z + 2P_o - P_w +$$

$$a\left(\frac{1-2n}{1-n}\right)(P_p - P_o) - P_p \quad \text{.....(36)}$$

For a penetrating type of fluid, the pore pressure (P_p) at the borehole wall is equal to the wellbore pressure, or $P_p = P_w$. Substituting this expression in the last equation and solving for P_w leads to:

$$P_f = P_W = \left(\frac{\left(\frac{2\nu}{1-\nu} \right)\sigma_z - S_t}{2-\alpha\left(\frac{1-2\nu}{1-\nu} \right)} \right) + P_o \ldots\ldots\ldots\ldots(37)$$

For a non penetrating type of fluid, the pore pressure ($\dot{P}_p$) at the borehole wall is the original formation pore pressure, or $\dot{P}_p = P_o$. From equation (36), after substituting $\dot{P}_p$ for $\dot{P}_o$:

$$P_f = P_W = \left(\frac{2\nu}{1-\nu} \right)\sigma_z - S_t + P_o \ldots\ldots\ldots\ldots(38)$$

The equations for $\dot{P}_W$ give the initiation criterion for vertical fractures. The fracture associated with the smaller $\dot{P}_W$ is the one initiated.

Fracture Extension Model

The main objective of the model is to determine the wellbore pressure at the fractured formation in each time step. Therefore, the determination of the flow rate that is being injected into the fracture is essential to analyze the extension of the fracture. This is done by assuming the fracture propagates in two wings, so the flow rate is equal to half of the flow rate calculated in the last cell of the wellbore model.

Although models such as Geertsma and de Klerk (1969), Nordgren (1972), Khristianovic and Zheltov (1955) and Perkins and Kern (1961) gave good results to predict the geometry of fracture in some cases, they just consider that the fracture expands in two dimensions. This can lead to miscalculations in cases where the fracture advances in three dimensions.

Also, 3-D models need parameters that are very difficult to measure. The comparison of predicted results among the existing models showed large variation in the results. In addition, the computer time to run a 3-D model is much larger than with 2-D models. This is another limitation for this kind of model because in the main program the 3-D model is coupled with a reservoir and a wellbore model.

On the other hand, a pseudo 3-D model considers the expansion of the fracture in three dimensions. This model needs few parameters, which can be obtained from field data. The predicted results are realistic when compared with some 3-D models. A limitation of this model occurs when the stress contrast between the fractured formation and the bounding layers is small. In this situation the model predicts unstable and unrealistic vertical fracture migration.

The unstable vertical fracture migration can be prevented by a vertical pressure gradient in the equations that predict the fracture height. Upon consideration of these characteristics, the authors decided to use a pseudo-3D model with some modifications to analyze the fracture.

The governing equations on which the pseudo-3D models are based had to be modified to consider the compressible nature of the fluid because in an underground blowout the fluid is a mixture of a gas and a liquid phase, such as mud or water. The fracture model also assumes that the liquid hold

up of the two-phase flow inside the fracture in each time step is the same as that calculated in the last cell of the wellbore model; therefore, it assumes that there is no slip or fluid segregation inside the fracture.

The pseudo-3D model used in this study assumes linear elasticity and uniform in-situ stress within each layer, so the width is calculated as follows:

$$w_T(x,y) = w_I - w_{II} - w_{III} + w_{IV} - w_V \ldots\ldots\ldots (39)$$

where:

$$w_I = \frac{4\left(P(x,t) - \sigma_1\right)}{E'}\sqrt{a^2 - y^2} \ldots\ldots\ldots\ldots\ldots (40)$$

$$w_{II} = \frac{4(\sigma_2 - \sigma_1)}{E'\pi}\left[-(b_2 - y)\cosh^{-1}\left(\frac{a^2 - b_2 y}{a|y - b_2|}\right) + \right.$$

$$\left. + \cos^{-1}\left(\frac{b_2}{a}\right)\sqrt{a^2 - y^2}\right] \ldots\ldots\ldots\ldots\ldots\ldots (41)$$

$$w_{III} = \frac{4(\sigma_3 - \sigma_1)}{E'\pi}\left[-(b_3 + y)\cosh^{-1}\left(\frac{a^2 + b_3 y}{a|y + b_3|}\right) + \right.$$

$$\left. + \cos^{-1}\left(\frac{b_3}{a}\right)\sqrt{a^2 - y^2}\right] \ldots\ldots\ldots\ldots\ldots\ldots (42)$$

$$w_{IV} = \frac{2}{E'} g_\sigma y\sqrt{a^2 - y^2} \ldots\ldots\ldots\ldots\ldots\ldots (43)$$

$$w_V = \frac{2}{E'} g_P y\sqrt{a^2 - y^2} \ldots\ldots\ldots\ldots\ldots\ldots (44)$$

$$E' = \frac{E}{(1 - \nu^2)} \ldots\ldots\ldots\ldots\ldots\ldots\ldots\ldots (45)$$

The height of the fracture is determined in terms of critical stress intensity factor at the top of the crack through the equation:

$$K_{Itop} = \frac{1}{\sqrt{\pi a}}\int_{-a}^{a} \Delta P(x,y,t)\sqrt{\frac{a+y}{a-y}}dy \ldots\ldots\ldots (46)$$

where:

$$\Delta P(x,y,t) = P(x,t) - g_P y - \sigma_3 + g_\sigma y + g_v y$$

$$for\ -a \le y < -b_3 \ldots\ldots\ldots\ldots\ldots\ldots\ldots\ldots\ldots\ldots (47)$$

$$\Delta P(x,y,t) = P(x,t) - g_P y - \sigma_1 + g_\sigma y + g_v y$$

$$for\ -b_3 \le y < 0 \ldots\ldots\ldots\ldots\ldots\ldots\ldots\ldots\ldots\ldots (48)$$

$$\Delta P(x,y,t) = P(x,t) - g_P y - \sigma_1 + g_\sigma y - g_v y$$

$$for\ 0 \le y < b_2 \ldots\ldots\ldots\ldots\ldots\ldots\ldots\ldots\ldots\ldots (49)$$

$$\Delta P(x,y,t) = P(x,t) - g_P y - \sigma_2 + g_\sigma y - g_v y$$

$$for\ b_2 \le y \le a \ldots\ldots\ldots\ldots\ldots\ldots\ldots\ldots\ldots\ldots (50)$$

and at the bottom by:

$$K_{Ibottom} = \frac{1}{\sqrt{\pi a}} \int_{-a}^{a} \Delta P(x,y,t) \sqrt{\frac{a+y}{a-y}}\, dy \ldots\ldots\ldots\ldots (51)$$

where:

$$\Delta P(x,y,t) = P(x,t) - g_P y - \sigma_2 + g_\sigma y + g_v y$$

$$for\ -a \le y < -b_2 \ldots\ldots\ldots\ldots\ldots\ldots\ldots\ldots\ldots\ldots (52)$$

$$\Delta P(x,y,t) = P(x,t) - g_P y - \sigma_1 + g_\sigma y + g_v y$$

$$for\ -b_2 \le y < 0 \ldots\ldots\ldots\ldots\ldots\ldots\ldots\ldots\ldots\ldots (53)$$

$$\Delta P(x,y,t) = P(x,t) - g_P y - \sigma_1 + g_\sigma y - g_v y$$

$$for\ 0 \le y < b_3 \ldots\ldots\ldots\ldots\ldots\ldots\ldots\ldots\ldots\ldots (54)$$

$$\Delta P(x,y,t) = P(x,t) - g_P y - \sigma_3 + g_\sigma y - g_v y$$

$$for\ b_3 \le y \le a \ldots\ldots\ldots\ldots\ldots\ldots\ldots\ldots\ldots\ldots (55)$$

The vertical pressure gradient ($\dot{g}_v$) is determined under the assumption that pressure in any cross section decreases in the direction of the tips in proportion to the pressure gradient for the lateral flow. This is the main point in a pseudo-3D model to avoid unstable vertical fracture migration. The authors assumed that this proportion depends on the ratio of height to length growth rate, or in equation form:

$$g_v = \frac{(a_t - a_{t-1})}{dx} \frac{P(x,t) - P_L}{L} \ldots\ldots\ldots\ldots\ldots\ldots (56)$$

where a_t and a_{t-1} are the half height of the cross section at current and previous time steps, respectively, and P_L is the pressure differential required to open the fracture at the crack front .

In the situation of uniform in-situ stress within each layer, the direct integration of equations (46) and (51) results in:

$$K_{Ic} = K_{I1} - K_{I2} - K_{I3} + K_{I4} - K_{I5} - K_{I6} \ldots\ldots (57)$$

where:

$$K_{I1} = \left(P(x,t) - \sigma_1\right)\sqrt{\pi a} \ldots\ldots\ldots\ldots\ldots\ldots\ldots (58)$$

$$K_{I2} = \frac{(s_2 - s_1)\sqrt{a}}{\sqrt{p}} \left(\cos^{-1}\left(\frac{b_2}{a}\right) + f_a \frac{\sqrt{a^2 - b_2^2}}{a} \right) \ldots\ldots\ldots\ldots (59)$$

$$K_{I3} = \frac{(s_3 - s_1)\sqrt{a}}{\sqrt{p}} \left(\cos^{-1}\left(\frac{b_3}{a}\right) - f_a \frac{\sqrt{a^2 - b_3^2}}{a} \right) \ldots\ldots\ldots\ldots (60)$$

$$K_{I4} = \frac{a}{2} f_a g_\sigma \sqrt{\pi a} \ldots\ldots\ldots\ldots\ldots\ldots\ldots\ldots (61)$$

$$K_{I5} = \frac{a}{2} f_a g_P \sqrt{\pi a} \ldots\ldots\ldots\ldots\ldots\ldots\ldots\ldots (62)$$

$$K_{I6} = \frac{2a^{1.5} g_v}{\sqrt{\pi}} \ldots\ldots\ldots\ldots\ldots\ldots\ldots\ldots\ldots (63)$$

where f_c = +1 for upper or -1 for lower fracture tip of vertical section.

The final solution (57) presents two equations, one for the upper and other for the lower tip. These two equations together with an additional geometry constraint of:

$$b_3 = h_f - b_2 \ldots\ldots\ldots\ldots\ldots\ldots\ldots\ldots\ldots\ldots (64)$$

give the solution for a, b_2, and b_3.

The fluid flow in a pseudo-3D model is considered as being one-dimensional flow along the fracture length. The governing equations are basically the continuity equation for a compressible flow and the pressure gradient equation.

The continuity equation is given by:

$$-\frac{\partial\left(\rho_{mix}(x,t)Q(x,t)\right)}{\partial x}=\rho_{mix}(x,t)Q_L(x,t)+$$

$$+\frac{\partial\rho_{mix}(x,t)A_{cr}(x,t)}{\partial t}\ldots\ldots\ldots\ldots\ldots\ldots\ldots\ldots(65)$$

where

$$A_{cr}(x,t)=\int_{-a}^{a}w(x,y,t)dy\ldots\ldots\ldots\ldots\ldots\ldots\ldots(66)$$

$$Q_L(x,t)=\frac{4Ca}{\sqrt{t-\tau(x)}}\ldots\ldots\ldots\ldots\ldots\ldots\ldots\ldots(67)$$

The thickness of the fractured formation is used instead of the height of fracture in equation (67) for cases where the bounding layers are impermeable.

Integration of equation (66) and the use of equation (39) allow equation (65) to be written as:

$$-\frac{\partial\left(\rho_{mix}(x,t)Q(x,t)\right)}{\partial x}=\rho_{mix}(x,t)Q_L(x,t)+$$

$$+\frac{2\pi}{E'}\frac{\partial\rho_{mix}(x,t)a^2P(x,t)}{\partial t}\ldots\ldots\ldots\ldots\ldots\ldots\ldots(68)$$

The pressure gradient equation after applying the concept of apparent viscosity yields:

$$\frac{\partial P}{\partial x}+\frac{12\mu_{mix}q_x}{w^3}=0\ldots\ldots\ldots\ldots\ldots\ldots\ldots\ldots\ldots(69)$$

and after integrating $\dot{q}_x$ over the fracture height gives:

$$Q(x,t)=\int_{-a}^{a}\left(\frac{w^3(x,y,t)}{12\mu_{mix}}\left|\frac{\partial P(x,t)}{\partial x}\right|\right)dy\ldots\ldots\ldots(70)$$

This equation can be solved for the pressure gradient to obtain:

$$\frac{\partial P(x,t)}{\partial x}=\frac{12\mu_{mix}Q(x,t)}{\int_{-a}^{a}w^3(x,y,t)dy}\ldots\ldots\ldots\ldots\ldots\ldots(71)$$

The two-phase fluid viscosity or apparent viscosity is given as stated in Brill and Beggs (1978) by:

$$\mu_{mix}=H_l\mu_{apl}+(1-H_l)\mu_g\ldots\ldots\ldots\ldots\ldots\ldots(72)$$

where the liquid apparent viscosity is calculated through:

$$\mu_{apl} = \mu_l + 5.441x10^{-5}\frac{\tau_y A_{cr}^2}{perQ_l} \ldots\ldots\ldots\ldots\ldots\ldots(73)$$

and per is the perimeter of the fracture cross section.

The boundary conditions of equations (68) and (71) are given by:

$$Q(0,t) = \frac{q_i(t)}{2} \ldots\ldots\ldots\ldots\ldots\ldots\ldots\ldots\ldots\ldots(74)$$

$$\Delta P\left(L(t)/2,t\right) = P_L \ldots\ldots\ldots\ldots\ldots\ldots\ldots\ldots(75)$$

The value of P_L is calculated by assuming that the fracture height at its front is equal to the height of the fractured formation. So from equation (57):

$$P_L = \frac{K_{Ic}}{\sqrt{\pi a}} + \sigma_1 \ldots\ldots\ldots\ldots\ldots\ldots\ldots\ldots\ldots(76)$$

The pseudo-3D equations were solved by advancing the fracture front at a distance, ΔL, during an assumed time step, Δt, and by integrating the two flow equations by Runge-Kutta method after substituting the term involving $\frac{\partial \rho_{mix}(x,t)a^2 P(x,t)}{\partial t}$ by the difference relation:

$$\frac{\partial \rho_{mix}(x,t)a^2 P(x,t)}{\partial t} =$$

$$= \bar{a}^2 \frac{r_{mix}(x,t+\Delta t)P(x,t+\Delta t) - r_{mix}(x,t)P(x,t)}{\Delta t} \ldots\ldots\ldots\ldots(77)$$

where $\bar{a}$ corresponds to the average half height of the fracture between the instant t and $t+\Delta t$ respectively.

The value of $Q(0,t)$ obtained is compared with $q_i(t)/2$, and if they do not agree, another value for Δt is assumed. An iterative process repeats the calculation until the values come within an acceptable range.

This calculation procedure, unlike other pseudo-3D models, allows the calculation of the leak-off coefficient for each cell instead of using an average leak-off coefficient for all fracture extension.

The pseudo-3D model with a vertical pressure gradient was used in fracture prediction because it gives good predictions with less computer running time. This is very important because the wellbore model is also time consuming, and the simulation of an underground blowout would require a main frame if the simulation is too long. The use of personal computers to predict pressure and flow rate in an underground blowout is preferred due to their wide availability.

Global Calculation Procedure

This procedure achieves the coupling among three sub models: the reservoir, the wellbore, and the fracture sub models. The procedure assumes that the pressures and liquid holdup are common to contiguous models and cells and the mass flow rate is conserved. A listing of the dynamic kill program developed in this study in included as Appendix A.

The first step of the procedure is the calculation of the fracture initiation pressure with equations (36) or (37) for vertical fracture. The calculation procedure will continue with the assumption that the vertical fracture initiates at the same moment as the two-phase leading edge reaches the fractured formation.

Due to this assumption, it is necessary to calculate the variables required in the fracture model at the moment the fracture starts. For that, the procedure is to calculate the properties of each cell in the annulus within each time step until the two-phase fluid reaches the fractured formation. This is done by the wellbore model that simulates a circulation of mud and gas from the moment the influx started using the pressure at the fractured formation equal to the fracture initiation pressure. Once the two-phase fluid reaches the fractured formation, the fluid properties of the last cell in the wellbore are used in the fracture model. The propagation process then starts.

The algorithm for this calculation consists of the following steps:

a) Assume the liquid/mixture interface position and calculate the time increment by dividing the grid length by the mixture leading edge velocity for the previous time step.

b) Assume a bottom hole pressure and determine the other boundary conditions at bottom hole.

c) Determine the gas flow rate using the reservoir flow model

d) Determine the pressure drop throughout the annulus

e) Add the pressure drop to the fracture initiation pressure to determine the bottom hole pressure

f) Compare the assumed and calculated pressure values. If they are within an acceptable range, repeat the process for the next time step. If not, assume another bottom hole pressure and repeat the process.

After the two-phase leading edge reaches the fractured formation, the program starts simulating the fracture propagation and the underground blowout. This consists of the following steps:

a) With the total flow rate calculated in the last cell when the two-phase leading edge reaches the fractured formation, calculate the time step and pressure change for an assumed increment in the length of the fracture.

b) With the wellbore model using the same time step and pressure change calculated in the previous item, calculate the bottom hole pressure and the gas flow rate with the reservoir model and the pressure drop in the annulus.

c) Determine the total flow rate in the cell at the fracture formation and repeat the calculation from item (a).

d) Continue the process until the variation of pressure is negligible. The simulation for this time step is now over and the process is repeated for the next time step.

This procedure gives the variation of fracture pressure and gas flow rate produced as a function of time for the assumed mud flow rate in an underground blowout. The calculation is repeated for different mud flow rates until the appropriate rate to control the underground blowout is determined. As can subsequently be seen in the comparison of the results, this new procedure gives different results than those calculated in the previous models. This can potentially change significantly the planning for the kill of an underground blowout.

Leak off Volume Correlation

An experimental apparatus and operational procedure were designed to study the leak-off volume occurring inside the induced fracture during an under-ground blowout. This apparatus was used to develop controlled, physical measurements rather than the full-scale experiments mentioned in the original proposal. The full scale experiments were concluded to be impractical given the lack of a well with open hole available and the inability of determining physical rock properties behind casing. In essence, full-scale tests of this phenomenon were not economically feasible within this project scope and budget. The result of this study is used in a fracture model to predict pressures developed during an underground blowout.

The experimental apparatus, set up at the LSU Petroleum Engineering Research and Technology Transfer Laboratory, consisted of a fluid loss cell in which a two-phase fluid passes over and through a porous core due to pressure differential. The volume that passes through the core is the leak-off volume used in the fracture model.

Description of the experimental apparatus

The test apparatus used for all fluid runs is shown schematically in figure 6. It can be di-vided in three major parts: the mixing system, the fluid loss cell, and the collector system.

The mixing system consists of two nitrogen bottles charged with a maximum pressure of 2,500 psi, a 10 gal fluid vessel, a heater, and two 20-ft rheology loops.

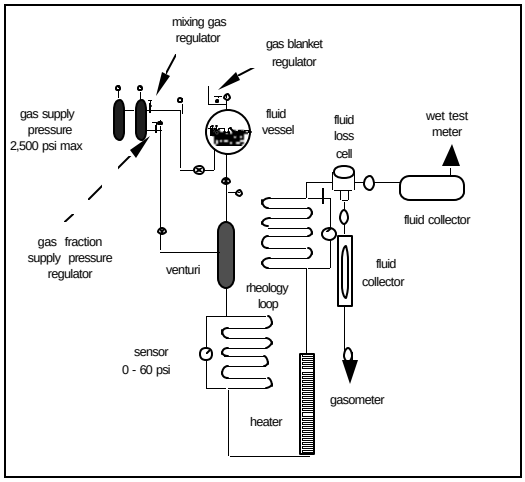

Figure 6 Experimental Apparatus

Base drilling fluid is prepared in a small tank, pumped into the fluid vessel, and pressurized at the required level to run the experiment. The two-phase fluid mixture is obtained by small adjustments in two needle valves situated on two lines upstream of the venturi. Once the pressure and gas flow rate are set at the start of the experiment, very little adjustment is needed to keep them at required levels. The gas and mud flow rates are measured in the collector system described later in this text.

The fluid loss cell is an apparatus in which a 0.94 x 1 inch core is set, and the fluid passes through a 1x1.5x0.13 inch slot over the core. The heater is used to maintain the fluid temperature at formation conditions, and it consists of a loop immersed in hot water. The collector system is used to collect the fluids that pass over and through the core, and to measure the total leak-off, the flow rate, and the gas void fraction.

Experimental Procedure

Before running the experiments, twelve Berea sandstone cores were dried in an oven for 12 hours at 250^{O}F, and the lateral surfaces of the cores were coated with a very thin layer of epoxy to avoid possible lateral flow during the experiment. The liquid permeability was then measured with a gas permeameter considering the Klinkenberg effect, and the porosity was measured by using mercury and an air pump.

At the end of the measurement, each core was put in a vacuum pump for three hours. Then, 50,000 ppm brine was introduced to the evacuated container to saturate the core. All the cores were allowed to saturate for a minimum of 10 days.

The fluid leak-off tests were run with five different pressure differentials of 200, 400, 600, 800, and 1,000 psi and gas void fractions varying from 0% up to 90% for each pressure differential. The pressure differential and gas void fraction were selected based on values that can be reached during an underground blowout and on values within the apparatus capacity. The mud used was a bentonite type with a viscosity of 10 cp and a density of 8.7 ppg.

The results of the total leak-off volume as function of time for all runs were plotted, and a general equation was found by using a curve fit program. The parallax error for the total leak-off volume measured in the experiment was estimated as 0.1 ml/sq cm. The equation is written as:

$$V = V_{sp}\left(1 - e^{-bt}\right) + v_D t \ldots\ldots\ldots\ldots\ldots\ldots\ldots\ldots\ldots\ldots (78)$$

where the parameters in this equation are spurt loss volume, the pack buildup factor, and the equilibrium Darcy flow velocity.

Those parameters depend on pressure differential, flow rate, core permeability, mud filtration property, rheological properties of the fluid, and gas void fraction.

Figure 7 shows the plot of the total leak-off volume data as function of time and gas void fraction for some runs (points in the graph), as well as the plot of equation (78) that fits the leak-off volume data (curves in the graph).

The use of equation (78) to predict the leak-off volume is possible when the spurt loss volume, the pack buildup factor, and the equilibrium Darcy flow velocity are known. The author analyzed those parameters as function of permeability, flow rate, pressure differential, viscosity, and gas void fraction.

The influence of gas void fraction on total leak-off volume is clear because the leak-off increases proportionally to gas void fraction, as can be seen in figure 7. The same conclusion is achieved about the pressure differential when observing the leak-off volume data. The influence of permeability, viscosity, and flow rate was not clear with the available data. The influence of the mud filtration property was not studied in this work because only one kind of mud was used in the experiment.

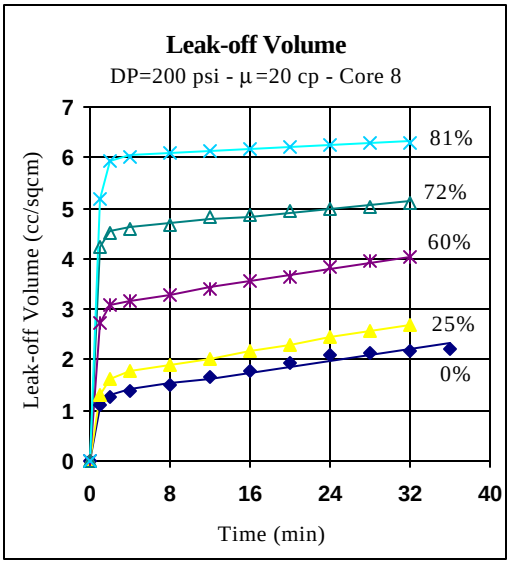

Figure 7 Leak-off Volume for Core 8

Results

Several simulations were performed using the program described above and in Appendix A. Case 1 is the simulation of a 9500 foot deep, offshore well in 500 feet of water. A wellbore diagram of the well showing the well's geometry is included figure 8. The bottomhole temperature is 190^0F. The fluid was a 9 lb/gal mud with a plastic viscosity of 10 cp and a yield point of 25 lb/100sf. The simulated reservoir is 35 feet thick with 25% porosity and 160 md permeability. The skin factor is 0, gas density is .65, water saturation is 20%, and temperature is 200^0F. The fractured zone taking flow is 55 feet thick with a fracture initiation pressure of 4640 psi and bounding zone stress of 5930 psi. The stress intensity factor is 216 psi-$ft^{.5}$, Poisson's ratio is .2, and Young's modulus is 2,100,000 psi.

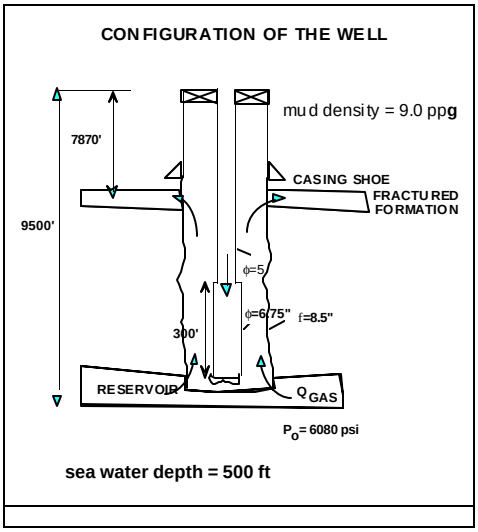

Figure 8 Wellbore Diagram for Case 1 Simulation

The bottomhole pressure variation with different flowrates over time is shown in figure 9. The bottomhole pressure is higher for larger mud flow rates as expected in a dynamic kill method. The bottomhole pressure also increases with time rapidly for the about the first 200 seconds then increases more slowly on a gradual upward trend as the fracture extends further from the reservoir

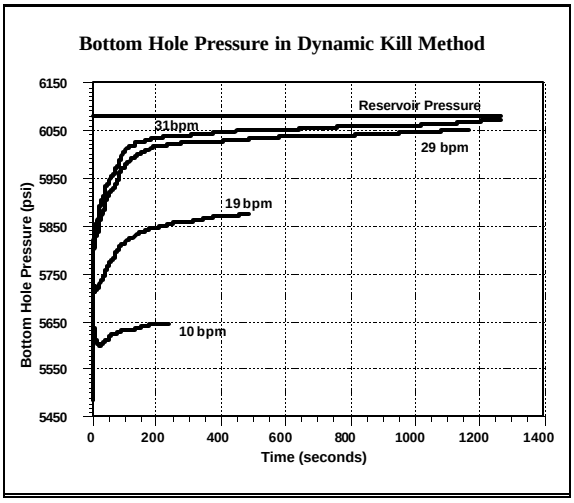

Figure 9 Bottom Hole Pressure for Case 1

Figure 10 shows the gas flow rate produced in the simulated control of this underground blowout using the dynamic kill method with different flow rates. The 31 bpm pump rate achieves dynamic control of the well after about 1300 seconds. The fracture extension pressure has a significant effect on bottom hole pressure in this case because the length of the open hole interval is relatively short. The combination of the fracture extension pressure, the frictional pressure losses, and the increase in hydrostatic head in this highest rate example cause the bottomhole pressure to reach a level equal to the formation pressure.

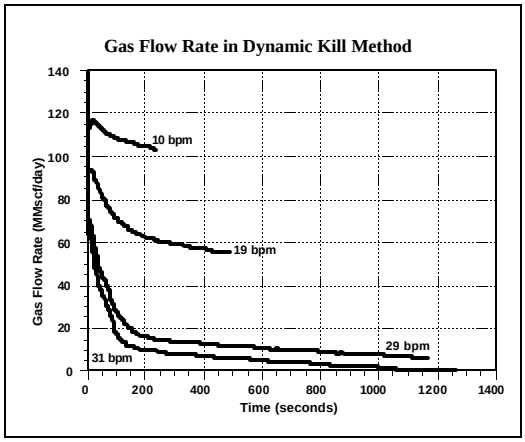

Figure 10 Gas Flow Rate for Case 1

The effect of increasing fracture pressure due to fracture extension is shown in figure 11. For the fracture characteristics in this case, there is very little difference in this pressure for the different pump rates. Consequently if knowing the small pressure increase versus time is not necessary, the effect of the fracture extension pressure for these conditions could be considered to be a constant pressure about 300 psi greater than the fracture initiation pressure.

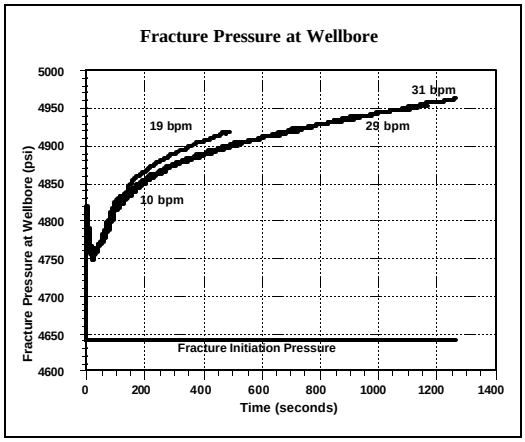

Figure 11 Fracture Pressure at Wellbore for Case 1

Figure 12 shows the effect of considering the fracture model explicitly as opposed to assuming that the pressure in front of the fracture is constant as with the "current" model. The pump rate calculated as required for a kill would be higher than 31 bpm if the effective of fracture extension was ignored. Ignoring this effect could result in assuming that the required pump capacity is too high or even that a dynamic kill is unfeasible with the pump capacity available. However, the difference in the predicted bottomhole pressures for the two methods is only about 100 psi.

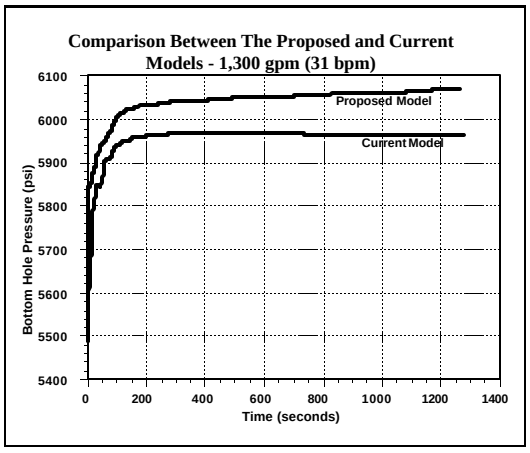

Figure 12 Bottomhole Pressure for Current and Proposed Model for Case 1

Case 2 is a simulation of an underground blowout in a shallow, 4600 foot offshore well in 500 feet of water. The loss zone is very shallow at 2625 feet. Figure 13 is a wellbore diagram for Case 2. The bottomhole temperature is 120^0F. The fluid was a 9 lb/gal mud with a plastic viscosity of 10 cp and a yield point of 25 lb/100sf. The simulated reservoir is 35 feet thick with 25% porosity and 110 md permeability. The skin factor is 0, gas density is .65, water saturation is 20%, and temperature is 130^0F. The fractured zone taking flow is 70 feet thick with a fracture initiation pressure of 1456 psi and bounding zone stress of 2400 psi. The stress intensity factor is 144 psi-$ft^{.5}$, Poisson's ratio is .2, and Young's modulus is 1,400,000 psi.

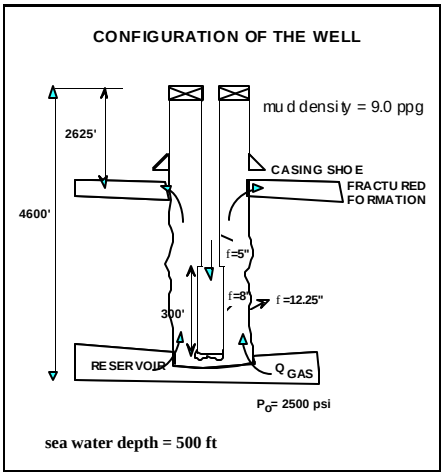

Figure 13 Wellbore Diagram for Case 2 Simulation

The bottomhole pressure variation with different flowrates over time is shown in figure 14. The bottomhole pressure is higher for larger mud flow rates as expected in a dynamic kill method. The rates required are higher than in Case 1 due to the larger wellbore diameter. The bottomhole pressure also continues to increase significantly over the period simulated. This occurs at the 38 and 43 bpm rates because of two factors. First, the hydrostatic effect of mud accumulating in the annulus is contributing to increasing bottomhole pressure. Second, the fracture is continuing to grow in height and length causing the pressure in front of the fracture to increase over almost the entire time period.

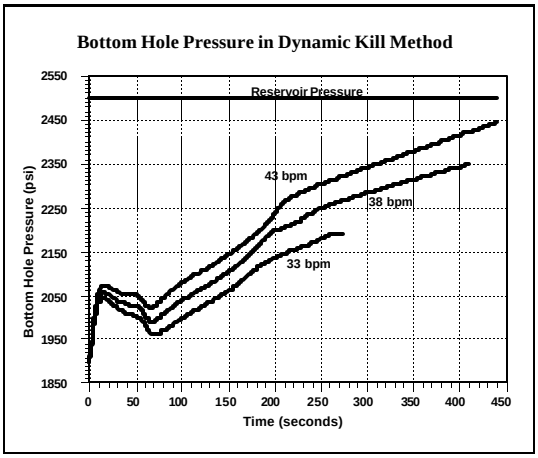

Figure 14 Bottom Hole Pressure for Case 2

Figure 15 shows the effect of considering the fracture model explicitly as opposed to assuming that the pressure in front of the fracture is constant as with the "current" model. The pump rate calculated as required for the kill considering the fracture model is 43 bpm. The bottomhole pressure after 400 seconds of pumping is calculated to be almost 400 psi greater than if a constant fracture pressure were assumed. However, the predicted difference in the pressure in front of the fracture is only about 200 psi, and it stabilizes as a maximum fracture height is reached.

The minimum rate required for a dynamic kill using the conventional assumption that fracture pressure is equal to a constant fracture initiation pressure is 76 bpm. However, a practical estimate of the minimum kill rate can be made, even with a conventional model, by assuming that the fracture extension pressure is slightly greater than the fracture initiation pressure. However, this simple assumption does not allow accurate prediction of pressure versus time in the manner of the proposed simulator. Also, as evidenced in this case of a shallow well, the importance of correctly estimating fracture extension pressure is greater in wells with short length or large diameter open hole intervals.

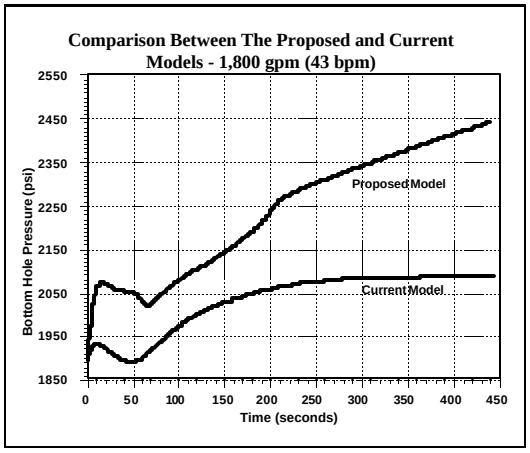

Figure 15 Current and Proposed Model for Case 2

It can be seen from figures 8 through 15 that the proposed model can differ from the current models significantly. The difference depends on the well geometry, the reservoir and fractured formation characteristics, and the distance between the fractured formation and the reservoir.

Comparison between the proposed model and field data was not possible. The two underground blowouts for which field data was available when evaluating this method were from Walters[6] and Flak and Gloger[19]. Both works mentioned an increase in the bottomhole pressure being caused by the injection of the fluid into a fractured formation. However, simulation of these cases was not possible because of the lack of data concerning the formations being fractured and the complex flow path in one of the cases.

Conclusions

It can be concluded from the simulations that:

1) The proposed model predicts a lower minimum mud flow rate than the current models to control an underground blowout.

2) The difference in the mud flow rate is directly proportional to the well diameter and inversely proportional to the distance between the reservoir and the fractured formation.

3) The leak-off volume is related to time, spurt loss volume, pack build-up factor, and the equilibrium Darcy flow velocity coefficient.

4) A pseudo 3D fracturing model with a pressure gradient factor predicts results that fit the results of other comprehensive 3D models.

5) The proposed model is significantly more complex, and therefore more difficult to use and maintain, than previous time-dependent and steady-state models.

6) The proposed model requires fracture zone mechanical properties, that are typically unknown, to give accurate predictions.

7) Simple models can be used to account for the effect of fracture propagation pressure being greater than fracture initiation pressure if an exact prediction of pressure versus time is not required.

Chapter 4

Steady-state Dynamic Kill Methods

Steady-state methods for designing and analyzing dynamic kills have also been the subject of recent research at LSU. This chapter describes that work.

Steady state methods have been used to design successful kills for a number of surface and underground blowouts. This section describes several published methods and models, application of these concepts to underground blowouts, and a steady-state method delivered as part of this report. The computer program implementing the method and its application to actual dynamic kills are described in Chapter 5.

Published Steady State Flow Models

E. M. Blount and E. Soeiinah (1981)[7]

A landmark model for an on - bottom dynamic kill of a surface blowout was presented by Blount and Soeiinah[7]. It was used during kill operations on Mobil Oil Indonesia's prolific Arun blowout in 1978. They described a dynamic kill as a technique for terminating a blowout utilizing flowing frictional pressure to supplement the hydrostatic pressure of the kill fluid being injected through a communication link. Hence, the flow rate must be maintained such that the sum of frictional and hydrostatic pressure exceeds the static formation pressure and the well ceases to produce. They pointed out that it can be important to avoid breaking down the formation so the maximum amount of fluid can be circulated through the well increasing the flowing frictional pressure, especially for surface blowouts. Therefore use two or more weights of mud was recommended, a light one to kill the well dynamically, then replacing it with a heavier one to kill the well hydrostatically.

Blount and Soeiinah proposed a simple model to find the necessary design parameters to carry out a dynamic kill with the drill string on - bottom. These kill parameters include:

Initial kill fluid density

They considered that the "initial dynamic kill fluid is to kill the well by exceeding the natural flow capacity of the wellbore". The density of the initial kill fluid can be determined by the following equation.

$$r_{ikf} = \frac{12.83 p_R}{D_V} \tag{79}$$

If the density of the initial kill fluid is lower than the density of the water, then water is used as the kill fluid in both dynamic and static condition.

Kill fluid injection rate

The required injection rate must generate a flowing frictional pressure to supplement the hydrostatic head of the kill fluid and exceed the static formation pressure. It is given by:

$$q_{kf} = \left[\frac{(p_R - p_h) d_e^5}{11.41 f_f L r_{ikf}} \right]^{1/2} \tag{80}$$

Where:

$$p_h = 0.052 r_{ikf} D_V \tag{81}$$

The equivalent diameter, d_e, is equal to the pipe diameter when the control fluid is pumped through the annular section. Contrarily, if the blowout control is carried out through the pipe and the flow is up the annulus the equivalent diameter becomes.

$$d_e^5 = (d_2 - d_1)^3 (d_2 + d_1)^2 \tag{82}$$

Fanning friction factor f_f in this procedure is calculated as follows.

$$f_f = \frac{0.25}{\left(2 \log \frac{d_h}{e} + 1.14 \right)^2} \tag{83}$$

Here the hydraulic diameter d_h is defined by.

$$d_h = d_2 - d_1$$

Size of the relief well

Blount's model[7] considers a blowout control through both a relief well and by injecting kill fluid internally in the blowout well through the surface. Thus, if the first option is taken the relief well size should be considered in the kill plan since the relief well must have adequate flow capacity to allow dynamic control. This parameter is calculated by

$$d_{e_{rw}} = \left[\left(\frac{d_e^5 \Delta p_f}{f_f L} \right)_{bw} \left(\frac{f_f L}{\Delta p_f} \right)_{rw} \frac{1}{k^2} \right]^{1/5} \tag{84}$$

Frictional pressure losses in the blowout well $\left(\Delta p_f\right)_{bw}$ can be obtained as follows

$$\left(\Delta p_f\right)_{bw} = p_R - p_h \tag{85}$$

On the other hand, $\left(\Delta p_f\right)_{rw}$ represents the frictional pressure losses in the relief well and is calculated by

$$\left(\Delta p_f\right)_{rw} = p_{ann} - p_F + p_{h_{rw}} \tag{86}$$

Where p_{ann} is the surface pressure on the relief well, and p_F represents the fracture pressure of the formation. The term k stands for fraction of flow entering blowout well and is given by the ratio between the kill fluid injection rate q_{kf}, flow up blowout well, and the injection rate required through annular section on the relief well q_{rw}. It is mathematically represented by

$$k = \frac{q_{kf}}{q_{rw}} \tag{87}$$

Equivalent diameter in the relief well $d_{e_{rw}}$ is computed with equation 2.6. Then reasonable values of outside diameter of the pipe d_1 and casing diameter d_2 are calculated utilizing the equivalent diameter concept (Equation 82). If it was not planned to run a pipe in the relief well, the equivalent diameter $d_{e_{rw}}$ is the casing diameter d_2.

Hydraulic horsepower

The required hydraulic horsepower to pump the kill fluid with the needed kill rate is obtained by considering the maximum pump pressure p_{ann}. It is given by

$$HHP = \frac{q_{rw} p_{ann}}{40.81} \tag{88}$$

Maximum allowable BHP to prevent drill pipe from being ejected

A force tending to eject the drill string from the blowout well is composed of the frictional drag and the hydraulic force acting on various cross sections of the drill string. The weight of the drillstring

resists the ejection force. Therefore, if ejection force is greater than the weight, the pipe will be ejected. Accordingly, the maximum allowable bottom hole pressure to prevent this effect is computed by

$$p_{BH\max} = \frac{W_s + A_{an} R p_h}{A_{ds} + A_{an} R} \tag{89}$$

Ratio of the total frictional drag R that applies to the drill pipe in the blowout well can be calculated as follows:

$$R = \frac{1}{2\log\left(\frac{d_2}{d_1}\right)} - \frac{d_1^2}{\left(d_2^2 - d_1^2\right)} \tag{90}$$

Blount and Soeiinah successfully used the above procedure to control an extremely difficult blowout in Indonesian's Arun field. The C-II-2 Arun well blew out and caught fire destroying the drilling rig and burned for 89 days at an approximate rate of 400 MMscfd. This method has been used for bringing several other blowouts under control around the world. It is important to point out that this method is intended to work when the drillstring is at the bottom of the well.

R. D. Lynch et al. (1981)[8]

Lynch et al[8] utilized the steady state system analysis approach for a dynamic kill to bring under control a CO_2, near - bottom blowout that occurred in 1982 in the Sheep Mountain Unit of Colorado. They considered that the following factors are of primary importance in the design of an on - bottom dynamic kill operation: bottomhole static formation pressure, pressure and hydraulic constraints, deliverability of the well, kill fluid density and injection rate.

The authors state that the selection of the kill fluid density is a trade - off between the advantages (higher hydrostatic and frictional pressure drops in the annulus) and disadvantages (higher friction pressure losses in the injection piping, which tend to reduce the injection rate) of a higher kill fluid density.

They found the required kill density and rate to control the blowout using the following steps. First, a reservoir model was used to calculate the reservoir performance curve (IPR). Then for a selected value of CO_2 flow rate and selected value of kill fluid injection rate, the pressure distribution in the well was calculated (wellbore hydraulics performance). A series of such calculations yielded a plot of bottom hole pressure versus CO_2 flow rate for various fixed values of kill fluid injection rate. Any wellbore hydraulics performance curve that lies entirely above the reservoir performance curve meets the conditions to control the well. Hence, the kill fluid density and injection rate utilized to construct that curve would be the ones that would kill the well.

W. L. Koederitz, F.E. Beck, J.P. Langlinais and A. T. Bourgoyne Jr. (1987)[9]

Koederitz et al[9] developed a systematic technique for handling shallow gas flows based on an on - bottom dynamic kill. A high circulating rate is used to increase annular frictional pressure losses. The method estimates the loads on the wellbore and diverter system during the kill operation for a

bottom supported marine rig, land rig, or a deep water-floating rig. The main goal is to avoid both underground fracturing, which may result in cratering and rig foundation problems, and failure of the diverter system. The authors presented the following procedure to apply this technique.

1. Plot the inflow performance of the reservoir to show flowing bottom hole pressure as a function of gas flow rate.

2. Superimpose on the plot of the step 1 the annular flow performance of the well for various liquid injection rates taking into account pressure change due to elevation, friction and acceleration.

3. Determine the kill injection rate from the plot as the line of constant injection rate which is just above the inflow performance line of the reservoir.

4. Plot the flowing annular pressure as a function of depth for various liquid injection rates up to the known kill injection rate.

5. Plot the casing seat depth and the fracture pressure as a function of depth on the graph of step 4. From the resulting plot, determine the fracture margin, which is defined as the minimum difference in the open hole interval between the fracture pressure and the annular wellbore pressure, expressed as an equivalent mud density.

6. Determine the frictional pressure losses in the injection string with and without friction reducers being present. The friction reducers are assumed to affect only the pressure losses in the injection string.

7. Determine surface injection pressure and hydraulic power requirements with and without friction reducers being present.

Parameters such as kill fluid rate and density, injection pressure, injection horsepower, a wellbore pressure profile, and diverter wellhead pressure can be determined from this analysis procedure.

G. E. Kouba, G. R. MacDougall, and B. W. Schumacher (1993)[10]

Kouba et al[10] presented three methods to determine the upper and lower limits of the injection rate needed to dynamically kill a well. These include a technique for establishing a conservative most probable minimum kill rate. A method for estimating the liquid accumulation below the injection point in an off - bottom kill was also proposed but is not reviewed here.

Multiphase Flow Solution.

They determined that the basic idea of this solution is that, for any successful kill rate, the bottom hole pressure prediction must be greater than the sand face pressure for any reservoir fluid flow rate. In graphical terms, the wellbore hydraulics curve must lie above or tangent to the inflow performance relationship. Kouba et al built the wellbore hydraulics performance curves for various combinations of injection and blowout rates by adding pressure losses resulting from hydrostatic head, friction and acceleration to the outlet pressure. It is mathematically represented by

$$p_{wf} = p_o + \frac{1}{144}\left[r_m D_V + \frac{K r_m v_m^2}{2g_c} + \frac{\Delta\left(r_m v_m^2\right)}{2g_c} \right] \tag{91}$$

Friction losses are included in the resistance coefficient, K. Kouba et al consider that homogeneous flow is very likely at high flow rates. This method was employed to calculate the minimum flow rate to achieve a kill in Indonesia's Arun blowout. The kill rate and density given by the method was accurate and essentially the same reported by Blount et al[7].

Bottomhole Pressure Match Solution (Lower Limit)

The authors proposed this solution to determine the liquid injection rate necessary to keep the bottomhole pressure equal to the reservoir pressure once the well has been killed. They substituted the reservoir pressure p_R for flowing bottomhole pressure p_{wf} in Equation (91), removed the acceleration pressure drop term, and solved for kill flow rate q_{kf}. The resulting equation was.

$$q_{kf} = A_{an}\left\{ \left[144\left(p_R - p_o\right) - r_{kf} D_V \right] \frac{2g_c}{K r_{kf}} \right\} \tag{92}$$

Equation (92) gives the necessary condition for determining the minimum kill rate; it is insufficient to guarantee that this rate will actually kill the well.

Zero Derivative Solution (Upper Limit)

Kouba et al[10] designed this solution to seek the kill rate for which the wellbore hydraulics performance curve passes through a pressure minimum as the formation rate approaches zero. A vanishing or zero derivative of bottomhole pressure with respect to formation fluid rate is therefore the criterion for this solution. In order to accomplish this, they derived Equation (91) with respect to the formation fluid rate and neglected the acceleration term. After applying the zero derivative condition ($q_g \rightarrow 0$), the following equation was obtained.

$$q_{kf} = \left(\frac{(r_{kf} - r_g)}{(r_{kf} + r)_g} \frac{2g_c A_{an}^2 D_V}{K} \right)^{1/2} \tag{93}$$

The authors suppose that the zero derivative technique ensures that there is, at most, one intersection between the wellbore hydraulics performance and the reservoir performance curves for any kill rate greater than or equal to the zero derivative kill rate. Furthermore, if the zero derivative kill rate is less than the lower limit rate necessary to sustain the kill, then the lower limit rate is also sufficient to kill the well.

Dhafer A. Al-Shehri (1994)[11]

Al-Shehri[11] developed a dynamic kill computer program based on steady state system analysis for controlling surface blowouts of oil and gas. The model simulates multiphase flow with the aid of the Beggs and Brill correlation in blowout and relief wells, and predicts and links the expected reservoir performance with wellbore hydraulics. This can be used to design a kill operation by studying the

effects of various injection rates, injection location, and the type of kill fluid on the flow behavior of blowing wells. The model was successfully tested for an on - bottom dynamic kill with data from the Indonesia's Arun blowout. The calculated kill parameters agree very well with the values reported by Kouba[10] and Blount[7].

P. Oudeman, and D. Mason (1998)[12]

Oudeman et al[12] designed, executed and analyzed a full-scale field test to study how a dynamic kill proceeds in a high rate gas well. They utilized a producing well with 5.5" tubing and 1.75" coiled tubing with a down hole pressure gauge. Several tests were carried out at different flow conditions using the coiled tubing to inject a brine control fluid. After analyzing the test results, the authors proposed equations to predict the following kill parameters for a successful and efficient kill job.

Pump rate

The authors propose that six parameters determine the minimum rate to kill the well. These parameters are the flow resistance of the blowout well, reservoir pressure, surface pressure, depth of interception (between kill and formation fluid), kill fluid density and average well effluent density. Their equation to obtain the pump rate is given by.

$$q_{kf} = \frac{1}{R}\left[\frac{p_R - p_s}{2\sqrt{gL}} - r_g\sqrt{gL}\right]\frac{1}{r_{kf} - r_g} \tag{94}$$

Where q_{kf}, is the kill flow rate (m^3/s), R, represents the flow resistance (m^{-4}), p_R, reservoir pressure ($kg/m\text{-}s^2$), p_s, surface pressure ($kg/m\text{-}s^2$), g, gravitational acceleration (m/s^2), L, true vertical depth of intersection (m), r_g, average gas density between the flowing bottomhole conditions and surface conditions (kg/m^3), and r_{kf}, is kill fluid density (kg/m^3).

Oudeman et al[12] obtained excellent results with the homogeneous flow model. They observed that at the high flow rates encountered in the blowing well, slip between gas and liquid do not play an essential role, and refined multiphase flow models did not yield answers significantly different from homogeneous one.

Pump time

The authors' experience obtained during the field tests to study hydraulic well killing indicated that the well is killed once a sufficient volume of fluid has been pumped to create a column to balance the reservoir pressure. Hence, they proposed the following equation to calculate the kill time.

$$t_k = \frac{A(p_R - p_s)}{q_{kf}\, g r_{kf}} \tag{95}$$

Where, t_k, is the time to kill the well (s), and A represents the area of the blowout conduit (m^2). The authors pointed out that Equation (95) may not be applicable when the formation pressure has to be balanced partially by the friction pressure drop of the kill fluid.

Kill volume

Oudeman et al[12] suggested one extra well volume be pumped to sweep the well clean, therefore the required mud volume can be calculated by

$$V_{kf} = q_{kf} t_k + V_{well} \tag{96}$$

Where, V_{kf} , is the volume of the kill fluid and V_{well} is the volume of the well (m^3).

Michael Wessel, and Brian Tarr (1991)[13]

Wessel and Tarr[13] have developed a method specifically to control underground blowouts based on the dynamic kill concept. The procedure proposes a set of equations to determine the pump rate to stop the flow with either an infinite volume of kill mud or when the first kill mud reaches the fractured formation. The derivations assumed homogeneous multi-phase flow.

They also derived an equation to estimate the time and kill mud volume required for controlling the well for any given kill mud density/pump rate combination.

Pump rate for infinite volume

The authors defined this kill rate as the minimum injection rate that will ever stop the flow. It can be calculated by

$$q_{kf\infty} = J\left(p_F - p_R + \frac{2r_{kf}E}{r_g} - E\right) - 2\sqrt{\left(\frac{r_{kf}E}{r_g} + p_F - p_R\right)\left(\frac{r_{kf}E}{r_g} - E\right)} \tag{97}$$

Where: $$E = \frac{V_{an} r_g \cos f}{A_{an}} \tag{98}$$

The advantage of defining this rate is the possibility that it may be achieved with the rig equipment. However, an infinite or very large volume of kill fluid may be needed.

Pump rate for minimum volume

Wessel and Tarr determined that this is the kill rate required to control the well as soon as the first control fluid reaches the fractured formation.

$$q_{kfOH} = \frac{J\left(E + p_F - p_R\right)^2}{2\left(\frac{r_{kf}E}{r_g} + p_F - p_R\right)} \tag{99}$$

Here E is defined by Equation (98).

Injection rates given by Equation (99) are usually high. Those high flow rate requirements may not be achievable with available rig equipment, and additional pumping units would be required. However, any combination between Equations (97) and (99) would fulfill the requirements to kill the flow.

The authors also derived a method for determining the time and therefore the kill mud volume to stop the underground flow and kill the well. It was based in numerical integration of the equations that predict the rate of influx from the formation and bottomhole pressure. They suggest that an estimate of the total kill mud volume required is the volume pumped during the time required to stop formation flow plus one annular volume. Once a kill pump rate and mud weight are selected, these calculations can be made. The required mud volume should be built before beginning the kill in order to execute the kill procedure without interruptions.

Wessel and Tarr pointed out that the productivity index of a gas zone flowing underground is approximately proportional to the product of the formation's permeability and thickness. If this product is low, there is a good probability of stopping the flow with the available rig equipment, but the opportunity diminishes as formation productivity increases. Hence, by estimating the formation permeability and thickness for a potential zone to be drilled, you can determine whether an underground gas flow from the zone could be controlled with the available rig equipment or whether additional pumping units or relief well would be required.

Mathematical Model and Methodology for Steady-state Dynamic Kill Analysis

The inflow performance and wellbore hydraulics relationships will interact to determine the conditions at which the dynamic kill will be achieved. Hence, the following section will describe a computer program and present a procedure applying this concept to determine the required kill parameters for a surface gas blowout. The gas case was selected because about 90% of all blowouts involve gas. An underground blowout is analyzed with the same technique, except that the pressure at and depth of the subsurface loss zone replaces the atmospheric surface pressure in the analysis. The mathematical procedure was implemented in an Excel™ spreadsheet using macros. This section describes the analytical models used, the global solution scheme, the process used in applying the method, and an example application of the method to actual surface and underground blowouts. A more detailed description of this method is given in the Ph.D. dissertation by Vallejo[20].

Dynamic Kill Mathematical Model

The dynamic kill mathematical model involves two major components, the wellbore and the reservoir. These were coupled, since a variation of the flow conditions in the wellbore will inevitably cause a change in inflow from the reservoir. The link between these two sections was the face of the production zone.

The dynamic kill analysis considered four sections in the system, three in the wellbore and one in the reservoir. Figure 1 illustrates a typical off - bottom blowout with the four zones to model the different areas of interest in the system. Zone 1 represents the producing formation, which produces the uncontrolled flow of formation fluid toward the surface. Zone 2 is in the wellbore and represents the section of single-phase, formation fluid, flow from the bottom of the well to the injection string depth. Zone 3 is also in the wellbore and represents the two-phase flow generated by the formation fluid and the kill fluid flowing through the annular section, from the string depth up to

the surface once the pumping operations begin. Finally zone 4 contains the single-phase control fluid flow down through the kill string.

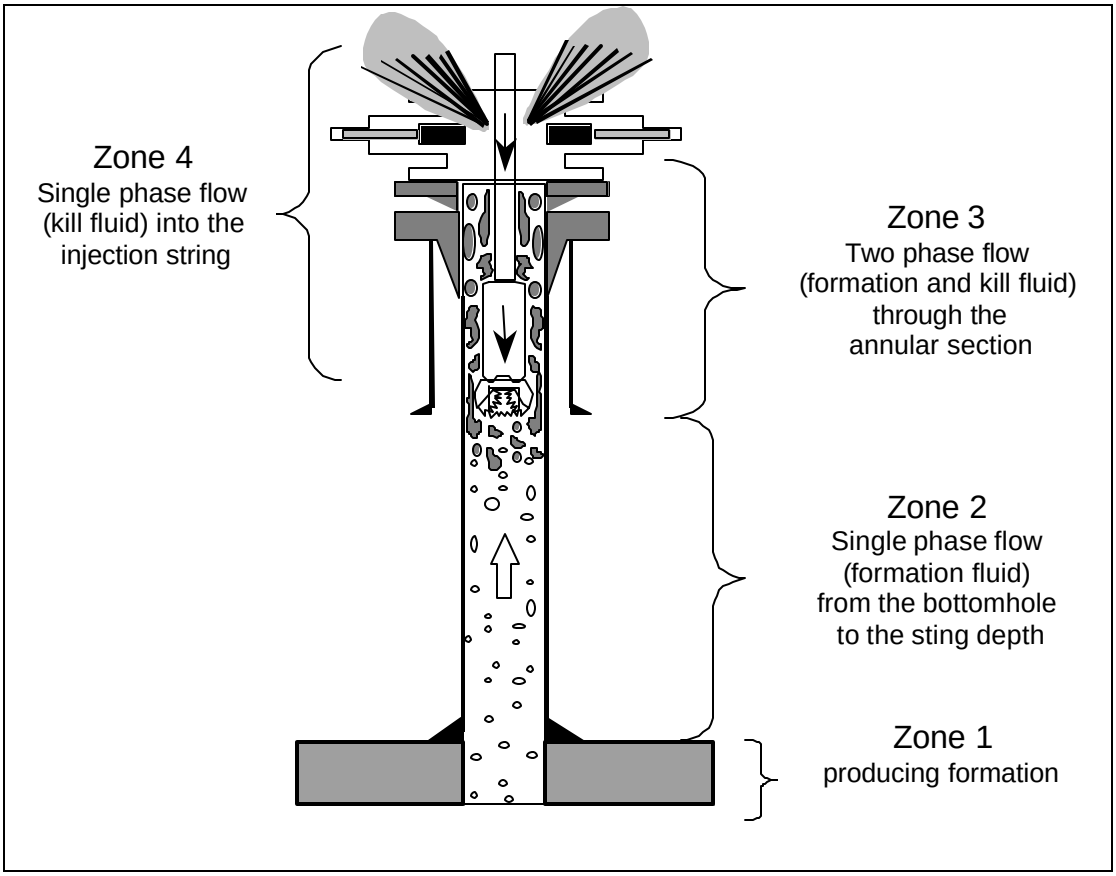

Figure 16 Interest zones to model the areas in the system

The mathematical model for each zone is explained in the following sections.

Model Assumptions

The following assumptions and considerations have been made in developing the dynamic kill model.

1. The flow system has one-dimensional spatial geometry along wellbore due to the limited cross sectional size compared with the axial wellbore length
2. The temperature gradient is constant and known
3. The formation fluid is single phase gas or liquid
4. The kill fluid has constant properties
5. Only single phase flow exists below the injection point until a dynamic kill is achieved
6. The injection rate of the kill fluid is constant
7. Flow rate of mud moving up annulus is constant and equal to the pump rate.
8. The producing formation is isotropic and the flow is radial

Wellbore Model

The wellbore model considers three zones, which were previously defined, see Figure 16. The equations employed to model the flow process in those zones are the conservation of linear momentum, conservation of mass, equation of state, gas velocity equation, and fluid and PVT property correlations. The conservation of linear momentum that is based on Newton's second Law of motion is given by

$$\frac{\partial}{\partial t}(rv)+\frac{\partial}{\partial L}(rv^2)=-\frac{\partial p}{\partial L}+\frac{frv^2}{2d}+rg \tag{100}$$

The Conservation of Mass is represented by

$$\frac{\partial}{\partial t}(r)+\frac{\partial}{\partial L}(rv)=0 \tag{101}$$

The combination of the above equations gives the well-known pressure gradient equation, given by

$$\left(\frac{dp}{dL}\right)_t=\left(\frac{dp}{dL}\right)_f+\left(\frac{dp}{dL}\right)_{el}+\left(\frac{dp}{dL}\right)_{acc} \tag{102}$$

The left-hand side term of Equation (102) is the total pressure gradient of the fluid in the interval studied. The first right-hand-side term accounts for frictional pressure losses due to the viscous shearing stress between the fluid and the wellbore/pipe wall and always causes a drop of pressure in direction of the flow. It is given in field units by

$$\left(\frac{dp}{dL}\right)_f=\frac{frv^2}{772.17d} \tag{103}$$

The second right-hand-side term accounts for the hydrostatic pressure of the fluid and acts in the direction of the gravitational field. It is given by

$$\left(\frac{dp}{dL}\right)_{el} = \frac{r}{144} \tag{104}$$

The third right-hand-side component accounts for pressure changes caused by fluid acceleration; a pressure drop occurs in the direction that the velocity increases. It is represented by

$$\left(\frac{dp}{dL}\right)_{acc} = \frac{r\Delta v^2}{9273.6\Delta L} \tag{105}$$

The friction pressure loss component represented by Equation (103) involves the calculation of the friction factor (f) which strongly depends on the rheological model of the fluid, i.e., whether the control fluid follows Newtonian or non-Newtonian behavior.

Newtonian Kill Fluids

Newtonian fluids such as water and brines are sometimes used in well control operations. The primary peculiarity of the Newtonian fluids is that the shear stress (t) is directly proportional to the shear rate ($\dot{g}$). The mathematical model is given by

$$t = m\dot{g} \tag{106}$$

where m is the constant of proportionality and is known as the viscosity of the fluid.

The friction factor in the friction term of the pressure gradient equation has not been analytically characterized except for laminar, single-phase flow. Hence it must be calculated by experimental work for turbulent flow. The friction factor is a function of both Reynolds number (N_{Re}) and relative roughness (e). The Moody friction factor (f, dimensionless), which is four times larger than the Fanning friction factor (f'), is adopted through this work.

$$f = 4f' \tag{107}$$

The procedure to evaluate the friction factor requires knowing whether the flow is laminar or turbulent. Laminar flow (considered to exist if the Reynolds number is less than 2,100) is calculated as follows:

$$f = \frac{64}{N_{\mathrm{Re}}} \tag{108}$$

$$f = \frac{64}{N_{\mathrm{Re}}} \tag{109}$$

Turbulent flow has no analytical representation, but several empirical equations have been proposed. In this work, the friction factor for non-Newtonian turbulent flow is calculated using the Serghides' equation. It is an explicit approximation to the Colebrook's correlation. Serghides' formula avoids the iterative solution and gives a maximum deviation of 0.0023%. It is given by

$$f = \left(A_7 - \frac{(A_8 - A_7)^2}{A_9 - 2A_8 + A_7} \right)^{-2} \tag{110}$$

where: $A_7 = -2\log\left(\frac{e/d}{3.7} + \frac{12}{N_{\mathrm{Re}}} \right)$

$$A_8 = -2\log\left(\frac{e/d}{3.7} + \frac{2.51A_7}{N_{\mathrm{Re}}} \right)$$

$$A_9 = -2\log\left(\frac{e/d}{3.7} + \frac{2.51A_8}{N_{\mathrm{Re}}} \right)$$

When the flow is through the annular section, d for essentially all of the equations used herein is computed using the equivalent circular diameter concept which is given by the slot approximation as

$$d_e = 0.816\left(d_2 - d_1\right) \tag{111}$$

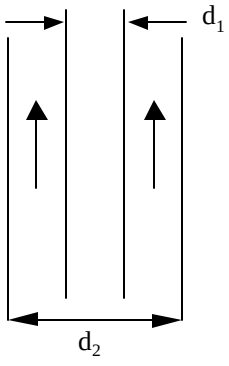

where:

d_e = Equivalent diameter (in).
d_1 = External diameter of injection pipe (in).
d_2 = Internal diameter of outer pipe or borehole (in).

Figure 17 Flow through annular section

The Reynolds number, N_{Re} (dimensionless), is defined by

$$N_{\mathrm{Re}} = \frac{124 r v d}{m} \tag{112}$$

The same equation can be used for flow through pipe or annulus, using d or d_e, respectively.

Non-Newtonian Kill Fluids

During well control operations, it is some times necessary to use a higher fluid density than water to control the well. Naturally this will depend on the productive zone properties. The only two ways to obtain those densities are by using either brines or drilling muds, but due to the cost and simplicity to prepare them in high densities, the most common kill fluids are muds. A complication is that those fluids have non-Newtonian behavior. That is, they do not exhibit a direct proportionality between shear stress and shear rate, making them more difficult to characterize. The non-Newtonian fluids used in drilling operations are pseudoplastic, fluids whose apparent viscosity decreases with increasing shear rate. The Bingham plastic and power law rheological models are most commonly utilized to represent a pseudoplastic behavior. In this work, the power law model is considered to best represent the non-Newtonian behavior of the kill fluid.

The power law fluids, like Newtonian fluids, will flow under any applied stress. However, as distinct from Newtonian fluids, the shear stress is not proportional to the shear rate, but to its nth power. It is defined by

$$t = K g^{n} \tag{113}$$

This model requires two parameters for fluid characterization. One of them is K, consistency index, and is indicative of the pumpability or overall thickness. The other parameter is n, flow behavior index, and it can be considered as a measure of the degree of deviation of a fluid from Newtonian behavior. For $n = 1$, the Equation 4.13 becomes the Newtonian fluid equation. The units of the consistency index (K) depend on the value of n. K has units of dyne-s^n/cm^2. In this work, a unit called equivalent centipoise, eq cp, will be used to represent 0.01 dyne-s^n/cm^2.

The determination of the flow behavior index (n) is computed with the following equations[1]:

$$n = 3.322 \log\left(\frac{q_{600}}{q_{300}}\right)$$

or

$$n = \frac{\log\left(\frac{q_{N_2}}{q_{N_1}}\right)}{\log\left(\frac{N_2}{N_1}\right)} \tag{114}$$

On the other hand, the consistency index is calculated as follows

$$K = \frac{510 q_{300}}{511^n}$$

or

$$K = \frac{510 q_N}{(1.703N)^n} \tag{115}$$

The dial readings used in these equations are measured with a standard Fann viscometer. For fully developed laminar flow, the friction losses can be predicted by the Metzner - Reed equations. For pipe it is given by

$$\frac{dp}{dL} = \frac{K\bar{v}^n}{144{,}000 d^{1+n}} \left(\frac{3+\frac{1}{n}}{0.0416}\right)^n \tag{116}$$

For the annulus the pressure loss gradient is given by

$$\frac{dp}{dL} = \frac{K\bar{v}^n}{144{,}000(d_2 - d_1)^{1+n}} \left(\frac{2+\frac{1}{n}}{0.0208}\right)^n \tag{117}$$

Where $\frac{dp}{dL}$ is the frictional pressure gradient when laminar flow is present.

The friction factor for turbulent non-Newtonian flow is calculated utilizing the Dodge and Metzner method. They suggested an implicit friction factor equation, which is calculated in an iterative procedure and is given by

$$\sqrt{\frac{1}{f'}} = \frac{4}{n^{0.75}} \log\left(N_{\mathrm{Re}} f'^{\left(1-\frac{n}{2}\right)}\right) - \frac{0.395}{n^{1.2}} \tag{118}$$

The Reynolds number is calculated utilizing the apparent Newtonian viscosity

$$N_{\mathrm{Re}_{M-R}} = \frac{124\,r\bar{v}d}{m_a} \tag{119}$$

Again the internal pipe or borehole diameter is used for pipe flow, and the equivalent diameter concept using Equation (111) is utilized for flow through annulus. The apparent viscosity (m_a) for flow through pipe is given by

$$m_a = \frac{Kd^{(1-n)}}{96\bar{v}^{(1-n)}}\left(\frac{3+\frac{1}{n}}{0.0416}\right) \tag{120}$$

On the other hand, the apparent viscosity for flow through annular section is computed by

$$m_a = \frac{K\left(d_2 - d_1\right)^{(1-n)}}{144\bar{v}^{(1-n)}}\left(\frac{2+\frac{1}{n}}{0.0208}\right) \tag{121}$$

A computer program can calculate the frictional pressure losses for both laminar and turbulent flow. Then, the larger value can be chosen as the correct one. This will avoid dependence on Reynolds number criteria.

Other parameters and fluid properties such as density, viscosity, and velocity are required to compute the friction factor and the total pressure gradient.

In - situ gas density is a function of pressure and temperature and will be calculated utilizing the real gas law, which is given by

$$r_g = 2.7g_g\frac{p}{zT} \tag{122}$$

Here g_g, is the specific gravity of the gas and is given by the ratio of the molecular weight of the gas ($\hat{M}_g$) to the molecular weight of dry air. It can be calculated by

$$g_g = \frac{\hat{M}_g}{28.96} \tag{123}$$

The gas compressibility factor (z) is computed using the Dranchuk & About - Kassem equation, which is a fitted equation of state to the data of Standing and Katz. It is given by the following equations.

$$z = 1 + \left(A_1 + \frac{A_2}{T_{pr}} + \frac{A_3}{T_{pr}^3} + \frac{A_4}{T_{pr}^4} + \frac{A_5}{T_{pr}^5} \right) r_r + \left(A_6 + \frac{A_7}{T_{pr}} + \frac{A_8}{T_{pr}^2} \right) r_r^2 - A_9 \left(\frac{A_7}{T_{pr}} + \frac{A_8}{T_{pr}^2} \right) r_r^5 + A_{10} \left(1 + A_{11} r_r^2\right) \left(\frac{r_{pr}^2}{T_{pr}^3} \right) EXP\left(- A_{11} r_r^2\right) \quad (124)$$

$$r_r = 0.27 \left[\frac{p_{pr}}{z T_{pr}} \right]$$

$$p_{pr} = \frac{p}{p_{pc}}$$

$$T_{pr} = \frac{T}{T_{pc}}$$

$$p_{pc} = 756.8 - 131 g_g - 3.6 g_g^2$$

$$T_{pc} = 169.2 + 349.5 g_g - 74 g_g^2$$

where the constants $A_1 - A_{11}$ are as follows:

$A_1 = 0.3265$	$A_5 = -0.05165$	$A_9 = 0.1056$
$A_2 = -1.0700$	$A_6 = 0.5475$	$A_{10} = 0.6124$
$A_3 = -0.5339$	$A_7 = -0.7361$	$A_{11} = 0.7210$
$A_4 = 0.01569$	$A_8 = 0.1874$	

The viscosity is utilized for determining the Reynolds number. In this work the in-situ gas viscosity (m) is calculated using the Carr, Kobayashi, and Burrows correlation. This correlation takes into account both fluid pressure and temperature for each calculation. It is given by

$$m_1 = \left(1.709 \times 10^{-5} - 2.062 \times 10^{-6} g_g\right) T + 8.188 \times 10^{-3} - 6.15 \times 10^{-3} \log g_g$$

The ratio of m / m_1 is evaluated from

$$\ln\left(\frac{m}{m_1} T_{pr} \right) = a_o + a_1 p_{pr} + a_2 p_{pr}^2 + a_3 p_{pr}^3 + T_{pr}\left(a_4 + a_5 p_{pr} + a_6 p_{pr}^2 + a_7 p_{pr}^3\right) + T_{pr}^2\left(a_8 + a_9 p_{pr} + a_{10} p_{pr}^2 + a_{11} p_{pr}^3\right) + T_{pr}^3\left(a_{12} + a_{13} p_{pr} + a_{14} p_{pr}^2 + a_{15} p_{pr}^3\right)$$

where the constants $a_0 - a_{15}$ are given by

$a_0 = -2.46211820\times10^{0}$ $a_6 = 2.60373020\times10^{-1}$ $a_{12} = 8.39387178\times10^{-2}$

$a_1 = 2.97054714\times10^{0}$ $a_7 = -1.04432413\times10^{-2}$ $a_{13} = -1.86408848\times10^{-1}$

$a_2 = -2.86264054\times10^{-1}$ $a_8 = -7.93385684\times10^{-1}$ $a_{14} = 2.03367881\times10^{-2}$

$a_3 = 8.05420522\times10^{-3}$ $a_9 = 1.39643306\times10^{0}$ $a_{15} = -6.09579263\times10^{-4}$

$a_4 = 2.80860949\times10^{0}$ $a_{10} = -1.49144925\times10^{-1}$

$a_5 = -3.49803305\times10^{0}$ $a_{11} = 4.41015512\times10^{-3}$

Finally the gas viscosity is obtained by:

$$m_g = \frac{m_1}{T_{pr}} \exp\left[\ln\left(\frac{m}{m_1} Tpr\right)\right] \tag{125}$$

The in-situ, single phase gas velocity (v_g), which is the same as the superficial gas velocity for a two-phase system is defined as

$$v_g = \frac{q_g}{A}$$

but:

$$q_g = q_{gscd} B_g \tag{126}$$

where B_g is the gas formation volume factor and is calculated from the gas real law as follows:

$$B_g = 0.02829 \frac{zT}{p} \tag{127}$$

Combining the above expressions and writing the superficial gas velocity in practical units:

$$v_g = 3.2743\times10^{-7} \frac{q_{gscd} zT}{pA} \tag{128}$$

Where A is the flow area, it can be pipe or annular.

Once the kill fluid reaches the injection point, there will be a mixture of the kill fluid and the formation fluid from the string depth to the surface. Therefore a two-phase flow model should be used for determining pressure losses.

Kouba[10] presented an analytical method that considers homogeneous flow for calculating the pumping requirements to achieve a dynamic kill. He concluded that the homogeneous model is very accurate at high flow rates. This has been proven accurate enough to characterize flow in the mist flow regime. Oudeman et al[12] designed, executed, and analyzed a full-scale field test to study how a dynamic kill proceeds in gas wells. They obtained excellent results with the homogeneous flow model, reportedly because at the high flow rates encountered in the blowing well, slip between gas and liquid do not play an essential role, and the refined multiphase flow models did not yield answers essentially different from the homogeneous model.

This dynamic kill model was also built considering homogeneous flow. The homogeneous flow pattern was adopted because it gives reliable results in high flow rates, which are present during this process. Therefore, the pressure gradient equation (102) for a two-phase flow mixture becomes

$$\left(\frac{dp}{dL}\right)_t = \frac{f r_m v_m^2}{772.17 d} + \frac{r_m}{144} + \frac{r_m \Delta v_m^2}{9273.6 \Delta L} \tag{129}$$

where r_m, is the mixture density, which can be calculated as

$$r_m = r_{kf}\, l + r_g a \tag{130}$$

The volumetric fraction of the control liquid (l) also called liquid holdup, is defined as the ratio of the volume occupied by the liquid component of the total volume, and for homogeneous flow, is given by

$$l = \frac{8085.6 q_{kf}}{8085.6 q_{kf} + q_g} \tag{131}$$

Here q_g is at in-situ conditions and is defined by equation (126). The formation fluid would occupy the remainder of the pipe segment, and for gas wells it is referred to as gas void fraction or gas holdup. It is obtained by

$$a = 1 - l \tag{132}$$

The term, v_m, in equation (129) is the mixture velocity, which is defined as the sum of superficial velocities of both fluid components. It can be estimated by

$$v_m = v_{kf} + v_g = \frac{1}{86,400}\left(\frac{q_g + 8085.6 q_{kf}}{A}\right) \tag{133}$$

The in-situ, superficial gas velocity (v_g) is given by Equation (128) and the superficial kill fluid velocity (v_{kf}) can be calculated by

$$\bar{v}_{kf} = \frac{17.16 q_{kf}}{d^2} \tag{134}$$

The Reynolds number of the mixture is given by

$$N_{\mathrm{Re}} = \frac{124 r_m v_m d}{m_m} \tag{135}$$

where m_m is the mixture viscosity which can be computed by

$$m_m = m_{kf}\, l + m_g a \tag{136}$$

Again, the internal pipe or borehole diameter is used for pipe flow, and the equivalent diameter concept in equation (111) is utilized for flow through annulus. The in-situ gas viscosity is given by equation (125).

Reservoir Model

Another major section that is involved in the dynamic kill model is the reservoir, shown as zone 1 in figure 17. As the conditions change in the wellbore, the producing zone will inevitably respond. In well control operations, the desired response is a decrease in the formation fluid influx rate. Therefore, a reservoir model should be coupled to the wellbore.

The reservoir model is based on the well-known Darcy's law, which is a mathematical relationship between formation flow rate and pressure drop in the reservoir. It states that the velocity of a fluid in a porous medium is proportional to the driving pressure and inversely proportional to the fluid viscosity.

For gas blowouts where the flow in the vicinity of the wellbore occurs at higher velocities, an additional pressure drop in the system takes place due to convective acceleration of the fluid passing through the pore space. Therefore, a non-Darcy term is taken into account. Under these circumstances, the appropriate flow model is the Forchheimer's equation, which is given by

$$p_R^2 - p_{bh}^2 = X q_{gscd} + Y q_{gscd}^2 \tag{137}$$

In the above equation (X) is the Darcy component or pressure drop due to laminar flow, and it is given by

$$X = \frac{1.422 m_g z_R T_R}{kh}\left[\ln\left(0.472\frac{r_e}{r_w}\right)\right] \tag{138}$$

On the other hand, the term (Y) is the non-Darcy flow component or pressure drop due to turbulence of the gas around the wellbore. It is mathematically represented by

$$Y = \frac{3.16\times10^{-18} b g_g z_R T_R}{h^2}\left(\frac{1}{r_w} - \frac{1}{r_e}\right) \tag{139}$$

Where b is the coefficient of inertial resistance, also called the turbulence factor, and is determined from an experimental relationship. The turbulence factor depends on formation permeability and it is given by

$$b = \frac{10^7}{\sqrt{k}} \qquad \text{for} \qquad k \geq 5{,}000 md \tag{140}$$

and

$$b = \frac{3.55\times10^{10}}{k^{1.35}} \qquad \text{for} \qquad k \leq 5{,}000 md \tag{141}$$

The gas formation properties in equations (138) and (139) are calculated at reservoir conditions.

Solving the quadratic equation, equation (137), it is possible to compute the deliverability potential of the reservoir as a function of differential pressure between the face formation and the producing formation limits.

$$q_{gscd} = \frac{-X + \sqrt{X^2 + 4Y\left(p_R^2 - p_{bh}^2\right)}}{2Y} \tag{142}$$

It can be seen in equation (142) that the gas flow rate is a function of the difference between reservoir pressure and bottomhole pressure, formation properties, formation fluid properties, and flow turbulence.

Formation Fluid Rate Determination

The formation fluid flow rate is estimated initially when the well has been completely unloaded of all the drilling mud and free flowing equilibrium conditions have been reached. That is, only formation fluid is flowing in the system from the reservoir to atmosphere. Under this situation, the mathematical relationship between the wellbore and the producing zone yields the maximum

formation flow rate that is possible given the well geometry. These conditions are considered as the initial conditions of the well control procedure.

The formation fluid flow rate depends on two important components, the reservoir inflow performance (IPR) and the wellbore hydraulics performance (WHP), also called inflow and outflow performance, respectively.

The IPR is the relationship between the production rate from the reservoir and bottomhole pressure and is a measure of the formation's capacity to produce to the wellbore. In this work, the IPR will be estimated by solving equation (137) for the bottomhole pressure, in the form shown as equation (143)

$$p_{bh}^2 = p_R^2 - \frac{1.422 m_g z_R T_R}{kh}\left[\ln\left(0.472\frac{r_e}{r_w}\right)\right] q_{gscd} - \frac{3.16\times10^{-18} b g_g z_R T_R}{h^2}\left(\frac{1}{r_w}-\frac{1}{r_e}\right) q_{gscd}^2 \tag{143}$$

The formation fluid properties such as the gas deviation factor (z_R) and gas viscosity (m_g) are calculated with equations (124) and (125), respectively. Then several gas flow rates are assumed and the bottomhole pressure is calculated for each specific rate employing equation (143). The resulting reservoir inflow performance curve is plotted on a graph of gas flow rate versus bottomhole pressure.

On the other hand, the WHP is the relationship between the production rate and the bottomhole pressure generated by that rate flowing to the surface through the wellbore. In this work, the WHP at the initial conditions with only gas flowing in the system will be calculated utilizing the Cullender and Smith equation, which is given by

$$\frac{1{,}000 g_g L}{53.356} = \int_{p_{bh}}^{p_s} \frac{\left(\frac{p}{Tz}\right)}{\frac{0.667 f q_{gscd}}{d^5} + \frac{1}{1{,}000}\frac{H}{L}\left(\frac{p}{Tz}\right)^2}\, dp \tag{144}$$

This is a widely used method to calculate flowing bottomhole pressure in gas wells. The Cullender and Smith method makes no simplifying assumptions for the variation of temperature and gas deviation factor in the wellbore. Equation (144) can be solved applying the trapezoidal rule for numerical integration.

When gas flow is through an annular section, the following equation for the diameter is used in equation (144):

$$d^5 = 0.816(d_2 - d_1)\left(d_2^2 - d_1^2\right)^2 \tag{145}$$

where d_2 and d_1 are schematically shown in figure 17.

The friction factor (f) and gas deviation factor (z) are calculated with equations (110) and (124) respectively. Again several gas flow rates are assumed, and the bottomhole pressure is calculated for each specific rate, employing equation (144). The resulted wellbore hydraulics performance curve is superimposed on the same graph as the IPR curve.

The simultaneous solution of the reservoir inflow performance and wellbore hydraulics performance is given at the intersection point between the curves generated by those equations (143) and (144), representing the natural flow point for that system. Thus, the conditions at that intersection point yield both the formation fluid flow rate and the flowing bottomhole pressure when only formation fluid is flowing through the wellbore.

Figure 18 displays a typical relationship between the IPR and the WHP. It can be seen that the intersection point is the natural flow point of the well and gives both the bottomhole pressure and the formation fluid flow rate when only formation fluid is flowing.

Once the gas flow rate is known, it is employed in equation (144), and the pressure profile in the system from the bottom to the surface is estimated.

Global Solution Scheme

The wellbore model and the reservoir model were coupled at the sand face to obtain a global solution as a basis for computing the flow conditions in the wellbore during the control process as a function of axial position at selected times. The solution scheme for applying the dynamic kill mathematical model utilizes a series of fully steady states solutions assuming that a given steady state flow condition exists for the time required for the mixture creating those conditions to reach the surface. By employing this approach, the approximate effect of time can be included in the process. As a consequence, the kill fluid volume required to reach the dynamic kill can be estimated. While much less accurate than the time-dependent model described in the previous chapter, this approach has the advantages of simplicity and being implemented in a common spreadsheet.

The solutions using this scheme predict the pressure behavior at any point in the wellbore and in the injection string as a function of spatial location along the flow path at selected times. The solution requires the specification of initial and boundary conditions to solve the flow equations.

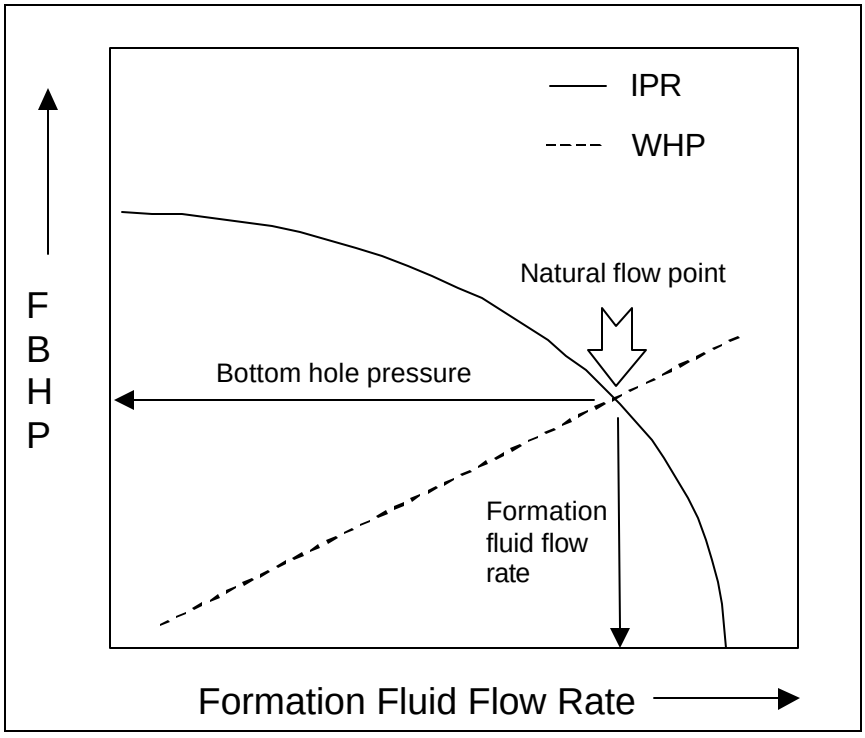

Figure 18 Formation fluid rate and bottomhole flowing pressure determination

Initial Conditions

The initial conditions are determined when the formation fluid has completely unloaded the well of all the drilling fluid. Under this circumstance, only formation fluid is flowing in the system, and the equilibrium conditions have been reached. At this point, the formation flow rate and pressure profile from the surface to the bottom of the well are calculated in the system as described in the previous section. Thus it is assumed that the blowout well has been flowing at a constant rate for a period of time such that steady state flow has been achieved inside the wellbore before and at the instant that the killing operation starts.

The wellbore is discretized into cells or grids of equal length along the length of the well. Hence, knowing the formation fluid flow rate, flowing bottom hole pressure, surface pressure, geothermal temperature gradient, and cell length, the initial conditions along the wellbore can be estimated.

The initial distribution of density, viscosity, flow rate, velocity, and pressure gradient along the axial position can be computed utilizing equations (122), (125), (126), (128), and (102), respectively, and a pressure traverse procedure as discussed in the next section. The process of calculating the initial distribution of conditions is schematically presented in Figure 19.

The pressure traverse procedure is applied at each cell and marching downward until reaching the bottom of the well. The velocity is corrected for changes in cross sectional area.

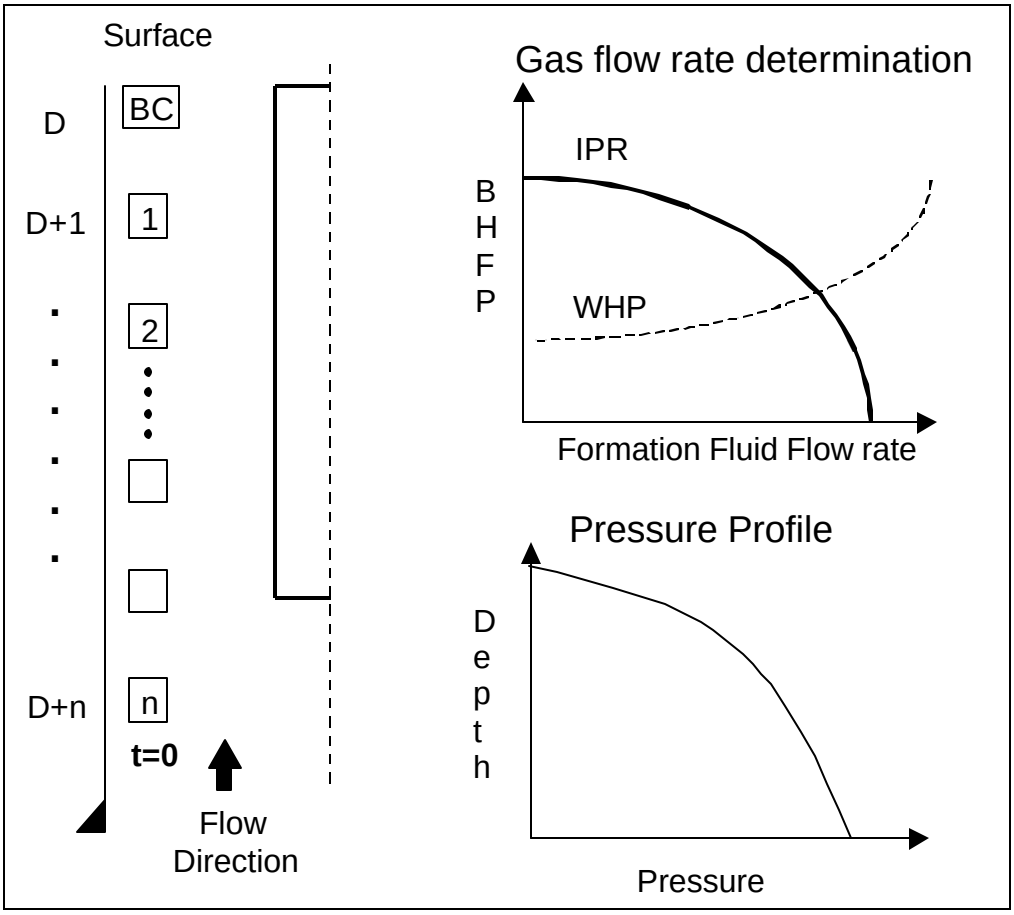

Figure 19 Determination of the initial conditions

Boundary Conditions

With a surface blowout in progress, it is assumed that the pressure and temperature conditions at the surface are known. So one known boundary condition is at the surface during the entire dynamic kill process. For the case of an underground blowout, the pressure, temperature, and depth of the subsurface loss zone can be specified. Another boundary is at the bottom of the well, where the wellbore is connected with the producing formation with known fluid properties and rock properties. Therefore, after the kill begins and a new bottomhole pressure is obtained by applying the pressure traverse procedure started at the surface or the subsurface loss zone, the reservoir mathematical model can be used to give a new formation fluid rate. This will be utilized to obtain the new distribution of densities, viscosities, velocities, flow rates, fluid fractions, and pressure gradient for a given time step.

The global solution procedure to describe the dynamic kill process is as follows. After the formation fluid rate and the pressure profile in the system have been computed, the initial fluid flow conditions throughout the wellbore are calculated, as described in the initial conditions section, utilizing the surface or loss zone boundary condition. Then, the control operations begin by pumping a control fluid of a given density and with constant properties at a given rate downward through the injection string.

The calculation procedure starts when the kill fluid is at the injection depth, that is just after the first droplet of liquid leaves the injection string and flows into the annulus. However, the time to fill the injection string is considered in the process. Therefore, the predictions of pressures while establishing a dynamic kill begin at the time required to fill the drillstring. Time zero or time at zero seconds is when the pumping operations just begin and the kill fluid is pumped into the injection string at the surface.

The dynamic kill model performs an approximate calculation of the time between steady-state conditions based on the mixture velocity. That is, if we know the cell length and the mixture velocity the program calculates the time required to travel from one cell to other. This procedure is performed at each cell until the kill fluid fills completely the annular section. The program then sums these times to obtain an estimate of the time required for fluids to reach the surface after a change in fluid input rates at the injection point.

For the case of a blowout up the annulus, the calculation procedure starts at the surface of the annular section considering the initial formation fluid rate and the kill fluid rate, expressed at standard conditions, as constant and equal in each cell. Then the pressure traverse for each cell is applied downward, using the wellbore mathematical model given in the earlier section, until it reaches the bottomhole. The fluid flow conditions along the wellbore and the bottomhole pressure can be determined for a specific time step. With the new bottomhole pressure, a new formation fluid rate is calculated utilizing the reservoir model as the boundary condition equation. Employing the new formation fluid rate, and the kill rate, the whole procedure is repeated to obtain the flow conditions, pressure gradient, and a formation fluid rate for a new time step. This process is schematically presented in figure 20.

Another flow condition is given for the injection string since single-phase kill fluid is flowing downward through it after the control starts. The pressure condition in the tubing and at the surface is obtained utilizing the pressure at the injection depth as a starting point. Then the upward pressure traverse calculation for single-phase flow is applied until reaching the surface. This procedure is also repeated for each time step.

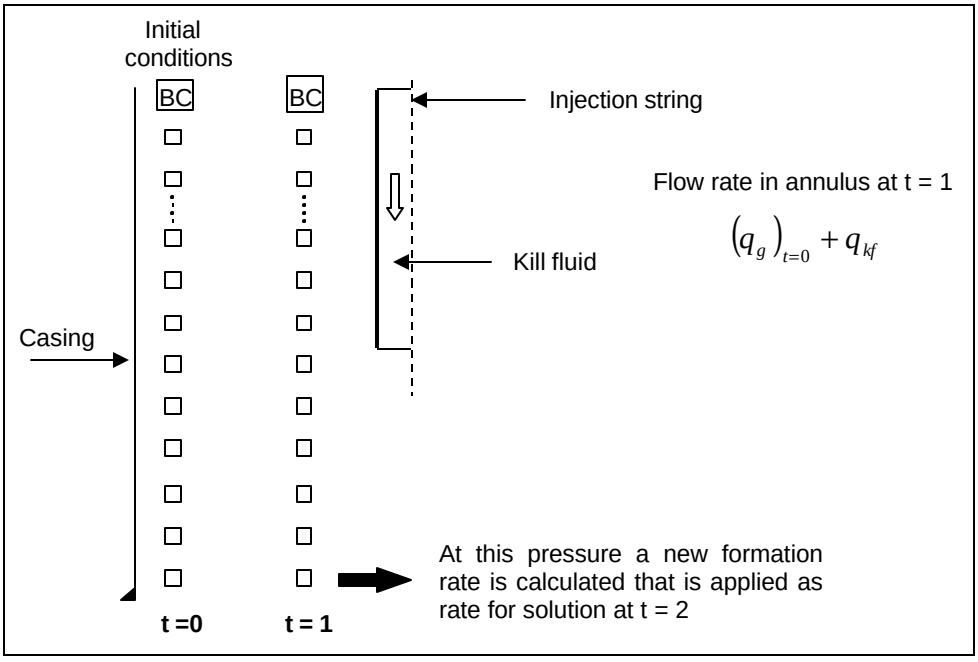

Figure 20 Wellbore conditions after the first time step is taken

Pressure Traverse Calculation

The pressure traverse calculation for a two-phase flow is a procedure that calculates the pressure gradient along the wellbore. It employs the pressure gradient equation for a two-phase flow mixture, equation (129), as well as the multi-phase flow properties given from equations (130) through (136).

The procedure is started at the top after applying the boundary conditions and marches downward over small length increments, considering the pipe geometry changes, until the bottom of the well is reached. The mixture properties are evaluated at average pressure and temperature in small increments. Then the pressure gradient is iteratively computed for each cell until a tolerance value of 0.00001 psi on the upstream pressure is attained. The following procedure explains the pressure traverse calculation to obtain the pressure gradient along the wellbore. The procedure is also shown as a flow chart in figure 21.

1. Taking the surface as starting point (L_0), compute fluid properties at surface conditions and select a length increment (ΔL).

2. Estimate the temperature increment (ΔT) corresponding to the length increment (ΔL).

3. Compute the pressure increment (Δp_0) corresponding to the length increment (ΔL) using the pressure gradient equation (129) and flow properties calculated in step 1.

4. Find the average temperature and pressure in the increment.

5. Calculate the fluid and PVT properties at the average temperature and pressure computed in step 4.

6. Compute the pressure gradient ($\Delta p / \Delta L$) in the increment utilizing the fluid and PVT properties obtained at average temperature and pressure determined in step 5 and the pressure gradient equation (129).

7. Find the pressure increment corresponding to the selected length increment, $\Delta p_1 = \Delta L(\Delta p / \Delta L)$.

8. Compare the estimated (Δp_0) and calculated (Δp_1) pressure values obtained in step 3 and 7. If they do not meet the given tolerance, consider Δp_1 as the new pressure estimate for Δp_0 and go to step 4. Repeat steps 4 through 8 until the tolerance value is attained.

9. Repeat the procedure from step 2, using $p_{i+1} = p_i + \Delta p_1$ as pressure at top of new (ΔL) until the sum of ΔL equals the total length of the well.

The length increment (ΔL) is obtained as follows. The program considers a total length of equal well geometry, i.e. with the same wellbore or casing size and same drill pipe or drill collar size, and then it is divided by the number of cells assigned by that section. This is done with the idea to always have the change in geometry at the boundary between two cells. In addition by utilizing this criteria, interpolation is not required in the last step since the computer program selects the sum of the increments equal to the total depth. Refer to figure 21 for a flow diagram of the entire process.

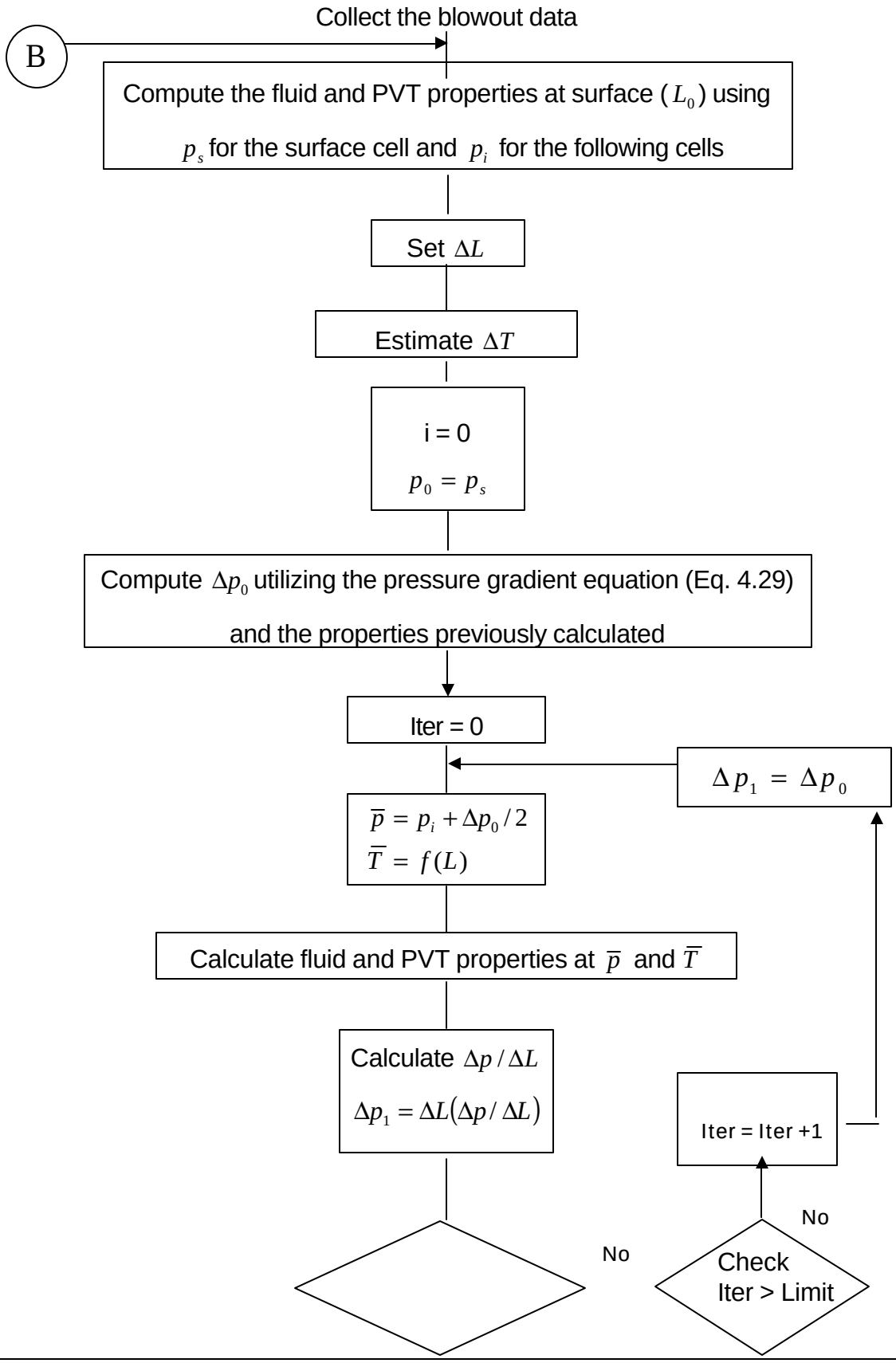
B
Collect the blowout data
Compute the fluid and PVT properties at surface (L_0) using
p_s for the surface cell and p_i for the following cells
Set ΔL
Estimate ΔT
i = 0
$p_0 = p_s$
Compute Δp_0 utilizing the pressure gradient equation (Eq. 4.29)
and the properties previously calculated
Iter = 0
$\Delta p_1 = \Delta p_0$
$\overline{p} = p_i + \Delta p_0 / 2$
$\overline{T} = f(L)$
Calculate fluid and PVT properties at $\overline{p}$ and $\overline{T}$
Calculate $\Delta p / \Delta L$
$\Delta p_1 = \Delta L(\Delta p / \Delta L)$
Iter = Iter +1
No
Check
Iter > Limit
No

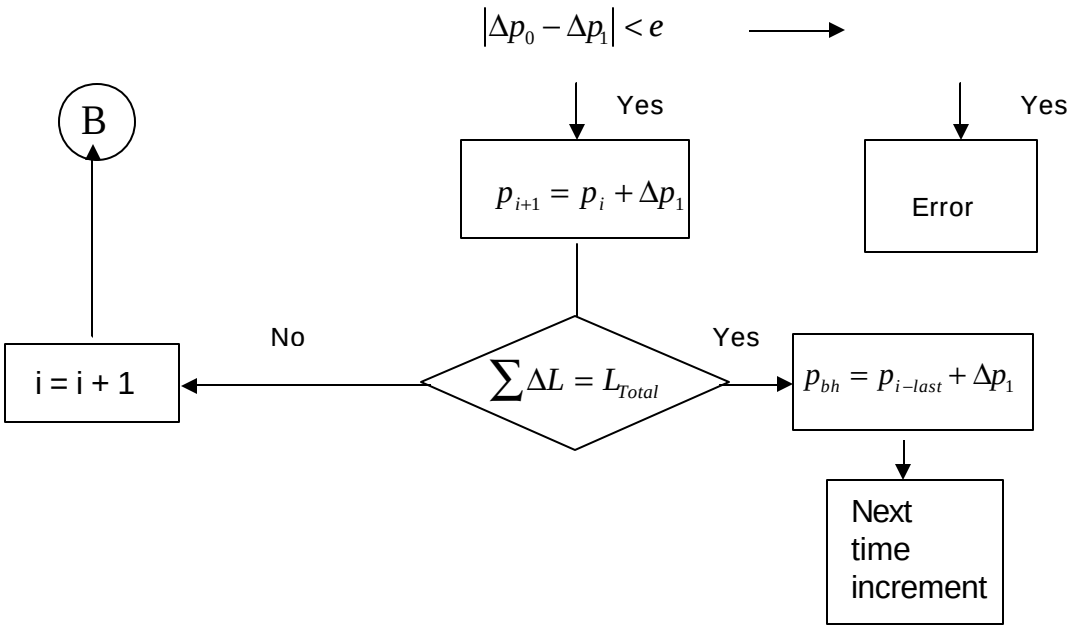

Figure 21 Marching algorithm for calculating a pressure traverse

Stepwise Procedure for Applying the Model

The required dynamic kill parameters for a surface or underground blowout include the following,

1. Gas flow rate under blowout conditions
2. Pressure profile in the system under blowout conditions
3. Kill fluid density
4. Kill fluid injection rate
5. Pressure profile in the system at the beginning of the control and after formation fluid influx stops
6. Surface pump pressure
7. Hydraulic horsepower required from pumps

The required steps to design and compute the above kill parameters utilizing the steady state system analysis approach are the following. These steps are all included in the calculations performed and plots created by the Excel™ spreadsheets, Surface Dynamic Kill.xls and Underground Dynamic Kill.xls, see Appendices B and C, that were used to implement the program described in the previous sections.

1. Compute the inflow performance relationship (IPR) for the reservoir and plot it as function of flowing bottom hole pressure versus gas flow rate. Determination of the inflow performance needs a connection between formation fluid flow rate and the sand face pressure. That relationship is given by the reservoir model, equation (143). The IPR is built assuming different gas flow rates and solving the equation for the bottomhole flowing pressure.

2. Compute the wellbore hydraulics performance curve and plot it as function of flowing bottom hole pressure versus gas flow rate superimposed on the plot of the IPR. Again determining the

wellbore performance requires a relationship between formation fluid flow rate and the bottom hole pressure, which is given by the Cullender and Smith model, equation (144). The wellbore hydraulic performance is completed assuming different gas flow rates and solving the equation at the sand face. Figure 18 displays a typical behavior of the system analysis. The IPR curve shows the performance of the reservoir, and the WHP curve represents the performance of the wellbore when flowing only gas, in other words the pressures required to move the resulting rates of gas through the wellbore system to the atmosphere or the subsurface loss zone.

3. Determine the gas flow rate under blowout conditions, which is given by the intersection of the inflow performance curve "IPR" and the wellbore hydraulics performance curve "WHP" on figure 18. This situation indicates that the well has been completely unloaded of all liquid, except any that is flowing from the formation, and a free flowing equilibrium condition has been reached.

4. Plot the pressure profile in the well under blowout conditions utilizing the gas flow rate obtained in the previous step and equation (144). This equation is solved for small depth increments in the wellbore.

5. Compute the wellbore hydraulics performance curve for each of various kill fluid injection rates with one selected kill fluid density in combination with a range of gas flow rates up to blowout flow rate, then plot them on the graph accomplished in step 2. These curves are calculated taking into account pressure changes due to elevation, friction, and acceleration of the mixture. They are obtained utilizing equation (129) and the respective fluid property correlations given earlier in this chapter. Figure 22 illustrates the wellbore hydraulics performance curves for different injection rates. Analyzing one of these lines, it can be seen that as the gas flow rate increases from zero, the bottom hole pressure typically decreases due to reduction in hydrostatic pressure. This portion of the curve shown as a dashed line is referred to as being hydrostatically dominated. On the other hand, further increases in the gas flow rate eventually increase the bottom hole pressure due to increasing frictional pressure losses. Consequently, this segment of the curve shown as a solid line is known as friction dominated.

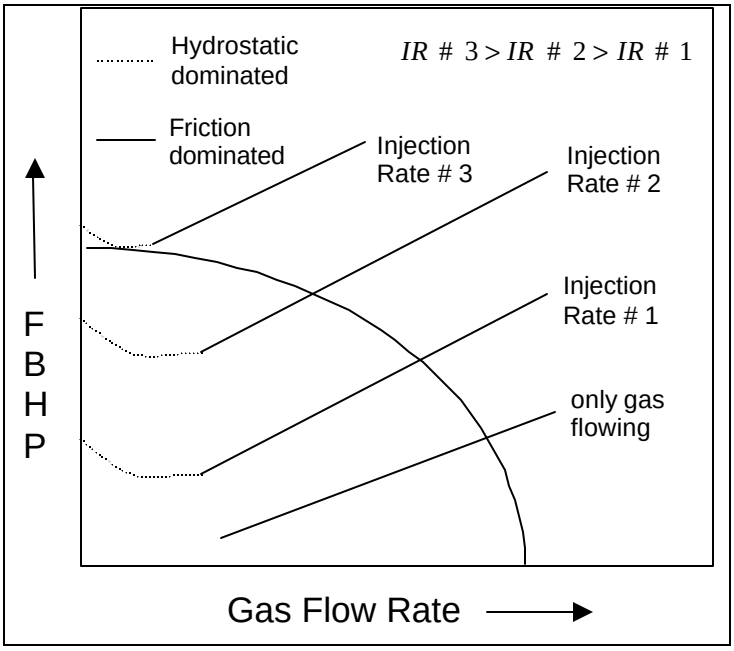

Figure 22 Wellbore hydraulics performance for various kill fluid injection rates

6. Select the kill injection rate from the plot as the line of constant injection rate, which is just above or tangent to the inflow performance relationship curve. Therefore, injection rate #3 on Figure 22 is the lowest rate that will achieve a kill. At that kill fluid rate, a stable gas lift flow condition would not be possible, and the well would be killed. On the other hand, if the wellbore hydraulics performance intersects the reservoir performance curve, as for injection rate #2, then a stable flow condition would result. That is, the reservoir would continue to produce at the rate corresponding to the point of intersection, and the well would not be killed.

7. If the selected kill injection rate is too high to handle with the available pumping equipment, repeat steps 5 and 6 with a higher kill density. Otherwise, proceed with step 8.

8. Plot the pressure profile in the system as a function of depth for the selected kill injection rate and density. This will give a good approximation of the pressure conditions in the wellbore just after the formation fluid influx stops. Hence those pressures can be compared with the burst ratings of the wellbore tubulars, and with the fracture pressure in any open hole interval for a surface blowout.

9. Estimate the frictional pressure losses and the hydrostatic pressure in the injection string utilizing equation (129) substituting kill fluid density for mixture density and basing mixture velocity on kill fluid rate using equation (134).

10. Calculate the surface injection pressure by summing the pressure losses in the injection string from step 9 with the injection pressure at the end of the injection string from step 8.

11. Determine the hydraulic horsepower requirement using the surface injection pressure and rate.

This procedure is also shown in the flow chart in figure 23, which shows the algorithm utilized to estimate the kill parameters.

A dynamic kill computer program following the previous procedure was created to accomplish the analysis. The program and its application to actual surface and underground blowouts are described in Chapter 5.

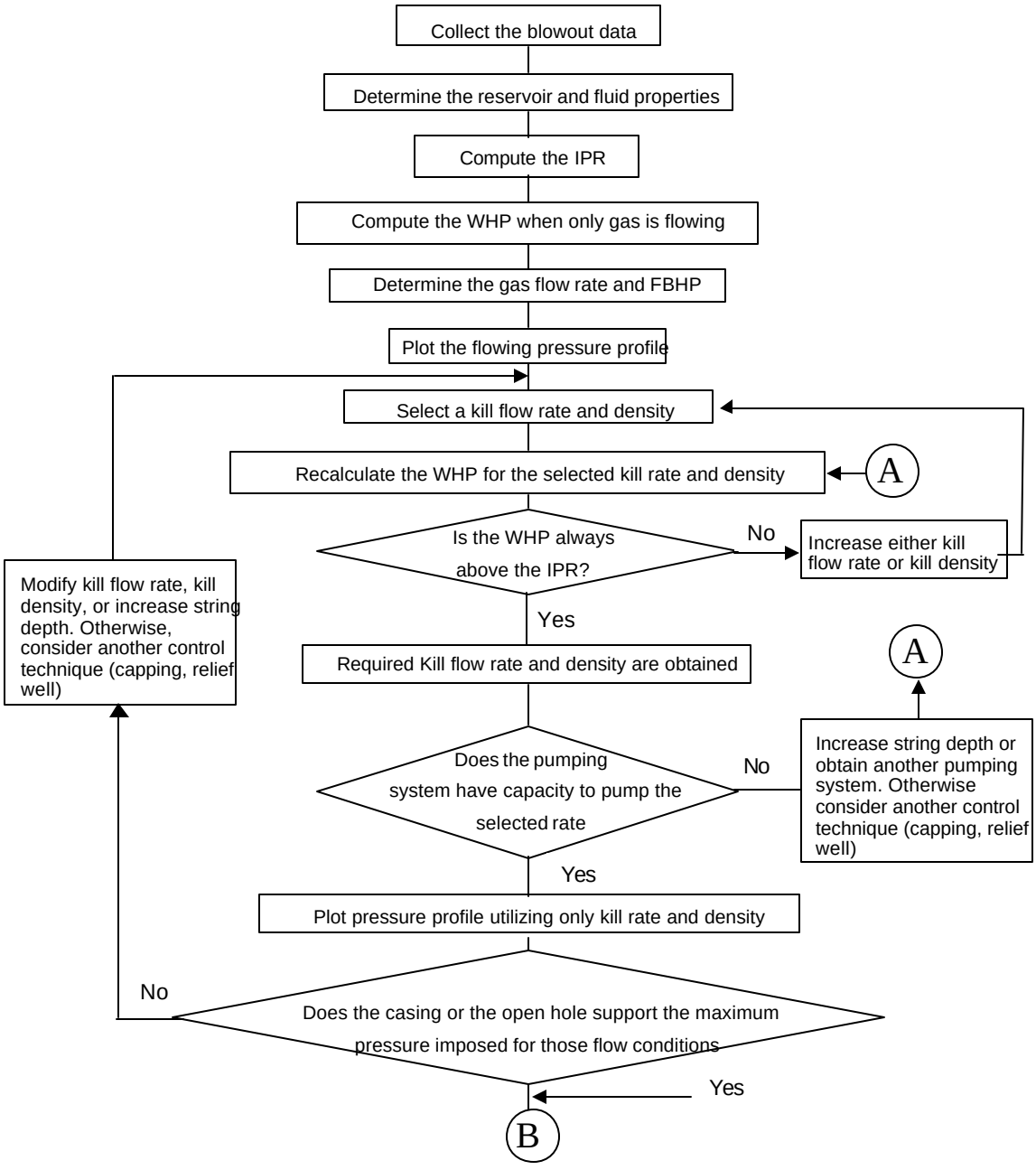

Figure 23 Algorithm to estimate the dynamic kill parameters (continued next page)

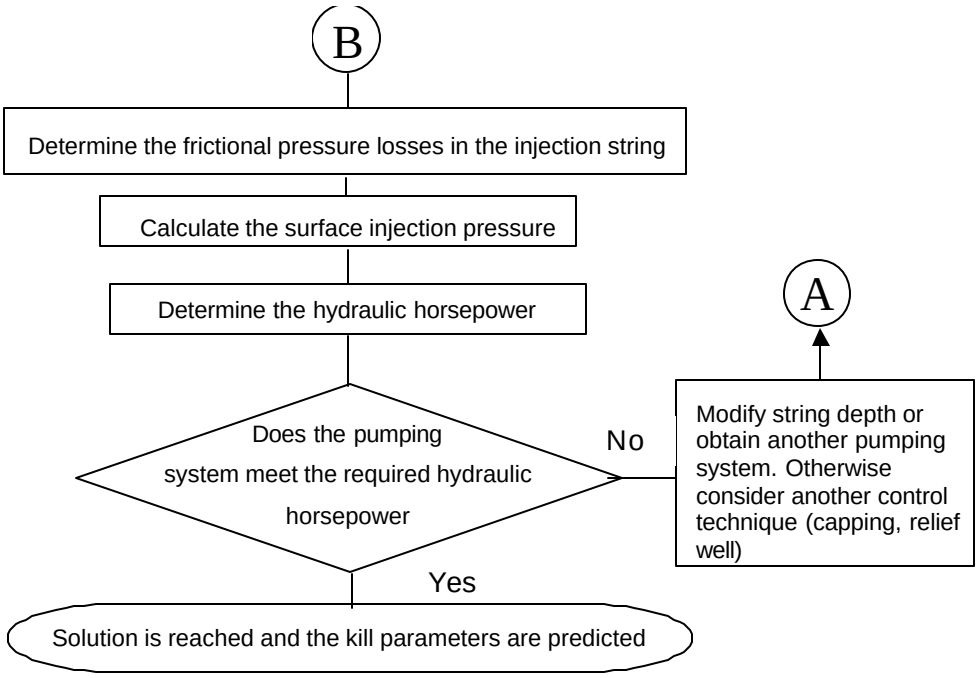

Figure 23 Algorithm to estimate the dynamic kill parameters

Conclusions

Steady-state models for both single and multi-phase flow are available to predict pressure versus rate behavior for both pipe and annulus flow. These models have been adapted by multiple authors as a basis for design and analysis of dynamic kills. The models have been used as the basis for the Excel™ spreadsheets to design and analyze dynamic kills for both surface and underground blowouts that are included in this report.

Nomenclature

A	=	area of flow, ft^2
B_g	=	gas volume factor, ft^3/scf
c_g	=	compressibility of the gas, psi^{-1}
c_r	=	reduced isothermal compressibility, dimensionless
c_t	=	total compressibility, psi^{-1}
D_V	=	vertical depth, ft
d	=	diameter of the pipe, in
d_1	=	outer diameter of the pipe, in
d_2	=	inner diameter of the pipe or borehole, in
d_e	=	equivalent diameter, in

d_{erw} = diameter of the relief well, in

d_h = hydraulic diameter, in

d_i = diameter of the pipe, ft

f = Moody friction factor, dimensionless

f' = Fanning friction factor, dimensionless

g = gravity acceleration, ft/sec^2

g_c = conversion factor 32.2 lbm-ft/lbf-sec^2

HHP = hydraulic horse power, hp

h = net pay thickness, ft

i_{kf} = injection flow rate, ft^3/sec

J = productivity index, gal/min-psi

K = consistency index of the fluid, eq cp

k = effective formation permeability, md

L = section length, ft

M_a = molecular weight of air, 28.96

$\hat{M}_g$ = molecular weight of gas

N = speed of the rotational viscometer, rpm

N_{Re} = Reynolds number, dimensionless

n = flow behavior index, dimensionless

p = pressure, psia

p_{bh} = bottomhole pressure, psi

p_F = formation fracture pressure, psi

p_f = frictional pressure losses, psi

p_h = hydrostatic pressure, psi

p_i = pressure at the top of the cell, psi

p_{i-last} = pressure at the top of the last cell, psi

p_n = pressure at interest depth, psia

p_{pc} = pseudo critical pressure, psia

p_{pr} = pseudo reduced pressure, dimensionless

p_R = reservoir pressure, psi

p_s = surface pressure, psi

p_{sd} = pressure at the injection string depth (kill fluid - formation gas), psi

p_{wf} = bottomhole flowing pressure, psi

$p(0)$ = bottomhole pressure at time 0, psi

$p(t)$ = bottomhole pressure at time t, psi

dp/dL = pressure gradient, psi/ft

q_g	=	in-situ gas flow rate, ft^3/day
q_{gsc}	=	gas flow rate at standard conditions, scf/sec
q_{gscd}	=	gas flow rate at standard conditions, scf/day
q_{kf}	=	kill flow rate, bpm
q_{kfOH}	=	kill rate for minimum volume, gpm
$q_{kf\infty}$	=	kill rate for infinity kill volume, gpm
q_{rw}	=	kill flow rate on the relief well, bpm
R	=	universal gas constant, 10.732 psia-ft^3/lbm-^oR
R_f	=	ratio of frictional drag, dimensionless
r_e	=	drainage radius, ft
r_w	=	wellbore radius, ft
T	=	temperature, ^oR
T_n	=	temperature at interest depth, ^oR
T_{pc}	=	pseudo critical temperature, ^oR
T_{pr}	=	pseudo reduced temperature, dimensionless
t	=	time, hr
t_k	=	kill time, sec
V_{an}	=	annular volume, gal
V_g	=	volume of gas flowing in an open formation, Mscf
V_{kf}	=	volume of kill fluid pumped into the well, ft^3
V_i	=	well volume, ft^3
v	=	velocity of the fluid, ft/sec
v_c	=	average velocity of the gas continuous phase, ft/sec
v_{kf}	=	velocity of the kill fluid, ft/sec
v_m	=	velocity of the mixture, ft/sec
W_s	=	weight of drillstring in air, lb
$z_{\overline{p}}$	=	gas compressibility factor at average pressure, dimensionless
z_n	=	gas compressibility factor at interest depth, dimensionless
z	=	gas compressibility factor, dimensionless

Greek Letters

a	=	fraction of the gas, fraction
b	=	turbulence factor, 1/ft
ΔL	=	length increment, ft
Δp_0	=	initial or first pressure increment, psi
Δp_1	=	final pressure increment, psi
ΔT	=	temperature increment, ^oF

e = absolute roughness, in
e = convergence tolerance
f = total porosity, fraction
g_g = gas specific gravity, dimensionless
l = fraction of the liquid, fraction
m = viscosity of the fluid, cp
m_a = apparent viscosity, cp
m_c = viscosity of the gas continuous phase, lbm/ft-sec
m_d = viscosity of the liquid phase, lbm/ft-sec
m_g = viscosity of the gas, cp
m_{kf} = viscosity of the kill fluid, cp
m_m = viscosity of the mixture, cp
m_1 = gas viscosity at one atmosphere and reservoir temperature, cp
q_N = dial reading of the rotational viscometer at N rpm
r = density of the fluid, lbm/ft^3
r_c = density of the gas continuous phase, lbm/ft^3
r_d = density of the liquid phase, lbm/ft^3
r_g = density of the gas, lbm/ft^3
r_{gsc} = density of the gas at standard conditions, lbm/ft^3
r_{if} = density of the influx fluid, ppg
r_{ikf} = density of the initial kill fluid, ppg
r_{kf} = density of the kill fluid, lbm/ft^3
r_m = density of the mixture, lbm/ft^3
r_{mw} = density of the mud weight in use, ppg
r_{pr} = pseudo reduced density, dimensionless
s = surface tension, dyne/cm

Subscripts

acc = acceleration
an = annulus
bw = blowout well
el = elevation
f = friction
kf = kill fluid
n = interest depth
R = reservoir
rw = relief well
t = total

Chapter 5

Steady-State Dynamic Kill Computer Program

Spreadsheet programs are used to apply steady-state methods for designing and analyzing dynamic kills to actual surface and underground blowouts.

The methods described in Chapter 4 are generally applied using computer programs to predict pressure gradients in the well and resultant surface and bottomhole pressures and formation flow rates. This chapter documents two Excel™ spread sheets that provide a steady state kill design and prediction method delivered as part of this report. It also describes the application of that method to actual dynamic kills of both surface and underground blowouts.

A dynamic kill computer program following the procedure in Chapter 4 was created to accomplish the design and predictive analysis of a dynamic kill. It is important to point out that the program was based on the conventional dynamic method, which assumes that only formation fluid is present below the injection point. This consideration is contemplated in nearly all current, published models, and most consider just the hydrostatic head of the fluid. In this program all the components of the pressure gradient equation are considered: hydrostatic head, friction losses, and acceleration.

Computer Program Implementing the Procedure

A computer program was developed to implement the global solution procedure discussed in Chapter 4. The results are presented numerically and graphically. The program is composed of several work sheets that are linked within an Excel™ file. Repetitive calculations are generally performed using "Macros" programmed in "Visual Basic." Therefore macros must be "enabled" to run the spreadsheet. The note when opening the spreadsheet that it is linked to previous spreadsheets is irrelevant, and should be answered with "no."

Work Sheet Descriptions

The following section will briefly explain the main characteristics of each sheet.

Data Sheet - The data sheet includes the required data to analyze an off - bottom blowout. It also schematically displays the wellbore geometry and a summary of the conditions in the well being analyzed.

IPR Sheet - This part of the program presents a table of the calculated reservoir inflow performance utilizing several gas flow rates. The table shows the flowing bottomhole pressure for each given gas formation rate.

WHP Sheet - This sheet is a table of the calculated wellbore hydraulic performance for different gas flow rates. The gas rates are the same as those utilized in the reservoir inflow performance calculation.

Gas Flow Rate Determination Plot - This sheet plots the previously calculated IPR and WHP. The intersection of these curves gives the gas flow rate assuming that the well has been completely unloaded of all the liquid and only formation gas is flowing in the system.

Pressure Profile Sheet - This sheet is a table of the pressure profile generated by the formation gas flowing through the well during blowout conditions. The pressure values are given for several depths in the well.

Pressure Profile Plot - This sheet plots the previously calculated pressure profile during blowout conditions as function of depth and presents the pressure behavior from the bottom of the well to the surface when only gas is flowing in the wellbore.

Gas Properties Sheet - The gas properties sheet displays the properties of the gas throughout the wellbore for the flow conditions previously obtained, which are used as the initial conditions of the control process.

Control Sheet - This segment of the program presents the process and flow conditions to reach the dynamic kill after a kill rate and kill fluid properties have been selected based on use of the dynamic kill sheet. After the kill fluid properties are input, the estimated flow conditions as function of time are presented in a table. Also the most important parameters such as time, gas flow rate, bottomhole pressure, injection depth pressure, surface pressure, and the pressure at any critical point in the well during the dynamic kill process are summarized and displayed.

Results Sheet - The results sheet summarizes the fluid properties and kill parameters for a given set of input variables that are being evaluated for possibly controlling an off - bottom blowout utilizing this concept. It also shows an estimated prediction of the bottomhole pressure, injection depth pressure, gas flow rate, and pressure at any point in the well as function of time during the whole control process.

Bottomhole Pressure Plot - This sheet plots the estimated bottomhole pressure as function of time during the whole control operation.

Surface Pressure Plot - This sheet presents a graph of the estimated surface pressure as function of time during the pumping operation.

Gas Flow Rate Plot - This section displays a plot versus time of the estimated gas flow rate from the reservoir to the wellbore during the dynamic kill development.

Dynamic Kill Sheet - The dynamic kill sheet presents the analysis of a possible blowout control employing the dynamic kill method. It takes exactly the same well, reservoir, and kill fluid data that

were input in the data sheet. It allows the user to test different kill fluid rates and properties to determine feasible steady state dynamic kill conditions.

Dynamic Kill Plot - This sheet presents the plot of the dynamic kill analysis and can be used to select an appropriate kill fluid rate and properties to control the blowout .

Input Data

Table 1 presents the required data to run the program. It also shows the respective units for each variable.

Table 1 Input data required by the computer program

Variable	Units
Wellbore Data	
First Casing	
Outside Diameter	Inches
Inside Diameter	Inches
Depth	Feet
Second Casing (Liner)	
Outside Diameter	Inches
Inside Diameter	Inches
Depth	Feet
Top Liner Depth	Feet
Injection string (first geometry)	
Outside Diameter	Inches
Inside Diameter	Inches
Depth	Feet
Injection string (second geometry)	
Outside Diameter	Inches
Inside Diameter	Inches
Length	Feet
Absolute roughness	Inches
Open hole	
Total well depth	Feet
Bit diameter	Inches
Reservoir Data	
Reservoir pressure	Psi
Reservoir temperature	ºF
Surface gas temperature	ºF
Gas specific gravity (air = 1.0)	Dimensionless
Permeability	md
Thickness	Feet
Porosity	Fraction
Total Compressibility	Psi^{-1}
Drainage Radius	Feet

Wellbore Radius	Feet
Kill Fluid Data	
Density	Lbm/ft^3
Viscosity	Cp
Standard Conditions	
Pressure	Psia
Temperature	°F

Potential Applications of the Program

The computer program described in this chapter can be utilized to analyze the control of surface and underground blowouts for both on- and off-bottom conditions with injection through an injection string, such as drillpipe, in either the blowout well or a relief well.

Example Application to Dynamic Kill of an Actual Surface Blowout

Once the computer program was finished, it was compared to previously published examples to evaluate its performance. This evaluation was carried out using field data from a surface blowout in Indonesia and compared to results from other models published in the literature. The program actually used is an Excel™ spreadsheet, which is included in this report as Appendix B and is named "FINAL-Surface Dynamic Kill (Arun).xls."

The program was run with data from the blowout that occurred in Mobil Oil Indonesia's Arun field well No. C-II-2. It is considered the largest gas blowout ever[11]. The results were compared with previously published models that used this information to calculate the kill parameters. Data were extracted from references 7, 10 and 11. Table 2 presents the blowout information. The program was run assuming equal measured and true vertical depths of 9650 feet with drillpipe 100 feet off bottom because the current program is for vertical wells only.

Figure 24 shows the reservoir inflow performance and wellbore hydraulics performance curves for different injection rates that were calculated and generated with the model built in this work and input data from the Arun blowout.

Table 2 Blowout data[7] from Mobil Oil Indonesia's Arun field well No. C-II-2

Input Data	
Reservoir pressure (psia)	7,100
Reservoir temperature (°F)	230
Gas specific gravity	0.6
Casing ID (in)	8.535
Drillpipe OD (in)	5.00
Drillpipe ID (in)	6.85 (equivalent in relief well)
Pipe roughness (in)	0.00065

Measured depth (ft)	10,210
True vertical depth (ft)	9,650

Analysis of the results of the Arun blowout calculation, see figure 24, showed the following. The inflow performance curve "IPR" shows the performance of the reservoir. The '0 bpm" curve represents the wellbore performance of the system when only gas is flowing. The intersection of the "IPR" curve and "0 bpm" curve corresponds to the well condition after all of the liquid has been unloaded from the wellbore and free flowing equilibrium condition has been reached. According to the calculations given by the program, the Arun field's well No. GII-2 was producing at an approximate rate of 450 MMscfd during the blowout, with a bottom hole pressure around 6,050 psi.

Figure 24 also shows that dynamic kill calculations indicate that a water injection rate of approximately 75 bpm would give a bottom hole pressure of just more than 7,100 psi, which would be enough to create sufficient backpressure at the formation face to prevent further gas flow from the reservoir.

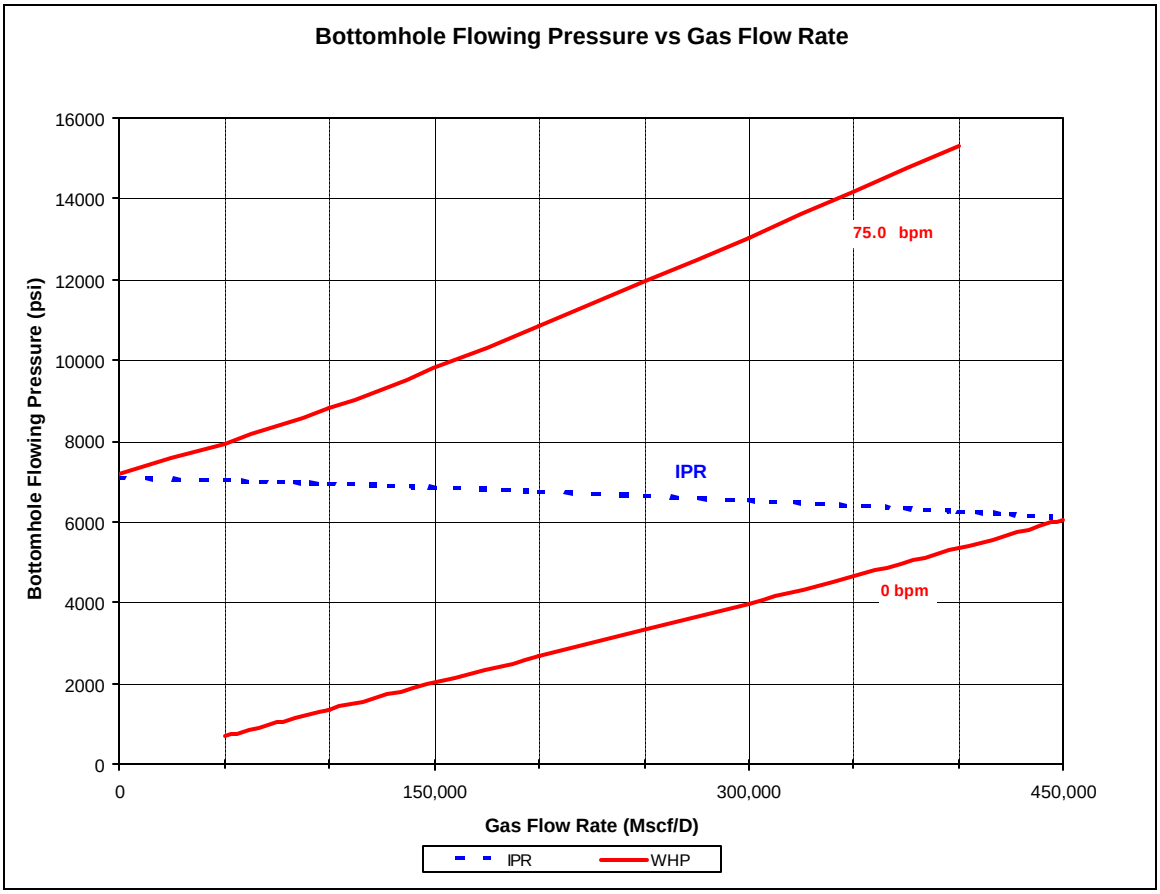

Fig. 24 Predicted kill flow rate for Arun blowout.

The solutions for the Arun blowout given by other authors' dynamic kill models are presented in Table 3. It can be seen that the dynamic kill computer program developed in this work predicts a similar blowout rate to Al-Shehri[11], which is higher than the rates predicted by Blount[7] or Kouba[10]. The assumption made herein that the measured depth was equal to the true vertical depth would result in a higher predicted rate due to ignoring the effect of additional friction over the longer actual measured depth. However this effect would only account for a fraction of the difference between the blowout rate predicted herein and those predicted by Blount and Kouba.

The kill rate of 75 bpm predicted by this program is similar to, but less than those calculated by Blount[7], Kouba[10], and Al-Shehri[11]. The predicted bottomhole pressure at Blount's proposed kill rate of 80 bpm is about 7550 psig versus about 7400 psi predicted by Bount. The principal difference in the calculations seems to be the basis for defining a friction factor for such highly turbulent flow. The use of a Newtonian/Bingham Plastic model for rheology in this program may overpredict frictional pressure losses and therefore underpredict the required kill rate. The actual kill rate used was much higher, but Blount attributed this to leak off into the formation between the relief well and the blowout well. Our conclusion is that this method and the program implementing it may be used with reasonable confidence to perform sensitivity analyses for different blowout scenarios and to assess the limitations of the dynamic kill method during blowout control operations.

Table 3 Results from different dynamic models for Arun gas blowout.

Model	Gas flow rate (Mscf/D)	Kill flow rate (bpm)	Kill fluid density (ppg)
Blount and Soeiinah [7]	360,000 to 380,000	80	8.33
Kouba [10]	370,000	84	8.33
Al-Shehri [11]	447,000	82	8.33
Surface Dynamic Kill Program	450,000	75	8.33

As noted in a previous section, the spreadsheet includes worksheets that attempt to give a rough approximation of the change in pressures versus time for a given kill fluid pump rate. In this case the predicted behavior is both unstable and unrealistic. This is probably because the high initial fluid velocities imply very rapid changes in the well conditions whereas the simplifying assumptions in the spreadsheet require that well conditions are almost steady state at each time step.

Example Application to Dynamic Kill of an Actual Underground Blowout

This field case is for an off - bottom underground blowout that occurred during a trip in the hole in a deep gas well described by Smith et al[21]. The drill string became stuck at more than 2,000 ft above total depth, and due to the previous history and excessive surface pressures, it was concluded that an underground blowout was in progress. Noise logs were run in the drillpipe, which confirmed flow from the objective sand to the casing shoe. The blowout data and scenario is presented in Figure 25.

The formation fluid path is through the openhole from the bottom of the hole to the injection string. Then, it is through the annular section between the drillstring and wellbore from the injection string depth to the 9 5/8" casing shoe.

Actual Kill Operations

The actual kill operation was performed utilizing the dynamic kill concept. It began by pumping 13.5 ppg mud at 3 bpm and staging up to 17 bpm. The initial pump pressure at 17 bpm was 6000psi. As mud began to fill the annulus, this pressure increased to 6,900 psi. A steady state condition of 6,800 psi at 16.3 bpm was achieved after pumping about 700 barrels.

Circulation continued for another 1000 barrels to help remove some of the remaining gas from the openhole and annulus. Then 1000 barrels of 15.5 ppg were pumped at a final rate and pressure of 14 bpm and 5,350 psi to provide additional overbalance. The 13.5 ppg mud weight from the injection depth back to the surface gives a bottomhole pressure adequate to overbalance the formation pressure. However, additional overbalance was desired to offset potential loss of hydrostatic pressure when gas from below the injection depth migrates upward into the annulus around the pipe. The actual kill parameters are presented in Table 4

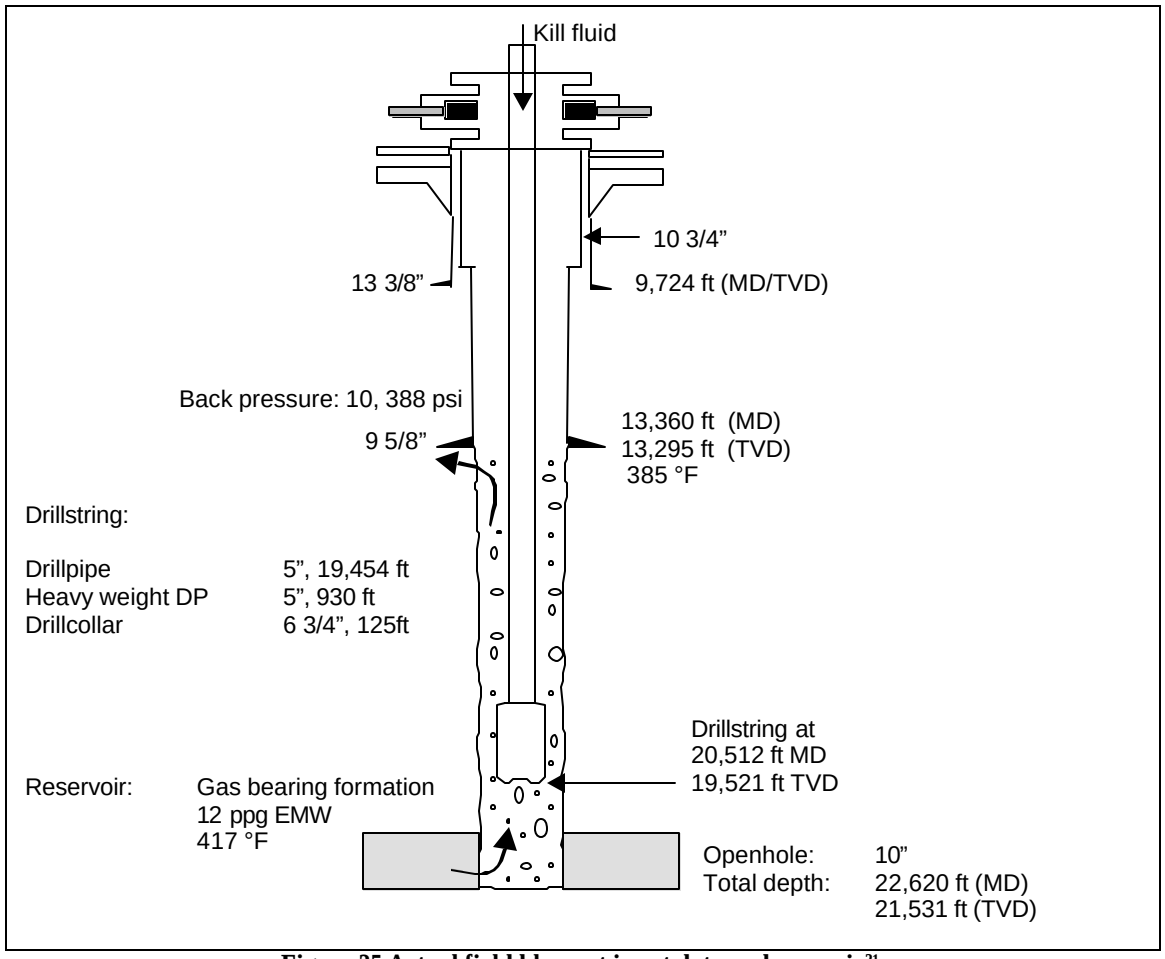

Figure 25 Actual field blowout input data and scenario[21]

Table 4 Actual kill parameters for the field case

Kill parameters utilized for controlling the well

Kill flow rate	17 bpm
Kill fluid density	13.5 ppg (101 lbm/ft^3)
Kill time	6,000 seconds (100 min)
Kill volume (13.5 ppg fluid)	1,700 bbl
Maximum peak pressure	6,900 psi
Maximum HHP	2,874

The proposed model was applied to simulate the kill performed in this field case and to compare the simulation results for an off-bottom dynamic kill to the actual results.

Simulation of Actual Case

The computer program was utilized to simulate the real well conditions during the control for the different pump rates and kill fluid densities utilized after the steady state conditions were reached. The program actually used is an Excel™ spreadsheet, which is included in this report as Appendix C and is named "Underground Dynamic Kill-FINAL..xls." In the field, a 13.5-ppg fluid and a rate of 17 bpm were used first, which resulted in a pump pressure of 6,900 psi. Then, the rate was reduced to 16.3 bpm obtaining a constant pressure of 6,800 psi. Finally, a 15.5 ppg fluid was pumped at a rate of 14 bpm, which reduced the pump pressure at 5,350 psi.

The computer program employed these flow conditions to compute the surface pressure considering that the steady state conditions were attained. Table 5 presents the actual surface pressures recorded during the control as well as the ones given by the program. In all cases, the surface pressures calculated by the program were significantly less than experienced in the field.

An attempt to account for known reasons for this difference is shown in the "corrected" column. The program is for vertical wells and consequently, true vertical depths were used in the calculations. Given that the measured drillstring length was 20,512 ft versus the true vertical length of 19,521 ft, the frictional pressure losses in the drillstring are expected to be about 5 percent higher than calculated with the program, or about 226 psi higher in the 17 bpm case. Also, the operator recorded that fracture pressure during pumping at the end of the job was approximately 10,700 psi rather than the 10,388 psi estimated as the fracture initiation pressure. This is likely due to the effect of fracture extension pressure described in Chapter 3 and adds another 312 psi to the surface pressure required at 17 bpm. These additional pressures result in a "corrected" estimate of 6280 psi for the surface pressure at 17 bpm. This is still about 600 psi less than the actual pressure recorded in the field.

Table 5 Actual and calculated surface pressures for the field case

Flow conditions		Surface pressure (psi)		
Kill flow rate	Kill density	Actual[21]	Calculated	"Corrected"
17 bpm	13.5 ppg	6,900	5,742	6,280

16.3 bpm	13.5 ppg	6,800	5,404	Not Calculated
14 bpm	15.5 ppg	5,350	3,583	Not Calculated

The real reasons for this discrepancy are unknown. The most likely cause cited by the operator was that a logging tool was stuck in the jars in the drillstring. This would create a significant restriction to flow that is not accounted for in either the program or the corrections. Two more possibilities include drillstring dimensions or fluid properties that are different than reported in the records for this case history. The drillstring was modeled with a 4.10 inch i.d. based on the length-weighted, root-mean-square average of the three different i.d. drillpipes used. Because frictional pressure losses are proportional to the pipe i.d. to the 4.75 power, a small reduction in actual pipe i.d. can cause a large increase in pressure loss. The fluid was modeled as a Newtonian fluid with a viscosity of 29 cp for the 13.5 ppg mud and 37 cp for the 15.5 ppg mud, equal to the plastic viscosities reported in the drilling records. The power-law friction loss model described in chapter 4 was not implemented in the program, but plastic viscosity is used in Bingham plastic friction loss models in exactly the same way as viscosity in the Newtonian model. Hand calculations for the Newtonian frictional pressure loss model confirmed that there were no significant errors in implementing this model in the program. In addition, use of a Power-law model would have actually resulted in the predicted surface pressures being somewhat lower for this example, and therefore is not a likely explanation for the discrepancy between calculated and actual pressures. Nevertheless, the actual viscosity of the large volumes of mud pumped could have been higher than reported. A final possibility is a significant error in the equations used in the spreadsheet for frictional pressure losses. Consequently, the operators's conclusion that the restriction due to the logging tool caused the higher than expected pressures seems logical. However, dimensions for the jars and logging tool are not available, and the increase in pressure due to this restriction cannot be estimated.

Figure 26 shows the reservoir inflow performance and wellbore hydraulics performance curves that were calculated and generated with the model built in this work and the input data for the underground blowout.

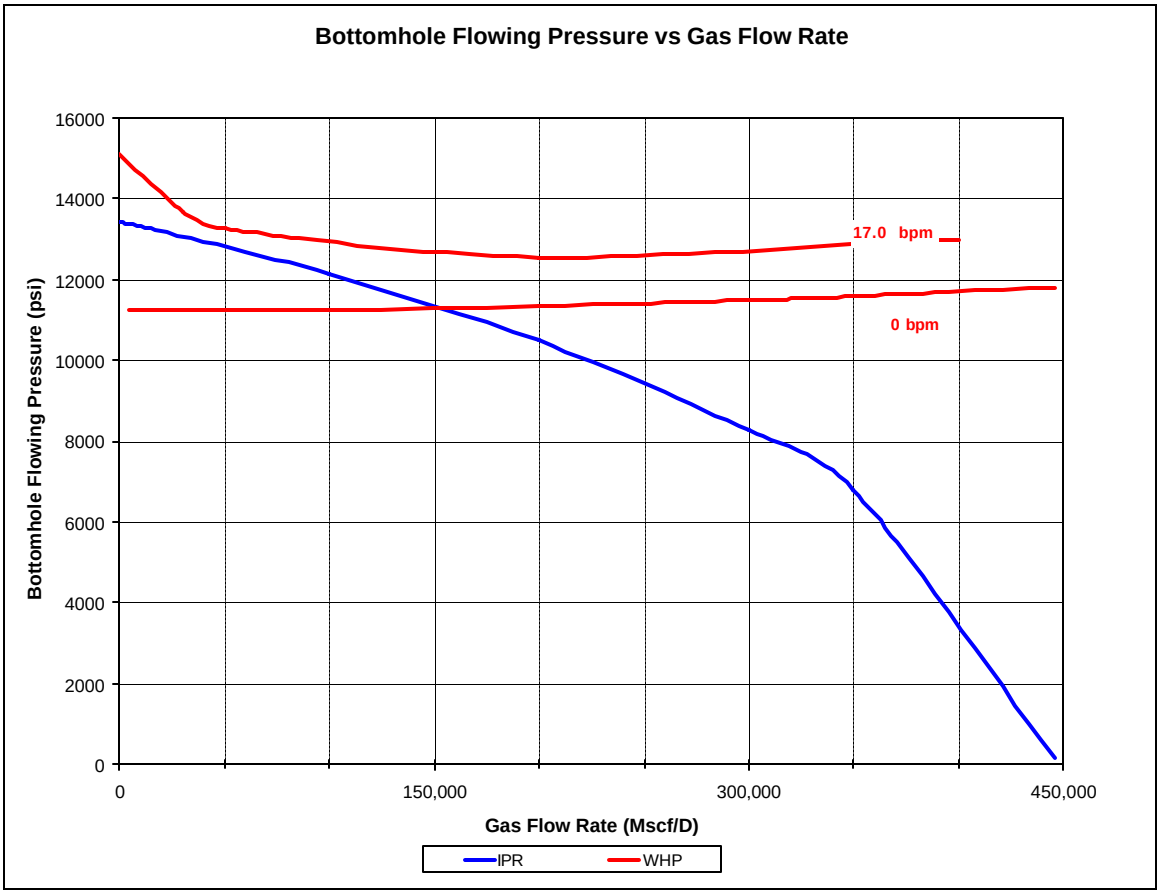

Figure 26 Predicted kill flow rate for Underground blowout.

Analysis of the results of these calculations, see figure 26, showed the following. The inflow performance curve "IPR" shows the performance of the reservoir. The "0 bpm" curve represents the wellbore performance of the system when only gas is flowing. The intersection of the "IPR" curve and "0 bpm" curve corresponds to the well condition after all of the liquid has been unloaded from the wellbore and free flowing equilibrium condition has been reached. According to the calculations given by the program, the well was producing a rate of approximately 150 MMscfd at a bottom hole pressure of about 11,300 psi during the underground blowout.

Figure 26 also shows that the dynamic kill calculations indicate an injection rate of approximately 17 bpm with 13.5 ppg mud would give a wellbore bottom hole pressure that is greater than the flowing formation pressure at any gas flow rate. Therefore, this “kill” rate is enough to create sufficient backpressure at the formation face to stop gas flow from the reservoir. Additional runs with the program further indicate that an injection rate of as little as 13 bpm would have also resulted in a successful kill.

The spreadsheet also computes crude estimates of the bottomhole pressure, figure 27, and the surface pressure, figure 28, as a function of time during the entire control process. It can be seen in figure 27 that after the pumping operations start, the bottomhole pressure begins to increase due to the flow of kill fluid in the annular section. This causes an increase in both frictional and hydrostatic pressure in the annulus. When the welbore pressure at the injection depth reaches a pressure that

causes bottomhole pressure to exceed the static formation pressure of 13,435 psi, gas flow from the formation stops. The program predicts that this would occur within about 800 seconds of beginning to pump the kill fluid at the rate of 17 bpm.

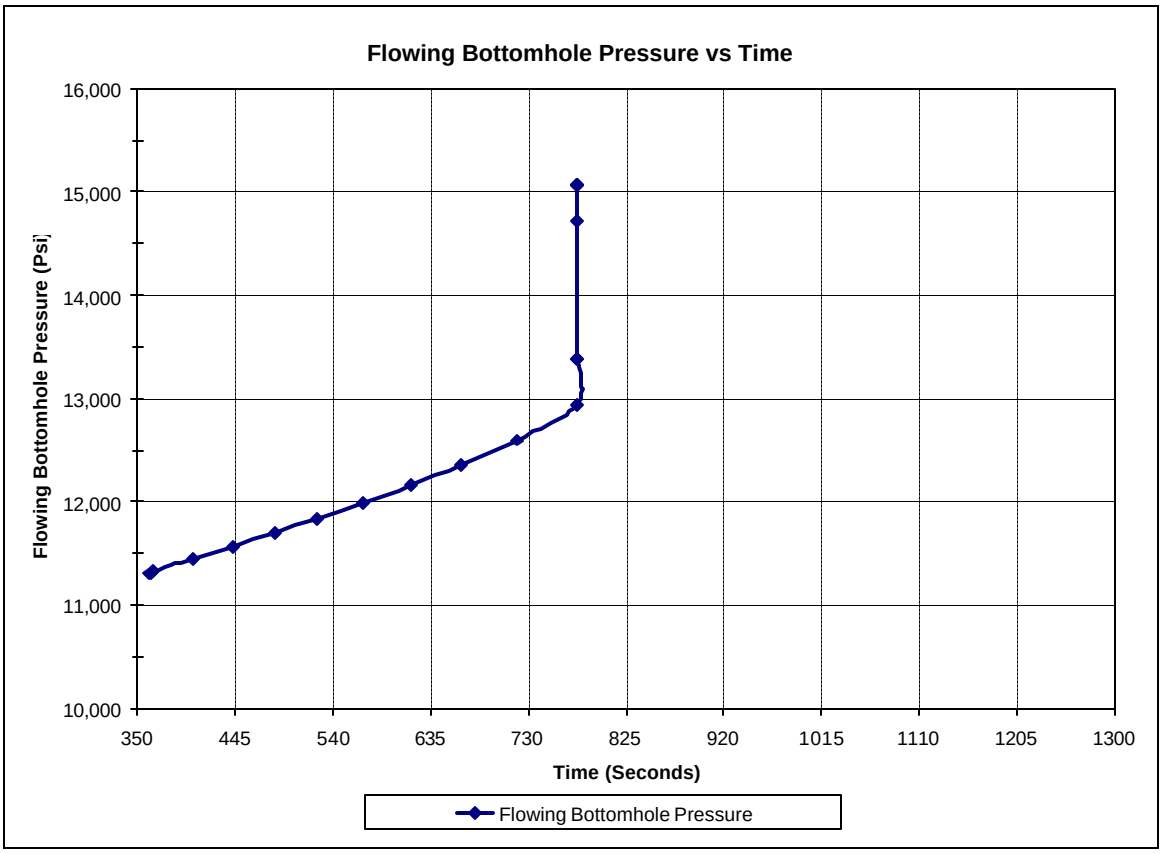

Figure 27 Estimated Bottomhole Pressure versus Time during Kill

The predicted surface pressure shown in figure 28 reinforce that common well control concept that pump pressure can be used as an indicator of bottomhole pressure. The increasing surface pressure is an indicator that bottomhole pressure is increasing both in the simulation and in the actual field results. Having already calculated the surface pressure when the kill is completed, tracking the trend of the actual surface pressure in the field can give a means to determine when the formation has become overbalanced and formation feed in has ceased.

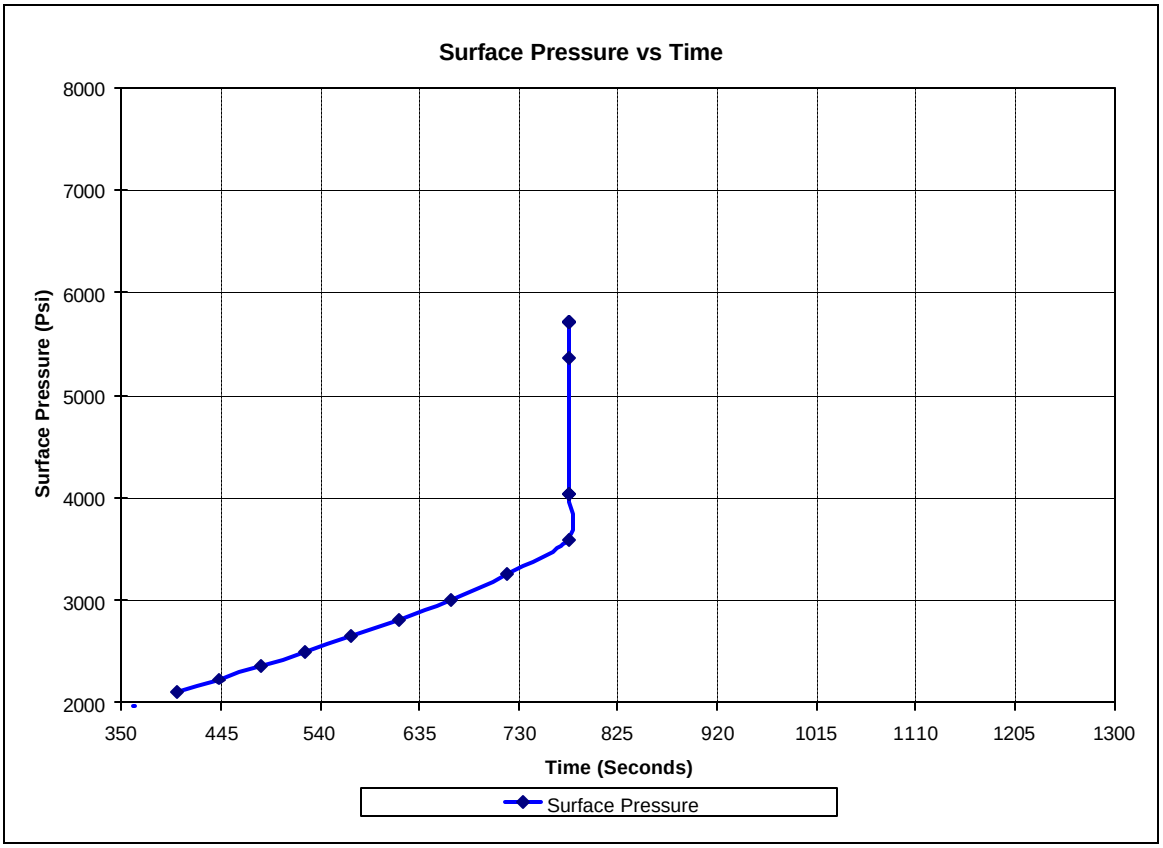

Figure 28 Estimated Surface Pressure versus Time during Kill

Summary Analysis of Results

The previous two comparisons to actual field experience provide some insights into the utility of and limitations of this steady-state approach to designing or analyzing dynamic kills for blowouts. In both cases, the calculations given by the spreadsheets were reasonable, but did not match the field results as well as expected.

One basis for comparison is surface pump pressure during kill operations. As noted already, surface pump pressure is often a useful indication of bottomhole pressure. In the case for the surface blowout in the Arun field[7], surface pressures calculated in the spreadsheet varied drastically during time. Nevertheless, the surface pressure calculated for 80 bpm at T1 = 354 seconds was 3624 psig. This compares very well for the measured surface pressure of 3600 psi during the kill at 80 bpm. However, the actual bottomhole pressure was determined to be 6514 psi in the relief well versus 6710 psi predicted by the spreadsheet. This difference is most likely due to the spreadsheet being configured for vertical wells only, whereas the relief well was a directional well. The actual frictional pressure loss was reported to be 1260 psi versus 1092 calculated with the spreadsheet. About half of this 168 psi difference is attributable to relief well's measured depth being greater than the true vertical depth used in the spreadsheet. The remaining difference has not been resolved. An additional possibility is inconsistency in applying dimensional approximations for the annular injection geometry used in the actual kill to the conventional pipe geometry considered for the injection string

in the program. In the underground blowout case, actual surface pressures were significantly higher than predicted, as shown in Table 5. As previously discussed, this is almost certainly due to the logging tool stuck n the drillstring jars.

Another basis for comparison is the kill rate used. In the Arun case, the required kill rate of 126 bpm was much higher than the 75 bpm calculated by our spreadsheet or the 80 bpm calculated by Blount and Soeiinah[7]. Blount and Soeiinah attribute this to leak off in the very high permeability reservoir between the relief well and the blowout well. The leak off resulted in only a fraction of the kill fluid actually flowing up the blowout well. In the case of the underground blowout[21], the operator's predicted kill rate of 17 bpm was successful. However, the spreadsheet predicted that a rate as low as 13 bpm would have been successful. In both cases, the spreadsheet predicted lower kill rates than anticipated by the operator. For the underground blowout case, the likely explanation lies with the use of the Newtonian rheology model for a non-Newtonian mud. The simplification of using plastic viscosity in lieu of the Newtonian viscosity is common, but it probably overestimates the frictional pressure losses for dynamic kill conditions. A power-law model would probably be more accurate at the high velocities experienced during dynamic kills.

Conclusions

1) The spreadsheets included in the attachments to this report provide reasonable estimates of steady state pressures and flows to be expected during surface and underground blowouts and the required kill operations.

2) Reasonable estimates of the pump rates required to kill a surface or underground blowouts can be made using the spreadsheets.

3) The quality of both pressure and kill rate calculations in the spreadsheets could be improved by implementing a power-law rheology model for friction loss calculations and by accounting for the longer measured depth flow path lengths in directional wells.

4) The time-based estimates of pressure versus time included in these spreadsheets are not accurate due to the assumption of steady-state gas flow throughout the well at each time step.

Chapter 6

Conclusions and Recommendations

Dynamic kills have been used to successfully control both surface and underground blowouts. This report describes a new computer program for time-based simulations that accounts for fracture extension pressure and a more conventional steady-state analysis implemented in a computer spreadsheet. These programs are intended to allow more consistent, effective design and analysis of control options for future blowouts.

The dynamic kill concept has been successfully applied to control of both surface and underground blowouts. The concept requires pumping a fluid into the well during the blowout such that the combination of fluid density and friction loss effects raises the bottomhole pressure to a value greater than the formation pressure. Both time-dependent and steady-state methods for designing and analyzing dynamic kills were studied. These methods can be used to determine the combination of fluid density and rate that will achieve a dynamic kill and to predict pressure response during the kill for better monitoring of the process. The following conclusions and recommendations are made as a result of this study.

Conclusions

Time-dependent Model accounting for Fracture Extension Pressure

1. The proposed model predicts a lower minimum mud flow rate than the current models to control an underground blowout.

2. The difference in the mud flow rate required versus current models is directly proportional to the well diameter and inversely proportional to the distance between the reservoir and the fractured formation.

3. The leak-off volume to the fracture is related to time, spurt loss volume, pack build-up factor, and the equilibrium Darcy flow velocity coefficient.

4. A pseudo 3D fracturing model with a pressure gradient factor predicts results that fit the results of other comprehensive 3D models.

5. The proposed model is significantly more complex, and therefore more difficult to use and maintain, than previous time-dependent and steady-state models.

6. The proposed model requires fracture zone mechanical properties, that are typically unknown, to give accurate predictions.

7. Simple models can be used to account for the effect of fracture propagation pressure being greater than fracture initiation pressure if an exact prediction of pressure versus time is not required.

Steady-state Model

8. Steady-state models for both single and multi-phase flow are available to predict pressure versus rate behavior for both pipe and annulus flow. These models have been adapted by multiple authors as a basis for design and analysis of dynamic kills. The models have been used as the basis for the Excel™ spreadsheets to design and analyze dynamic kills for both surface and underground blowouts that are included in this report.

9. The spreadsheets included in the attachments to this report provide reasonable estimates of steady-state pressures and flows to be expected during surface and underground blowouts and the required kill operations.

10. Reasonable estimates of the pump rates required to kill surface or underground blowouts can be made using the spreadsheets.

11. The quality of both pressure and kill rate calculations in the spreadsheets could be improved by implementing a power-law rheology model for friction loss calculations and by accounting for the longer measured depth flow path lengths in directional wells.

12. The time-based estimates of pressure versus time included in these spreadsheets are not accurate due to the assumption of steady-state gas flow throughout the well at each time step.

Recommendations

1) Design of dynamic kills should probably be performed using models or equations based on steady-state conditions. The beneficial effect of fracture extension pressure when killing an underground blowout should probably be ignored unless a small, 200 to 300 psi, increase in back pressure would significantly reduce kill design parameters.
2) The quality of the results from the spreadsheets delivered with this report could be improved by the following changes. These changes should be considered in any future development of this method.
   a) Implement a power-law rheology model for friction loss calculations
   b) Separate calculation of the hydrostatic, frictional, and acceleration components of the pressure change across a cell. This would allow simpler correction for frictional pressure losses in directional wells.

c) Define whether a flow path is a pipe or an annulus on the input data sheet.
d) Use pipe equations for frictional pressure losses.
e) Use the slot approximation as a basis for equivalent diameter in the pipe equations determining frictional pressure losses due to an annular flow.
f) Consider alternatives to the Serghides' equation for estimating friction factor for high velocity flows.
g) Delete unused "macros" for other definitions of equivalent diameters and flow parameters such as Reynolds number.
h) A simple calculation of surface pump pressure at a selected rate for the entire well filled with kill fluid should be added.

Acknowledgment

The authors would like to thank U.S. Minerals Management Service, Department of the Interior for funding this project, and Petrobras, PEMEX, and Louisiana State University for the financial support of the authors.

Bibliography

1. Bourgoyne, Adam T., Jr. and Kelly, O. Allen: “Development of Improved Procedures for Detecting and Handling Underground Blowouts in a Marine Environment - An Overview,” LSU/MMS Well Control Workshop, Baton Rouge, LA (3/30-31/94).

2. Geertsma, J., Haafkens, R.: “A Comparison of the Theories for Predicting Width and Extent of Vertical Hydraulically Induced Fractures,” Journal of Energy Resources Technology, (3/79), pp. 8-19.

3. Gidley, J.L., Holditch, S.A., Nierode, D.E., Veatch Jr., R.W.: Recent Advances in Hydraulic Fracturing, SPE Henry L. Doherty Series, Monograph Vol. 12, (1989).

4. Negrao, A.F.: Model for Planning Well Control Operations Involving an Induced Fracture, Ph.D. Dissertation, Louisiana State University, (12/94).

5. Santos, O.L.A.: A Dynamic Model of Diverter Operations for Handling Shallow Gas Hazards in Oil and Gas Exploratory Drilling, Ph.D. Dissertation, Louisiana State University, (1989).

6. Walters, J. V.: “Internal Blowouts, Cratering, Casing Setting Depths, and the Location of Subsurface Safety Valves,” SPE Drilling Engineering, (12/91), pp. 285-292.

7. Blount, E.M. and Soeiinah, E.: "Dynamic Kill: Controlling Wild Wells a New Way", World Oil, (10/81).

8. Lynch, R. D., McBride, E., Perkins, T., Wiley, M.: "Dynamic Kill of an Uncontrolled CO2 Well" SPE 11378, (7/85).

9. Koederitz, W. L., Beck, F.E., Langlinais, J.P. and Bourgoyne, A. T. Jr.: "Method for Determining the Feasibility of dynamic Kill of Shallow Gas Flows", SPE 16691 presented at the Annual Technical conference and Exhibition, Dallas Texas, (9/87).

10. Kouba, G.E., MacDougall, G.R. and Schumacher, B.W.: "Advanced in Dynamic Kill Calculations for Blowout Wells" SPE 22559 presented at the SPE Drilling & Completion Conference, (9/93).

11. Al-Shehri, Dhafer A.: A Study in the Dynamic Kill for the Control of Induced Surface Blowouts, Ph.D. Dissertation, Texas A & M University, (1994).

12. Oudeman, P., and Mason, D.: "Results of a Field Test to Improve Hydraulic Blowout Control Calculations", SPE 50577 presented at the European Petroleum Conference held in The Hague, The Netherlands (10/98).

13. Wessel, Michael and Tarr, Brian A.: "Underground Flow Well Control: The Key to Drilling Low-Kick-Tolerance Wells Safely and Economically," SPE Drilling Engineering, SPE 22217, Richardson, Texas (12/91).

14. Petersen, Johnny et al: "Kick with Lost Circulation Simulator, a Tool for Design of Complex Well Control Situations," SPE 49956, Perth Australia (10/12-14/98).

15. Leraand, Frode, Wright, J. W., Zachary, M. B., and Thompson, B. G.: "Relief-Well Planning and Drilling for a North Sea Underground Blowout," JPT, SPE 20420, (3/92).

16. Flak, Larry H., Muhanna, Ghassan A., and Al-Qassab, Mohamed: "Case History: Relief Well Control of Underground Blowout in Bahrain," SPE 29859, SPE Middle East Oil Show, Bahrain (3/11-14/95).

17. Smith, J. R. and Bourgoyne, A. T., Jr.: "Case History-Based Training for Control and Prevention of Underground Blowouts," SPE 38605, SPE ATCE, San Antonio, TX, (10/5-8/97).

18. Smith, John Rogers, Bourgoyne, A. T. Jr., Waly, Sherif M., and Hoff, Eileen B.: "Underground Blowout Training Modules," Report issued to MMS, Louisiana State University, (2/12/02).

19. Flak, L.H. and Gloger, D., "Blowout Control: Response, Intervention, and Management," World Oil, (7/94).

20. Vallejo-Arrieta, Victor Gerardo: Analytical Model to Control Off-Bottom Blowouts Utilizing the Concept of Simultaneous Dynamic Seal and Bullheading, Ph.D. Dissertation, Louisiana State University, (8/02).

21. Smith J. R., Bourgoyne, A. T. Jr., Waly, S. M., and Hoff, E. B., "Case Histories Bring Reality to Well Control Training", IADC Well Control Conference of the Americas. (8/25-26/99).

NOTE: A more extensive bibliography covering topics relating to underground blowouts and well control in general is provided in: SPE Reprint Series No. 42 – Well Control, SPE, Richardson, TX (1996).

Appendix

A

Time-Dependent Dynamic Kill Program

This appendix contains a listing for the program to perform time-dependent simulation for a dynamic kill of an underground blowout, which accounts for the effect of fracture extension pressure.

```
C
C  THIS PROGRAM SIMULATES THE PROFILE OF AN UNDERGROUND
C  BLOWOUT INTO A INDUCED FRACTURE
C  VERSION : 10/21/94 - ALVARO NEGRAO
C
C
C
C  REMARKS: 1) THE PROGRAM ASKS FOR THE INITIAL VALUE FOR THE
C  TIME STEP SIZE.THIS VALUE IS NECESSARY FOR THE THE FIRST CELL
C  CALCULATION
C
C         2) THIS PROGRAM COMPRISES THREE PHASES:
C              I. TWO-PHASE LEADING EDGE TRAVELS BETWEEN DC-
C                WELLBORE ANNULUS
C              II. TWO-PHASE LEADING EDGE TRAVELS BETWEEN DP-
C                 WELLBORE ANNULUS
C              III. ONLY A TWO-PHASE MIXTURE FLOWS INSIDE THE SYSTEM
C
C  INPUT PARAMETERS:
C      DAT - NAME OF THE DATA FILE FROM WHICH THE PROGRAM READS
C      THE INPUT PARAMETERS (DEFINED IN THE DATA FILE MDATA.DAT)
C      RESUL - NAME OF THE DATA FILE INTO WHICH THE PROGRAM WRITES
C      THE RESULTS (DEFINED IN THE DATA FILE MDATA.DAT)
C      BW - WELL DEPTH FROM KELLY BUSHING, FT
C      DCL - UNCASED WELL LENGTH,FT
C      DDC - DRILL COLLAR LENGTH,FT
C      CAL - UNCASED WELL DIAMETER, INCHES
C      CAU - CASING INSIDE DIAMETER, INCHES
C      ODP - DRILL PIPE OUTSIDE DIAMETER, INCHES
C      ODC - DRILL COLLAR OUTSIDE DIAMETER, INCHES
C      DM - MUD DENSITY, LBM/GAL
C      XN - MUD FLOW BEHAVIOR INDEX
C      XK - MUD CONSISTENCY INDEX
C      VISL - MUD PLASTIC VISCOSITY
C      ST - MUD SURFACE TENSION
C      AR - PIPE ABSOLUTE ROUGHNESS
C      GD - GAS SPECIFIC GRAVITY
C      SURT - SURFACE TEMPERATURE
```

```
C     BHT - BOTTOMHOLE TEMPERATURE
C     QLIQ - MUD FLOW RATE (IF A NONCIRCULATION CASE, USE QLIQ = .1)
C     AF - ADJUSTMENT FACTOR
C     IMAX - NUMBER OF TIME STEPS
C     IDC - NUMBER OF CELLS IN THE DRILL COLLAR PORTION OF THE WELL
C     IDP - NUMBER OF CELLS IN THE UNCASED DRILL PIPE PORTION OF THE
C           WELL
C     POR - RESERVOIR POROSITY
C     HF - RESERVOIR THICKNESS,FT
C     RW - WELLBORE RADIUS,FT
C     RK - RESERVOIR PERMEABILITY
C     PI - RESERVOIR PRESSURE, PSI
C     S - SKIN FACTOR
C     RT - RESERVOIR TEMPERATURE
C     TS - STANDART CONDITIONS TEMPERATURE
C     PS - STANDART CONDITIONS PRESSURE
C     SWI - RESERVOIR INITIAL WATER SATURATION
C     QKILL - FLOW RATE USED IN DYNAMIC KILL, GPM
C     HFR - THICKNESS OF THE FRACTURED FORMATION, FT
C     SIG2 - STRESS IN THE UPPER LAYER
C     SIG3 - STRESS IN THE LOWER LAYER
C     AKLCBOT - FRACTURE TOUGHNESS OF LOWER LAYER
C     AKLCTOP - FRACTURE TOUGHNESS OF LOWER LAYER
C     EFR - YOUNGS MODULUS OF FRACTURED FORMATION
C     DELX - PROPAGATION OF THE FRACTURE WITHIN TIME STEP, FT
C  RESULTS IN THE FOLLOWING ORDER:
C     T - TIME
C     P - BOTTOMHOLE PRESSURE
C     H - TWO-PHASE FLOW LEADING EDGE DEPTH
C     QREC - GAS FLOW RATE PRODUCED BY THE GAS RESERVOIR (MMSCF/DAY)
C     PSHOE - PRESSURE AT CASING DEPTH
C
C  MAIN PROGRAM
C
      IMPLICIT REAL*8 (A-H,O-Z)
      DIMENSION D(80,4),P(80,4),V(80,4),HL(80,4),VG(80,4)
      DIMENSION T(0:500),VMIX(80,4),TD(0:500),TI(0:500),QFR(0:500),
     *QR(0:500),DQ(0:500)
      DIMENSION TFR(0:500),PFR(0:500),PANT(0:500),WF(0:30),WFM(0:30),
     *AFANT(0:500),AF1ANT(0:500),AFATM(0:500),AF1ATM(0:500),
     *DANT(0:500),D1ANT(0:500),DANTM(0:500),D1ANTM(0:500),
     *P1ANT(0:500)
      DIMENSION VSANT(0:500),V1SANT(0:500)
      COMMON/MAT/FRC(80,4),ELEV(80,4),CMOM(80,4),FMOM(80,4),KJ,KG
      COMMON/REO/VISL
      COMMON/MAINP/AF,VSLI
      COMMON/FLAG/IFLAG
      COMMON/RESULTS/DSHOE
      COMMON/RESER/XMPI,TDFAC,DFAC,QFAC,S,TI,QREC,QR,DQ
      COMMON/FRAC/SIG1,SIG2,SIG3,AKLCBOT,AKLCTOP,HFR,EFR,DPFR,PL
      COMMON/BLOCK3/ SWD,DW,XMATD,DEPF,REFD,PHIO,PDC,POIS,STR,
     *ALPHA,PO,AK,PHI,VISC,TALY
      COMMON/VAR/QMIX,AMVF,DGASF,DTFRAC,IFC,TFRAC,PFRAC,KFR,
     *COEF,CS,QL
      COMMON/TEMP/GT,SURT,TEMPFR
      COMMON/FRAPAR/PFR,PANT,WF,WFM,AFANT,AF1ANT,AFATM,
     *AF1ATM,DANT,
     *D1ANT,DANTM,D1ANTM,P1ANT,TFR
```

```
      COMMON/DIMFRA/AREA1,AREXP1,PER1,AF1,BF1,ARC,XLF,AF2,BF,DELX,
     *ARCEXP,PERC
      COMMON/VOL/VSANT,V1SANT
      OPEN(2,FILE="MMS.DAT",STATUS='UNKNOWN')
      OPEN(3,FILE="RESUL.DAT",STATUS='UNKNOWN')
      OPEN(4,FILE="FRAC1.DAT",STATUS='UNKNOWN')
      OPEN(5,FILE="PSDFRAC.OUT",STATUS='UNKNOWN')
      READ(4,*) QKILL,HFR,SIG2,SIG3,TALY
      READ(4,*) AKLCBOT,AKLCTOP,EFR,DELX
      CLOSE(4)
      DO 111 I=1,80
      DO 112 J=1,4
      D(I,J)=0.
      P(I,J)=0.
      V(I,J)=0.
      VG(I,J)=0.
  112 CONTINUE
  111 CONTINUE
C
C  READ PARAMETERS FROM DATA FILES
C
      READ(2,*)BW,DDC,CAL,CAU,ODP,ODC
      READ(2,*)DM,XN,XK,VISL,ST,AR
      READ(2,*)GD,SURT,BHT,QLIQ
      READ(2,*)AF
      READ(2,*)IMAX,IDC,IDP
      READ(2,*)POR,HF,RW,RK,PI,S
      READ(2,*)RT,TS,PS,SWI,DTFRAC
      READ (2,*) SWD,DW,XMATD,DEPF,REFD,PHIO,PDC
      READ(2,*) POIS,STR,ALPHA,PO,AK,PHI
      CLOSE(2)
C
C  ESTIMATION OF THE FRACTURE PRESSURE
C
      VISC=VISL
      OVERB=0.052*(SWD*DW+XMATD*(DEPF-DW)-((XMATD-REFD)*PHIO/PDC)*
     *(1.-EXP(-PDC*(DEPF-DW))))
      KFL=0
      WRITE(*,1000)
 1000 FORMAT(1X,'TYPE 1 IF FLUID IS PENETRATING--->',\\)
      READ(*,*)KFL
      IF(KFL.EQ.1) THEN
      PFV=(2*POIS*(OVERB-PO)/(1.-POIS)-STR)/(2.-ALPHA*((1.-2*POIS)/
     *(1.-POIS)))+PO
      PFH=(OVERB-PO-STR)/(1-ALPHA*(1.-2.*POIS)/(1.-POIS))+PO
      ELSE
      PFV=2*POIS*(OVERB-PO)/(1.-POIS)-STR+PO
      PFH=OVERB-STR
      END IF
      IF (PFH.LT.PFV) THEN
      IFRAC=1
      PFRAC=PFH
      PIC=PFH
      ELSE
      PFRAC=PFV
      PIC=PFV
      END IF
      SIG1=PIC
```

```
C
C  INITIALIZE SOME VARIABLES
      CALL SINIT(CDCC,CDPC,CDDC,CAL,CAU,ODP,ODC)
      CALL GCOM(PI,RT,GD,CG)
      CALL GASVIS(RT,GD,PI,GVI)
      CI=CG*(1-SWI)
      TDFAC=.000264*2.2454*RK/(POR*GVI*CI*RW**2)/3600.
      DFAC=.0518*GD/(GVI*HF*RW*RK**.201)
      QFAC=RK*HF*(TS+460.)/(5.792D7*PS*(RT+460.))
      CALL GASPSE(RT,GD,PI,XMPI)
      QREC=0.
      DXC=DDC/FLOAT(IDC)
      DCL=BW-DEPF-DDC
      DXP=DCL/FLOAT(IDP)
      I=1
      TD(1)=BHT
      IT1=IDC+1
      IT2=IDC+IDP+1
      GT=(BHT-SURT)/BW
      H=BW
      VSLI=QLIQ/(448.8*CDDC)
      CALL DPMUD1(1.D0,H,DDC,DCL,BW,VSLI,VSLI,XN,XK,CAL,
     *ODP,ODC,DM,CDCC,CDDC,DPMUD,PIC)
      IF(DPMUD.GE.PI)THEN
        WRITE(*,*)' BOTTOMHOLE PRESSURE GREATER THAN RES. PRESSURE'
        STOP
      END IF
      P(1,1)=DPMUD
      V(1,1)=VSLI
      V(2,1)=V(1,1)
      VG(2,1)=0.D0
      VG(1,1)=0.D0
      D(2,1)=0.D0
      D(1,1)=0.D0
      HL(2,1)=AF
      HL(1,1)=1.
      CALL PARCEL(D(1,1),V(1,1),HL(1,1),VG(1,1),P(1,1),TD(1),GD,XN,XK,
     *CAL,ODC,AR,VMIX(1,1),DM,FMOM(1,1),CMOM(1,1),ELEV(1,1),FRC(1,1),
     *VISL)
      FMOM(2,1)=FMOM(1,1)
      CMOM(2,1)=CMOM(1,1)
      ELEV(2,1)=ELEV(1,1)
      FRC(2,1)=FRC(1,1)
      T(1)=0.D0
      ICCF=1
        TEMPFR=SURT+GT*DEPF
        AKLC=MIN(AKLCBOT,AKLCTOP)
        PL=AKLC/(DSQRT(1.5708*HFR))+SIG1
        PFR(0)=PL
        XLF=0.
        TFR(0)=0.
        DPFR=10.
        AF1=HFR
        AF2=HFR
        BF1=HFR/2.
        BF=HFR/2.
        AFATM(0)=0.5*HFR
        AFANT(0)=0.5*HFR
```

```
      AFATM(1)=0.5*HFR
      AFANT(1)=0.5*HFR
      PANT(0)=PL
      PANT(1)=PL
      P1ANT(0)=PL
      P1ANT(1)=PL
      CNFR=1.
      VSANT(0)=0.
      V1SANT(0)=0.
      VSANT(1)=0.
      V1SANT(1)=0.
      CALL WIDTH(EFR,POIS,HFR,SIG1,SIG2,SIG3,PL,HFR/2.,HFR/2.,WF,
     *ARC,ARCEXP,CNFR,PERC)
      AREA1=ARC
      AREXP1=ARCEXP
      PER1=PERC
C  TIME STEP DO-LOOP
      DO 10 I=2,IMAX
        IF(I.LE.IT1)THEN
          VGC=VG(I-1,1)
          IF(I.EQ.2)THEN
            WRITE(*,*)' ENTER INITIAL VALUES FOR DT'
            READ(*,*)DT
            WRITE(*,*)
            WRITE(*,2)
            IIA=1
            WRITE(*,1)IIA,T(1),DPMUD,H,QREC,DSHOE,AF2,BF
            WRITE(3,1)IIA,T(1),DPMUD,H,QREC,DSHOE,AF2,BF
          ELSE
            DT=DXC/VGC
          END IF
          H=H-DXC
          TD(I)=SURT+H*GT
        ELSE IF(I.GT.IT1.AND.I.LE.IT2)THEN
          DT=DXP/VG(I-1,3)
          H=H-DXP
          TD(I)=SURT+H*GT
        ELSE
          DT=DTFRAC
          QLIQ=QKILL
          VSLI=QLIQ/(448.8*CDDC)
        END IF
        T(I)=T(I-1)+DT
        TI(I)=0.
        DO 50 J=2,I
   50   TI(J)=TI(J)+DT
        P(1,2)=P(1,1)
        IF(I.LE.2)GO TO 20
          DIF=PTEMP-P(1,1)
          P(1,2)=P(1,1)-DIF*DT/DTA
          IF(I.EQ.3)P(1,2)=P(1,1)
   20   IF(P(1,2).GT.PI)P(1,2)=PI-2.
C  CALL SUBROUTINE ROOT TO CALCULATE PRESSURES FOR THE CURRENT
C  TIME
      CALL ROOT(P,V,D,HL,VG,TD,CDCC,GD,I,IT1,DT,DXC,AR,DXP,H,PIC,BW,
     *XN,XK,CAL,CAU,ODP,ODC,DM,CDPC,CDDC,IT2,ST,VMIX,DCL,DDC,
     *QFR,ICCF,PI)
        PTEMP=P(1,1)
```

```
      DTA=DT
C
C  UPDATE FLOW VARIABLES
C
      IUM=I
      IF(I.GT.IT1)IUM=IT1
      DO 30 IU=1,IUM
        P(IU,1)=P(IU,2)
        V(IU,1)=V(IU,2)
        VG(IU,1)=VG(IU,2)
        D(IU,1)=D(IU,2)
        HL(IU,1)=HL(IU,2)
        FRC(IU,1)=FRC(IU,2)
        ELEV(IU,1)=ELEV(IU,2)
        CMOM(IU,1)=CMOM(IU,2)
        FMOM(IU,1)=FMOM(IU,2)
   30   CONTINUE
      VMIX(I,1)=VMIX(I,2)
      V(I+1,1)=VMIX(I,1)
      IF(I.EQ.IT1)THEN
        HL(IT1,3)=HL(IT1,1)
        P(IT1,3)=P(IT1,1)
        D(IT1,3)=D(IT1,1)
        V(IT1,3)=V(IT1,1)*CDDC/CDCC
        VG(IT1,3)=VG(IT1,1)*CDDC/CDCC
        VMIX(IT1,3)=VMIX(IT1,1)*CDDC/CDCC
        V(IT1+1,3)=VMIX(IT1,3)
        CALL PARCEL(D(IT1,3),V(IT1,3),HL(IT1,3),VG(IT1,3),P(IT1,3),
     *     TD(IT1),GD,XN,XK,CAL,ODP,AR,VM,DM,
     *     FMOM(IT1,3),CMOM(IT1,3),ELEV(IT1,3),FRC(IT1,3),VISL)
      END IF
      IF(I.LE.IT1)GO TO 60
      IUM=I
      IF(I.GT.IT2) THEN
      IUM=IT2
    DO 39 NTF=1,IFC
    AFANT(NTF)=AF1ANT(NTF)
    AFATM(NTF)=AF1ATM(NTF)
    PANT(NTF+1)=P1ANT(NTF+1)
    DANT(NTF+1)=D1ANT(NTF+1)
    DANTM(NTF+1)=D1ANTM(NTF+1)
    VSANT(NTF+1)=V1SANT(NTF+1)
39   CONTINUE
    KFR=1
    DT=DTFRAC
    END IF
      DO 40 IU=IT1,IUM
        P(IU,3)=P(IU,4)
        V(IU,3)=V(IU,4)
        VG(IU,3)=VG(IU,4)
        HL(IU,3)=HL(IU,4)
        D(IU,3)=D(IU,4)
        FRC(IU,3)=FRC(IU,4)
        ELEV(IU,3)=ELEV(IU,4)
        CMOM(IU,3)=CMOM(IU,4)
        FMOM(IU,3)=FMOM(IU,4)
   40   CONTINUE
      VMIX(I,3)=VMIX(I,4)
```

```
      V(I+1,3)=VMIX(I,3)
60    PSHOE=DSHOE
      T(I)=T(I-1)+DT
      WRITE(*,1)I,T(I),P(1,2),H,QREC,PIC,AF2,BF
      WRITE(3,1)I,T(I),P(1,2),H,QREC,PIC,AF2,BF
10    CONTINUE
    1 FORMAT(2X,I3,8F9.2)
    2 FORMAT(1X,' STEP    TIME    BHP    TP. TOP    QGAS   PFRAC
     *FRAC HEIG  B')
      CLOSE(3)
      CLOSE(4)
      STOP
      END
C  THIS SUBROUTINE ITERATES THE BOTTOMHOLE PRESSURE FOR EACH TIME STEP
C
      SUBROUTINE ROOT(P,V,D,HL,VG,TD,CDCC,GD,I,IT1,DT,DXC,AR,DXP,H,
     *PIC,BW,XN,XK,CAL,CAU,ODP,ODC,DM,CDPC,CDDC,IT2,ST,VMIX,DCL,
     *DDC,QFR,ICCF,PI)
      IMPLICIT REAL*8 (A-H,O-Z)
      DIMENSION D(80,4),P(80,4),V(80,4),HL(80,4),VG(80,4)
      DIMENSION T(0:500),VMIX(80,4),TD(0:500),TI(0:500),QFR(0:500),
     *QR(0:500),DQ(0:500)
      DIMENSION TFR(0:500),PFR(0:500),PANT(0:500),WF(0:30),WFM(0:30),
     *AFANT(0:500),AF1ANT(0:500),AFATM(0:500),AF1ATM(0:500),
     *DANT(0:500),D1ANT(0:500),DANTM(0:500),D1ANTM(0:500),
     *P1ANT(0:500)
      DIMENSION VSANT(0:500),V1SANT(0:500)
      COMMON/BLOCK3/ SWD,DW,XMATD,DEPF,REFD,PHIO,PDC,POIS,STR,
     *ALPHA,PO,AK,PHI,VISC,TALY
      COMMON/VAR/QMIX,AMVF,DGASF,DTFRAC,IFC,TFRAC,PFRAC,KFR,
     *COEF,CS,QL
      COMMON/TEMP/GT,SURT,TEMPFR
      COMMON/FRAPAR/PFR,PANT,WF,WFM,AFANT,AF1ANT,AFATM,
     *AF1ATM,DANT,D1ANT,DANTM,D1ANTM,P1ANT,TFR
      COMMON/DIMFRA/AREA1,AREXP1,PER1,AF1,BF1,ARC,XLF,AF2,BF,DELX,
     *ARCEXP,PERC
      COMMON/FRAC/SIG1,SIG2,SIG3,AKLCBOT,AKLCTOP,HFR,EFR,DPFR,PL
      COMMON/VOL/VSANT,V1SANT
      ICA=0
      K=1
      ZERO=0.D0
      PINC=1.D0
      IF(I.LE.3)PINC=10.
      PGA=P(1,2)
   10 CALL PREST(P,V,D,HL,VG,TD,CDCC,GD,I,IT1,DT,DXC,AR,DXP,H,
     *BW,PIC,XN,XK,CAL,CAU,ODP,ODC,DM,CDPC,CDDC,ST,VMIX,IT2,DCL,
     *DDC,IC,DIFF,QFR,ICCF)
      IF(K.EQ.1.AND.(IC.EQ.1.OR.IC.EQ.2))THEN
        IF(IC*ICA.EQ.2)PINC=PINC/2.
        IF(IC.EQ.1)P(1,2)=P(1,2)-PINC
        IF(IC.EQ.2)P(1,2)=P(1,2)+PINC
        PGA=P(1,2)
        ICA=IC
        GO TO 10
      END IF
      IF(K.EQ.2.AND.(IC.EQ.1.OR.IC.EQ.2))THEN
        FM=FM/2.
        IF(IC.EQ.1)PGP=PGA-FM
```

```
      IF(IC.EQ.2)PGP=PGA+FM
      P(1,2)=PGP
      GO TO 10
    END IF
    IF(K.GT.2.AND.(IC.EQ.1.OR.IC.EQ.2))THEN
      CE=CE/2.
      PGP=B-CE
      P(1,2)=PGP
      GO TO 10
    END IF
    IF(K.GT.2)GO TO 20
    IF(K.EQ.1)THEN
    IF(DABS(DIFF).LT.1.D-2)RETURN
      PCA=DIFF
      FM=.3D0
      IF(DIFF.GT.0.)FM=-.3D0
      PGP=PGA+FM
      P(1,2)=PGP
      K=K+1
      IF(I.GT.IT2) THEN
      TFRAC=TFRAC-DTFRAC
      IFC=IFC-1
      END IF
      GO TO 10
    END IF
    PCP=DIFF
 30 IF(PCA*PCP.LE.ZERO)THEN
      A=PGA
      FA=PCA
      GO TO 100
    END IF
    A=PGA
    B=PGP
    F=PCA
    C=PCP
    PGA=PGP
    PCA=PCP
    IF(DABS(A-B).LT.1.D-7) THEN
    P(1,2)=PGP-DIFF/2.
    CALL RES(GD,TD(1),P(1,2),QSC,I)
    RETURN
    END IF
    E=(F-C)/(A-B)
    CE=C/E
    PGP=B-CE
    P(1,2)=PGP
    K=K+1
      IF(I.GT.IT2) THEN
      TFRAC=TFRAC-DTFRAC
      IFC=IFC-1
      END IF
    GO TO 10
 20 PCP=DIFF
    IF(DABS(DIFF).LT.1.D0.AND.I.EQ.2)RETURN
    IF(DABS(DIFF).LT.1.D-2)RETURN
    IF(K.GT.100)STOP 50
    GO TO 30
100 B=P(1,2)
```

```
      FB=DIFF
        IF(I.GT.IT2) THEN
        TFRAC=TFRAC-DTFRAC
        IFC=IFC-1
        END IF
      CALL ZBRENT(P,V,D,HL,VG,TD,CDCC,GD,I,IT1,DT,DXC,AR,H,DDC,
     *BW,XN,XK,CAL,CAU,ODP,ODC,DM,CDPC,CDDC,ST,IT2,DXP,A,FA,B,FB,
     *DCL,DIFF,IC,VMIX,PIC,QFR,ICCF)
      RETURN
      END
C
C  THIS SUBROUTINE ITERATES THE BOTTOMHOLE PRESSURE FOR EACH
C  TIME STEP. IT IS CALLED BY ROOT SUBROUTINE WHEN THE INTERVAL
C  THAT CONTAINS THE ROOT IS KNOWN. IT IS USED TO SPEED UP THE
C  CONVERGENCY PROCESS.
C
      SUBROUTINE ZBRENT(P,V,D,HL,VG,TD,CDCC,GD,I,IT1,DT,DXC,AR,H,DDC,
     *BW,XN,XK,CAL,CAU,ODP,ODC,DM,CDPC,CDDC,ST,IT2,DXP,A,FA,B,FB,DCL,
     *DIFF,IC,VMIX,PIC,QFR,ICCF)
      IMPLICIT REAL*8 (A-H,O-Z)
      PARAMETER (ITMAX=100,EPS=3.E-8,TOL=.0001)
      DIMENSION P(80,4),V(80,4),D(80,4),HL(80,4),VG(80,4),
     *VMIX(80,4),TD(0:500),QFR(0:500)
      DIMENSION VSANT(0:500),V1SANT(0:500)
      COMMON/VAR/QMIX,AMVF,DGASF,DTFRAC,IFC,TFRAC,PFRAC,KFR,COEF,CS,QL
      COMMON/VOL/VSANT,V1SANT
      IF(FB*FA.GT.0.) PAUSE 'ROOT MUST BE BRACKETED FOR ZBRENT.'
      FC=FB
      DO 11 ITER=1,ITMAX
        IF(FB*FC.GT.0.) THEN
          C=A
          FC=FA
          DY=B-A
          E=DY
        ENDIF
        IF(DABS(FC).LT.DABS(FB)) THEN
          A=B
          B=C
          C=A
          FA=FB
          FB=FC
          FC=FA
        ENDIF
        TOL1=2.*EPS*DABS(B)+0.5*TOL
        XM=.5*(C-B)
        IF(DABS(XM).LE.TOL1 .OR. DABS(FB).LT.1.D-3)THEN
          RETURN
        ENDIF
        IF(ITER.GT.1.AND.I.GT.IT2) THEN
        TFRAC=TFRAC-DTFRAC
        IFC=IFC-1
        END IF
        IF(DABS(E).GE.TOL1 .AND. DABS(FA).GT.DABS(FB)) THEN
          XS=FB/FA
          IF(A.EQ.C) THEN
            PX=2.*XM*XS
            Q=1.-XS
          ELSE
```

```
            Q=FA/FC
            R=FB/FC
            PX=XS*(2.*XM*Q*(Q-R)-(B-A)*(R-1.))
            Q=(Q-1.)*(R-1.)*(XS-1.)
          ENDIF
          IF(PX.GT.0.) Q=-Q
          PX=DABS(PX)
          IF(2.*PX .LT. MIN(3.*XM*Q-DABS(TOL1*Q),DABS(E*Q))) THEN
            E=DY
            DY=PX/Q
          ELSE
            DY=XM
            E=DY
          ENDIF
        ELSE
          DY=XM
          E=DY
        ENDIF
        A=B
        FA=FB
        IF(DABS(DY) .GT. TOL1) THEN
          B=B+DY
        ELSE
          B=B+DSIGN(TOL1,XM)
        ENDIF
        P(1,2)=B
        CALL PREST(P,V,D,HL,VG,TD,CDCC,GD,I,IT1,DT,DXC,AR,DXP,H,BW,PIC,
     *XN,XK,CAL,CAU,ODP,ODC,DM,CDPC,CDDC,ST,VMIX,IT2,DCL,DDC,IC,DIFF,
     *QFR,ICCF)
        FB=DIFF
   11 CONTINUE
      PAUSE 'ZBRENT EXCEEDING MAXIMUM ITERATIONS.'
      RETURN
      END
C
C  SUBROUTINE RES CALCULATES GAS FLOW RATE FOR A CERTAIN BOTTOMHOLE PRESSURE
C
      SUBROUTINE RES(GD,RT,BHP,QC,I)
      IMPLICIT REAL*8 (A-H,O-Z)
      COMMON/RESER/XMPI,TDFAC,DFAC,QFAC,S,TI,QREC,QR,DQ
      DIMENSION TI(0:500),QR(0:500),DQ(0:500)
      CALL GASPSE(RT,GD,BHP,XMBHP)
      A=(XMPI-XMBHP)*QFAC
      B=0.
      QR(1)=0.
      IF(I.GT.2)THEN
      DO 15 J=2,I-1
        TD=TI(J)*TDFAC
   15 B=B+DQ(J)*DLOG10(TD)
      END IF
      C=DLOG10(TI(I)*TDFAC)
      F=(B-A-C*QR(I-1))/(.87*DFAC)
      E=(.87*S+C)/(.87*DFAC)
      QC=(-E+DSQRT(E**2-4.*F))/2.
      DQ(I)=QC-QR(I-1)
      QR(I)=QC
      QREC=QC
      RETURN
```

```
      END
C
C  THIS SUBROUTINE CALCULATES THE REAL GAS POTENTIAL
C
      SUBROUTINE GASPSE(RT,GD,P,XMP)
      IMPLICIT REAL*8 (A-H,O-Z)
      DIMENSION PVZ(0:500)
      PA=P+14.7
      NINC=10
      PVZ(1)=0.
      XMP=0.
      PINC=PA/NINC
      PA=0.
      N=NINC+1
      DO 30 I=2,N
        PA=PA+PINC
        CALL ZFACHY (RT,PA-14.7,GD,Z)
        CALL GASVIS (RT,GD,PA-14.7,GV)
        PVZ(I)=PA/(GV*Z)
        DMP=(PVZ(I-1)+PVZ(I))*PINC
        XMP=XMP+DMP
   30 CONTINUE
      RETURN
      END
C
C  THIS SUBROUTINE CALCULATES THE GAS COMPRESSIBILITY
C
      SUBROUTINE GCOM(P,T,GD,CG)
      IMPLICIT REAL*8 (A-H,O-Z)
      CALL ZFACHY(T,P,GD,Z)
      PB=P*.95
      PA=P*1.05
      CALL ZFACHY(T,PA,GD,Z2)
      CALL ZFACHY(T,PB,GD,Z1)
      CG=1./(P+14.7)-(1/Z)*(Z2-Z1)/(PA-PB)
      RETURN
      END
C
C  THIS SUBROUTINE CONTAINS THE GLOBAL SOLUTION PROCEDURE FOR PHASES I,
C  II AND IV
C
      SUBROUTINE PREST(P,V,D,HL,VG,TD,CDCC,GD,I,IT1,DT,DXC,AR,DXP,H,BW,
     *PIC,XN,XK,CAL,CAU,ODP,ODC,DM,CDPC,CDDC,ST,VMIX,IT2,DCL,DDC,IC,
     *DIFF,QFR,ICCF)
      IMPLICIT REAL*8 (A-H,O-Z)
      DIMENSION P(80,4),V(80,4),D(80,4),HL(80,4),VG(80,4),TD(0:500),
     *VMIX(80,4),QFR(0:100)
      DIMENSION TFR(0:500),PFR(0:500),PANT(0:500),WF(0:30),WFM(0:30),
     *AFANT(0:500),AF1ANT(0:500),AFATM(0:500),AF1ATM(0:500),
     *DANT(0:500),D1ANT(0:500),DANTM(0:500),D1ANTM(0:500),
     *P1ANT(0:500)
      DIMENSION VSANT(0:500),V1SANT(0:500)
      COMMON/MAT/FRC(80,4),ELEV(80,4),CMOM(80,4),FMOM(80,4),KJ,KG
      COMMON/MAINP/AF,VSLI
      COMMON/REO/VISL
      COMMON/BLOCK3/ SWD,DW,XMATD,DEPF,REFD,PHIO,PDC,POIS,STR,
     *ALPHA,PO,AK,PHI,VISC,TALY
      COMMON/VAR/QMIX,AMVF,DGASF,DTFRAC,IFC,TFRAC,PFRAC,KFR,COEF,CS,QL
```

```
      COMMON/FRAC/SIG1,SIG2,SIG3,AKLCBOT,AKLCTOP,HFR,EFR,DPFR,PL
      COMMON/TEMP/GT,SURT,TEMPFR
      COMMON/FRAPAR/PFR,PANT,WF,WFM,AFANT,AF1ANT,AFATM,AF1ATM,DANT,
     *D1ANT,DANTM,D1ANTM,P1ANT,TFR
      COMMON/DIMFRA/AREA1,AREXP1,PER1,AF1,BF1,ARC,XLF,AF2,BF,DELX,
     *ARCEXP,PERC
      COMMON/VOL/VSANT,V1SANT
      IC=0
C     CALCULATE VARIABLES AT BOTTOM OF THE WELL
      CALL RES(GD,TD(1),P(1,2),QSC,I)
      CALL VELD(QSC,P(1,2),TD(1),CDDC,GD,VSGI)
      D(1,2)=GDEN(P(1,2),TD(1),GD)
      IF(VSLI.LT.1.D-3)THEN
        HL(1,2)=0.
        V(1,2)=0.D0
        VG(1,2)=VSGI
      ELSE
        CALL LIQHU(VSLI,VSGI,ST,DM,D(1,2),CAL,ODC,V(1,2),VG(1,2),
     *   HL(1,2))
      END IF
      CALL PARCEL(D(1,2),V(1,2),HL(1,2),VG(1,2),P(1,2),TD(1),GD,XN,XK,
     *CAL,ODC,AR,VM,DM,FMOM(1,2),CMOM(1,2),ELEV(1,2),FRC(1,2),VISL)
C  CALCULATIONS FOR PHASE I
      IF(I.LE.IT1)THEN
        HL(I,1)=AF
        CALL PARCEL(D(I,1),V(I,1),HL(I,1),VG(I,1),P(I,1),TD(I),GD,XN,
     *   XK,CAL,ODC,AR,VM,DM,FMOM(I,1),CMOM(I,1),ELEV(I,1),FRC(I,1),
     *   VISL)
        CALL FINDI1(P,V,D,HL,VG,I,IT1,TD,GD,DT,DXC,CAL,ODC,AR,DFGAS,
     *   XN,XK,DM,ST,VMIX,IC)
        IF(IC.EQ.1.OR.IC.EQ.2)RETURN
        CALL DPMUD1(DT,H,DDC,DCL,BW,VMIX(I-1,1),VMIX(I,2),XN,XK,CAL,
     *   ODP,ODC,DM,CDCC,CDDC,DPMUD,PIC)
        PINJC=DPMUD+DFGAS
        DIFF=PINJC-P(1,2)
        RETURN
C  CALCULATIONS FOR PHASE II
      ELSE IF(I.GT.IT1.AND.I.LE.IT2)THEN
        HL(I,3)=AF
        CALL PARCEL(D(I,3),V(I,3),HL(I,3),VG(I,3),P(I,3),TD(I),GD,XN,
     *   XK,CAL,ODP,AR,VM,DM,FMOM(I,3),CMOM(I,3),ELEV(I,3),FRC(I,3),
     *   VISL)
        CALL FINDI1(P,V,D,HL,VG,I,IT1,TD,GD,DT,DXC,CAL,ODC,AR,DFGAS1,
     *   XN,XK,DM,ST,VMIX,IC)
        IF(IC.EQ.1.OR.IC.EQ.2)RETURN
        V(IT1,4)=V(IT1,2)*CDDC/CDCC
        VG(IT1,4)=VG(IT1,2)*CDDC/CDCC
        HL(IT1,4)=HL(IT1,2)
        P(IT1,4)=P(IT1,2)
        D(IT1,4)=D(IT1,2)
        CALL PARCEL(D(IT1,4),V(IT1,4),HL(IT1,4),VG(IT1,4),P(IT1,4),
     *   TD(IT1),GD,XN,XK,CAL,ODP,AR,VM,DM,
     *   FMOM(IT1,4),CMOM(IT1,4),ELEV(IT1,4),FRC(IT1,4),VISL)
        CALL FINDI2(P,V,D,HL,VG,I,IT1,IT2,TD,GD,DT,DXP,CAL,ODP,AR,
     *   XN,XK,DM,DFGAS2,ST,VMIX,IC)
        IF(IC.EQ.1.OR.IC.EQ.2)RETURN
        CALL DPMUD2(DT,H,VMIX(I-1,3),VMIX(I,4),XN,XK,CAL,ODP,DM,
     *   DPMUD,PIC,DEPF)
```

```
      PINJC=DPMUD+DFGAS1+DFGAS2
      DIFF=PINJC-P(1,2)
C  CALCULATIONS FOR PHASE IV
     ELSE
      CALL FINDI1(P,V,D,HL,VG,I,IT1,TD,GD,DT,DXC,CAL,ODP,AR,DFGAS,
     *  XN,XK,DM,ST,VMIX,IC)
      IF(IC.EQ.1.OR.IC.EQ.2)RETURN
      V(IT1,4)=V(IT1,2)*CDCC/CDPC
      VG(IT1,4)=VG(IT1,2)*CDCC/CDPC
      HL(IT1,4)=HL(IT1,2)
      P(IT1,4)=P(IT1,2)
      D(IT1,4)=D(IT1,2)
      CALL PARCEL(D(IT1,4),V(IT1,4),HL(IT1,4),VG(IT1,4),P(IT1,4),
     *  TD(IT1),GD,XN,XK,CAU,ODP,AR,VM,DM,
     *  FMOM(IT1,4),CMOM(IT1,4),ELEV(IT1,4),FRC(IT1,4),VISL)
      CALL FINDI2(P,V,D,HL,VG,I,IT1,IT2,TD,GD,DT,DXP,CAU,ODP,AR,
     *  XN,XK,DM,DFGAS2,ST,VMIX,IC)
      IF(IC.EQ.1.OR.IC.EQ.2)RETURN
      IF(I.GT.IT2)THEN
     IF(I.EQ.IT2+1)THEN
      AMVF=HL(IT2,4)
      QMIX=VMIX(IT2,4)*CDCC/2.
      CNFR=1.
      KFR=1
      KPFR=1
      RHO=GDEN(PL,TEMPFR,GD)
      DANT(0)=RHO*(1.-AMVF)/7.48+AMVF*DM
      DANT(1)=DANT(0)
      DANTM(1)=DANT(0)
      D1ANTM(1)=DANT(0)
      D1ANT(0)=DANT(0)
      D1ANT(1)=DANT(1)
      IF(ICCF.EQ.1) THEN
      DTFRAC=(20.*ARC*DELX)/QMIX
      ICCF=0
      END IF
      IFC=1
      VFR=DELX/DTFRAC
      DPR=PL-PO
      TANT=0.
      TPOS=DTFRAC
      CALL LECOE(DPR,AMVF,TANT,TPOS,DVCOE,CS)
      TMCELL=0.5*(TANT+TPOS)
      IF(DVCOE.LT.CS) THEN
      COEF=0.
      ELSE
      COEF=(DVCOE-CS)/(2*DSQRT(TMCELL))
      END IF
      QL=VFR*ARC+2.22144*COEF*DSQRT(VFR)*(HFR)**1.5+2.*CS*HFR*VFR
      IF(QL.GE.QMIX) QL=QMIX-.1
      IFC=1
      TFRAC=0.
     ELSE
      IFC=IFC+1
      KPFR=1
      TFRAC=TFRAC+DTFRAC
      AF1=HFR
      BF1=HFR/2.
```

```
      END IF
        AMVF=HL(IT2,4)
        QMIX=VMIX(IT2,4)*CDCC/2.
        CNFR=1.
      END IF
      CALL FRACTURE(IFC,DTFRAC,QL,DPFR,QMIX,VFR,EFR,POIS,SIG1,SIG2,
     *SIG3,PL,CNFR,DM,DEPF,AMVF,TALY,VISC,KFR,KPFR,AKLC,AKLCBOT,
     *AKLCTOP,GD,HFR,COEF,CS,PIC,PO)
        PWD=DFGAS+DFGAS2+PIC
        DIFF=PWD-P(1,2)
      END IF
      RETURN
      END
C
C  SUBROUTINE FOR SOLVING THE TWO-PHASE UNSTEADY STATE FLOW IN THE
C  UNCASED PORTION OF THE WELL
C
      SUBROUTINE FINDI1(P,V,D,HL,VG,I,IT1,TD,GD,DT,DXC,DA,DB,AR,DFGAS,
     *XN,XK,DM,ST,VMIX,IC)
      IMPLICIT REAL*8 (A-H,O-Z)
      DIMENSION P(80,4),V(80,4),D(80,4),HL(80,4),VG(80,4),TD(0:99),
     *VMIX(80,4)
      COMMON/MAT/FRC(80,4),ELEV(80,4),CMOM(80,4),FMOM(80,4),KJ,KG
      KG=2
      VC=DXC/DT
      N=I-1
      IF(I.GT.IT1)N=IT1-1
      DO 10 J=1,N
        KJ=J
        K=1
        V(J+1,2)=VG(J,2)
        PGA=V(J+1,2)
        J1=J+1
        FM=4.
   20   CALL SOL(DXC,VC,D(J1,1),D(J,2),D(J1,2),V(J,2),V(J1,2),
     *   VG(J,2),VG(J1,2),HL(J1,1),HL(J,2),HL(J1,2),DM,TD(J1),GD,
     *   DA,DB,AR,XN,XK,P(J,2),P(J1,2),DIFF,VMD,ST,D(J,1),HL(J,1),
     *   IAFN)
        IF(V(J1,2).LE.0.D0)THEN
          IC=1
          RETURN
        END IF
        IF(P(J1,2).LE.0.D0)THEN
          IC=2
          RETURN
        END IF
        IF(K.GE.1) THEN
        IF(IAFN.EQ.1) THEN
        FM=FM/2.
        PGP=PGA+FM
        V(J+1,2)=PGP
        GO TO 20
        END IF
        END IF
        VMIX(N+1,2)=VMD
        IF(K.GT.2)GO TO 40
        IF(K.EQ.1)THEN
          PCA=DIFF
```

```
          FM=4.D0
          IF(DIFF.LT.0.)FM=-4.D0
          PGP=PGA+FM
          V(J+1,2)=PGP
          K=K+1
          GO TO 20
        END IF
        IF(DABS(DIFF).GT.DABS(PCA))THEN
          FM=FM/2.D0
          PGP=PGA+FM
          V(J+1,2)=PGP
          GO TO 20
        END IF
        IF(K.EQ.2)PCP=DIFF
   30   A=PGA
        B=PGP
        F=PCA
        C=PCP
        PGA=PGP
        PCA=PCP
        IF(DABS(A-B).LT.1.D-7)THEN
          IC=2
          RETURN
        END IF
        E=(F-C)/(A-B)
        CE=C/E
        PGP=B-CE
        V(J+1,2)=PGP
        K=K+1
        GO TO 20
   40   PCP=DIFF
        IF(DABS(DIFF).GT.DABS(PCA))THEN
          CE=CE/2.D0
          PGP=B-CE
          V(J+1,2)=PGP
          GO TO 20
        END IF
        IF(DABS(DIFF).LT.1.D-2)GO TO 60
        IF(K.GT.100)STOP 2
        GO TO 30
   60   CALL CRITV(TD(J+1),GD,DM,P(J+1,2),HL(J+1,2),CRIV)
        IF(VMD.GT.CRIV)THEN
          WRITE(*,*)'CRITICAL FLOW AT CASING SHOE'
        END IF
   10 CONTINUE
      DFGAS=P(1,2)-P(N+1,2)
      RETURN
      END
C
C  SUBROUTINE FOR SOLVING THE TWO-PHASE UNSTEADY STATE FLOW IN THE
C  CASED PORTION OF THE WELL
C
      SUBROUTINE FINDI2(P,V,D,HL,VG,I,IT1,IT2,TD,GD,DT,DXP,DA,DB,AR,
     *XN,XK,DM,DFGAS,ST,VMIX,IC)
      IMPLICIT REAL*8 (A-H,O-Z)
      DIMENSION P(80,4),V(80,4),D(80,4),HL(80,4),VG(80,4),TD(0:99),
     *VMIX(80,4)
      COMMON/MAT/FRC(80,4),ELEV(80,4),CMOM(80,4),FMOM(80,4),KJ,KG
```

```
      KG=4
      VC=DXP/DT
      N=I-1
      IF(I.GT.IT2)N=IT2-1
      DO 10 J=IT1,N
        KJ=J
        K=1
        V(J+1,4)=V(J,4)
        PGA=V(J+1,4)
        J1=J+1
        FM=8.
   20   CALL SOL(DXP,VC,D(J1,3),D(J,4),D(J1,4),V(J,4),
     *  V(J1,4),VG(J,4),VG(J1,4),HL(J1,3),HL(J,4),HL(J1,4),DM,TD(J1),
     *  GD,DA,DB,AR,XN,XK,P(J,4),P(J1,4),DIFF,VMD,ST,D(J,3),HL(J,3),
     *  IAFN)
        IF(V(J1,4).LE.0.D0)THEN
          IC=1
          RETURN
        END IF
        IF(P(J1,4).LE.0.D0)THEN
          IC=2
          RETURN
        END IF
        IF(K.GE.1) THEN
        IF(IAFN.EQ.1) THEN
        FM=FM/2.
        PGP=PGA+FM
        V(J+1,4)=PGP
        GO TO 20
        END IF
        END IF
        VMIX(N+1,4)=VMD
        IF(K.GT.2)GO TO 40
        IF(K.EQ.1)THEN
          PCA=DIFF
          FM=4.D0
          IF(DIFF.LT.0.)FM=-2.D0
          PGP=PGA+FM
          V(J+1,4)=PGP
          K=K+1
          GO TO 20
        END IF
        IF(DABS(DIFF).GT.DABS(PCA))THEN
          FM=FM/2.D0
          PGP=PGA+FM
          V(J+1,4)=PGP
          GO TO 20
        END IF
        IF(K.EQ.2)PCP=DIFF
   30   A=PGA
        B=PGP
        F=PCA
        C=PCP
        PGA=PGP
        PCA=PCP
        IF(DABS(A-B).LT.1.D-7)THEN
          IC=2
          RETURN
```

```
      END IF
      E=(F-C)/(A-B)
      CE=C/E
      PGP=B-CE
      V(J+1,4)=PGP
      K=K+1
      GO TO 20
   40   PCP=DIFF
      IF(DABS(DIFF).GT.DABS(PCA))THEN
        CE=CE/2.D0
        PGP=B-CE
        V(J+1,4)=PGP
        GO TO 20
      END IF
      IF(DABS(DIFF).LT.1.D-2)GO TO 10
      IF(K.GT.100)STOP 3
      GO TO 30
   10 CONTINUE
     DFGAS=P(IT1,4)-P(N+1,4)
     RETURN
     END
C
C  SUBROUTINE FOR SOLVING THE SYSTEM OF EQUATIONS OF THE TWO-PHASE
C  UNSTEADY STATE FLOW INSIDE EACH CELL
C
     SUBROUTINE SOL(DX,VC,DD,DUP,DDP,VUP,VDP,VGUP,VGDP,HD,HUP,
    *HDP,DM,T,GD,D1,D2,AR,XN,XK,PUP,PDP,DIFF,VMDP,ST,DU,HU,IAFN)
     IMPLICIT REAL*8 (A-H,O-Z)
     COMMON/REO/VISL
     COMMON/MAT/FRC(80,4),ELEV(80,4),CMOM(80,4),FMOM(80,4),KJ,KG
     IAFN=0
     R=D2/D1
     XK1=.345-.037*R+.235*R*R-.134*R*R*R
     XK2=1.1
     HDP=(VUP*HUP+VC*(HD+HU-HUP)/2.)/(VDP+VC/2.)
     IF(HDP.GE.1.) HDP=0.99999
     IF(HDP.GE..85)THEN
       VSB=.4774*(ST*(DM-DUP/7.48)/DM**2)**.25*HDP**.5
       VGDP=(VDP*XK2*HDP+VSB)/(1.-XK2+XK2*HDP)
     ELSE IF(HDP.LT..85.AND.HDP.GE..75)THEN
       VSB=.4774*(ST*(DM-DUP/7.48)/DM**2)**.25*.85**.5
       VGDPB=(VDP*XK2*.85+VSB)/(1.-XK2+XK2*.85)
       VSS=XK1*1.637*DSQRT(D1*(DM-DUP/7.48)/DM)
       VGDPS=(VDP*XK2*.75+VSS)/(1.-XK2+XK2*.75)
       VGDP=VGDPB+(HDP-.85)*(VGDPS-VGDPB)/(.75-.85)
     ELSE IF(HDP.LT..75.AND.HDP.GE..45)THEN
       VSS=XK1*1.637*DSQRT(D1*(DM-DUP/7.48)/DM)
       VGDP=(VDP*XK2*HDP+VSS)/(1.-XK2+XK2*HDP)
     ELSE IF(HDP.LT..45.AND.HDP.GE..10)THEN
       VSS=XK1*1.637*DSQRT(D1*(DM-DUP/7.48)/DM)
       VGDPS=(VDP*XK2*.45+VSS)/(1.-XK2+XK2*.45)
       VGDPA=VDP
       VGDP=VGDPS+(HDP-.45)*(VGDPA-VGDPS)/(.10-.45)
     ELSE
       VGDP=VDP
     END IF
     XNUM1=(DD*(1.-HD)+DU*(1.-HU)-DUP*(1.-HUP))*VC/2.
     XNUM2=DUP*(1-HUP)*VGUP
```

```
      DEN=(1-HDP)*(VGDP+VC/2.)
      DDP=(XNUM1+XNUM2)/DEN
      IF(DDP.GT.62.4) THEN
      IAFN=1
      RETURN
      END IF
      CALL ZFACHY(T,PUP,GD,Z)
      PDP=(DDP*(T+460.)*Z)/(2.7*GD)-14.7
      CALL PARCEL(DDP,VDP,HDP,VGDP,PDP,T,GD,XN,XK,D1,D2,AR,VMDP,DM,
     *FMOM(KJ+1,KG),CMOM(KJ+1,KG),ELEV(KJ+1,KG),FRC(KJ+1,KG),VISL)
      AA=(-FMOM(KJ,KG)+FMOM(KJ+1,KG-1)-FMOM(KJ,KG-1)+FMOM(KJ+1,KG))
      A=.000108*AA
      BB=(CMOM(KJ,KG)-CMOM(KJ+1,KG-1)-CMOM(KJ,KG-1)+CMOM(KJ+1,KG))
      B=.000108*BB*VC
      CC=ELEV(KJ,KG)+ELEV(KJ+1,KG-1)+ELEV(KJ,KG-1)+ELEV(KJ+1,KG)
      C=.001736*DX*CC
      E=.25*(FRC(KJ,KG)+FRC(KJ+1,KG-1)+FRC(KJ,KG-1)+FRC(KJ+1,KG))*DX
      DIFF=A+B+C+E+PDP-PUP
      RETURN
      END
C
C  THIS SUBROUTINE CALCULATES LIQUID HOLD-UP AT BOTTOM OF THE WELL
C
      SUBROUTINE LIQHU(VSL,VSG,ST,DM,D,D1,D2,V,VG,HC)
      IMPLICIT REAL*8 (A-H,O-Z)
      R=D2/D1
      XK1=.345-.037*R+.235*R*R-.134*R*R*R
      J=0
      H=VSL/(VSL+VSG)
   20 IF(H.GE..85)THEN
        VS=.4774*(ST*(DM-D/7.48)/DM**2)**.25*H**.5
        XK2=1.1
      ELSE IF(H.LT..85.AND.H.GE..75)THEN
        VSB=.4774*(ST*(DM-D/7.48)/DM**2)**.25*.85**.5
        VSS=XK1*1.637*DSQRT(D1*(DM-D/7.48)/DM)
        VS=VSB+(H-.85)*(VSS-VSB)/(.75-.85)
        XK2=1.1
      ELSE IF(H.LT..75.AND.H.GE..45)THEN
        VS=XK1*1.637*DSQRT(D1*(DM-D/7.48)/DM)
        XK2=1.1
      ELSE IF(H.LT..45.AND.H.GE..10)THEN
        VSS=XK1*1.637*DSQRT(D1*(DM-D/7.48)/DM)
        VSA=0.
        VS=VSS+(H-.45)*(VSA-VSS)/(.10-.45)
        XK2=1.1+(H-.45)*(1.0-1.1)/(.10-.45)
      ELSE
        VS=0.
        XK2=1.0
      END IF
      VG=XK2*(VSG+VSL)+VS
      HC=1-VSG/VG
      IF(ABS(H-HC).LT..001)GO TO 10
      H=HC
      J=J+1
      IF(J.GT.20)STOP 22
      GO TO 20
   10 IF(HC.GT.1.) HC=0.99999
      V=VSL/HC
```

```
      RETURN
      END
C
C  THIS SUBROUTINE CALCULATES CAPACITIES
C
      SUBROUTINE SINIT(CDCC,CDPC,CDDC,CAL,CAU,ODP,ODC)
      IMPLICIT REAL*8 (A-H,O-Z)
      CDCC=.0054541539*(CAL**2-ODP**2)
      CDPC=.0054541539*(CAU**2-ODP**2)
      CDDC=.0054541539*(CAL**2-ODC**2)
      RETURN
      END
C
C  THIS SUBROUTINE PRESSURE GRADIENTS
C
      SUBROUTINE PARCEL(D,V,H,VG,P,T,GD,XN,XK,D1,D2,AR,VM,DM,A,B,C,E,
     *VISL)
      IMPLICIT REAL*8 (A-H,O-Z)
      A=DM*7.48*V**2*H+D*VG**2*(1-H)
      B=DM*7.48*V*H+D*VG*(1-H)
      C=DM*7.48*H+D*(1-H)
      VSL=V*H
      VSG=VG*(1.-H)
      VM=VSL+VSG
      HLNS=VSL/VM
      IF(HLNS.GT..99999.OR.HLNS.LT..00001)GO TO 10
      Y=HLNS/(H**2)
      X=DLOG(Y)
      S=X/(-.0523+3.182*X-.8725*X**2+.01853*X**4)
      IF (Y.GT.1.AND.Y.LT.1.2) S=DLOG(2.2*Y-1.2)
      XM=DEXP(S)
      CALL GASVIS (T,GD,P,VISG)
      DENSM=D*(1.-HLNS)+DM*HLNS*7.48
      VISCM=VISG*(1.-HLNS)+VISL*HLNS
      CALL FRICG (VM,VISCM,D1,D2,AR,DENSM,1,GFM)
      E=XM*GFM
   10 IF(HLNS.GT..99999)CALL FRICM (VM,XN,XK,D1,D2,DM,1,E)
      IF(HLNS.LT..00001)THEN
      CALL GASVIS (T,GD,P,VISG)
      CALL FRICG (VM,VISG,D1,D2,AR,D,1,E)
      END IF
      RETURN
      END
C
C  THIS SUBROUTINE SINGLE-PHASE PRESSURE DROPS FOR PHASE I
C
      SUBROUTINE DPMUD1(DT,H,DDC,DCL,BW,VMCB,VMCA,XN,XK,CAL,ODP,
     *ODC,DM,CDCC,CDDC,DPMUD,PIC)
      IMPLICIT REAL*8 (A-H,O-Z)
      COMMON/RESULTS/DSHOE
      COMMON/MAINP/AF,VSLI
      DB=0.
      VMP=VMCA*CDDC/CDCC
      IF(ABS(VMCA).LE.1.D-3)THEN
      GMC=0.
      GMP=0.
      ELSE
      CALL FRICM (VMCA,XN,XK,CAL,ODC,DM,1,GMC)
```

```
      CALL FRICM (VMP,XN,XK,CAL,ODP,DM,1,GMP)
      END IF
      DVEL=VMCA-VMCB
      DVMP=DVEL*CDDC/CDCC
      GHM=.052*DM
      GAC=.001615*DM*DVEL/DT
      GAP=.001615*DM*DVMP/DT
      DPC=(GHM+GMC+GAC)*(DDC-BW+H)
      DPP=(GHM+GMP+GAP)*DCL
      DSHOE=PIC
      DPMUD=DPC+DPP+PIC
      RETURN
      END
C
C  THIS SUBROUTINE SINGLE-PHASE PRESSURE DROPS FOR PHASE II
C
      SUBROUTINE DPMUD2(DT,H,VMPB,VMP,XN,XK,CAL,ODP,DM,DPMUD,PIC,DEPF)
      IMPLICIT REAL*8 (A-H,O-Z)
      COMMON/RESULTS/DSHOE
      COMMON/MAINP/AF,VSLI
      DB=0.D0
      CALL FRICM(VMP,XN,XK,CAL,ODP,DM,1,GMP)
      DVP=VMP-VMPB
      GHM=.052*DM
      GAP=.001615*DM*DVP/DT
      DPP=(GHM+GMP+GAP)*(H-DEPF)
      DPMUD=DPP+PIC
      RETURN
      END
C
C  THIS SUBROUTINE CALCULATES TWO-PHASE CRITICAL VELOCITY BASED ON
C  WALLIS' EQUATION
C
      SUBROUTINE CRITV(T,SG,DM,P,HL,CRIV)
      IMPLICIT REAL*8 (A-H,O-Z)
      CW=3.D-6
      CALL ZFACHY(T,P,SG,Z)
      D=2.7*SG*(P+14.7)/(Z*(T+460.))
      CRGAS=41.4*SQRT(1.3*Z*(460.+T)/SG)
      CRLIQ=68.1*SQRT(1./(CW*DM*7.48))
      PAR1=(1-HL)*D+HL*DM*7.48
      PAR2=(1-HL)/(D*CRGAS**2)
      PAR3=HL/(DM*7.48*CRLIQ**2)
      A=PAR1*(PAR2+PAR3)
      CRIV=DSQRT(1./A)
      RETURN
      END
C
C  SUBROUTINE TO CALCULATE FLOW VELOCITIES
C
      SUBROUTINE VELD(QSC,P,T,CAP,SG,GVEL)
      IMPLICIT REAL*8 (A-H,O-Z)
      CALL ZFACHY(T,P,SG,Z)
      Q=.32719*QSC*Z*(T+460.)/(P+14.7)
      GVEL=Q/CAP
      RETURN
      END
C
```

```
C  SUBROUTINE TO CALCULATE GAS DENSITIES
C
      FUNCTION GDEN(P,T,SG)
      IMPLICIT REAL*8 (A-H,O-Z)
      CALL ZFACHY(T,P,SG,Z)
      GDEN=2.7*SG*(P+14.7)/(Z*(T+460.))
      RETURN
      END
C
C
C  SUBROUTINE TO CALCULATE GAS VISCOSITIES
C
      SUBROUTINE GASVIS (T,SGFG,PI,GVIS)
      IMPLICIT REAL*8 (A-H,O-Z)
      P=PI
      IF(P.LE.-14.5)P=-14.5
      TABS=T+460.
      W=SGFG*29.
      AK=(9.4+.02*W)*(TABS**1.5)/(209.+19.*W+TABS)
      X=3.5+(986./TABS)+.01*W
      Y=2.4-.2*X
      CALL ZFACHY (T,P,SGFG,Z)
      RHOG=(P+14.7)*W/(10.72*Z*TABS*62.4)
      GVIS=AK*DEXP(X*RHOG**Y)/10000.
      RETURN
      END
C
C  SUBROUTINE TO CALCULATE FRICTIONAL PRESSURE DROPS FOR NEWTONIAN
C  FLUIDS
C
      SUBROUTINE FRICG (V,VIS,D1,D2,AR,GDP,I,GGF)
      IMPLICIT REAL*8 (A-H,O-Z)
      GD=GDP/7.48
      RR=AR/(D1-D2)
      IF(I.EQ.1)GO TO 10
      RN=928*GD*V*D1/VIS
      IF(RN.GT.2000.)GO TO 20
      FF=16./RN
      GO TO 30
   20 CALL FRFACT(RN,RR,FF)
   30 GGF=FF*GD*V**2/(25.8*D1)
      RETURN
   10 RN=928.*GD*V*(D1-D2)/VIS
      IF(RN.GT.2000.)GO TO 40
      FF=24./RN
      GO TO 50
   40 CALL FRFACT(RN,RR,FF)
   50 GGF=FF*GD*V**2/(25.8*(D1-D2))
      RETURN
      END
C
C  SUBROUTINE TO CALCULATE FRICTIONAL PRESSURE DROPS FOR POWER-LAW
C  FLUIDS
C
      SUBROUTINE FRICM(V,XN,XK,D1,D2,DM,I,GGF)
      IMPLICIT REAL*8 (A-H,O-Z)
      RNL=3470.-1370.*XN
      IF(I.EQ.1)GO TO 10
```

```
      RN=1.86*DM*DABS(V)**(2.-XN)*(D1/96.)**XN/XK
      IF(V.LE.0.D0)RN=-RN
      IF(RN.GT.RNL)GO TO 20
      FF=16/RN
      GO TO 30
   20 FF=FRIC(RN,XN)
   30 GGF=FF*DM*V**2/(25.8*D1)
      RETURN
   10 XKA=XK*((8.*XN+4.)/(9.*XN+3.))**XN
      RN=2.79*((D1-D2)/144.)**XN*DABS(V)**(2.-XN)*DM/XKA
      IF(V.LE.0.D0)RN=-RN
      IF(RN.GT.RNL)GO TO 40
      FF=24./RN
      GO TO 50
   40 FF=FRIC(RN,XN)
   50 GGF=FF*DM*V**2/(25.8*(D1-D2))
      RETURN
      END
C
C  SUBROUTINE TO CALCULATE DODGE-METZNER FRICTION FACTOR
C
      FUNCTION FRIC(RN,XN)
      IMPLICIT REAL*8 (A-H,O-Z)
      I=0
      F=.0791/RN**.25
      TL=1.D-4
   20 FC=(1/((4.*DLOG10(RN*F**(1.-XN/2.))/XN**.75)-.4/XN**1.2))**2.
      IF(DABS(F-FC).LE.TL)GO TO 10
      IF(I.GT.30)STOP 10
      I=I+1
      F=FC
      GO TO 20
   10 FRIC=FC
      RETURN
      END
C
C
C
C  FUNCTION TO CALCULATE MOODY FRICTION FACTOR
C
      FUNCTION FRFACM(REY,ED)
      IMPLICIT REAL*8 (A-H,O-Z)
      IF (REY.GT.2000) GO TO 1
      FF=64./REY
      GO TO 8
    1 FGI=0.0056+0.5/REY**0.32
      I=1
    5 DEN=1.14-2.*DLOG10(ED+9.34/(REY*SQRT(FGI)))
      FF=(1./DEN)**2
      DIFF=ABS(FGI-FF)
      IF (DIFF.LE.0.0001) GO TO 8
      FGI=(FGI+FF)/2.
      I=I+1
      IF (I.LT.10) GO TO 5
      FF=FGI
    8 CONTINUE
      FRFACM=FF
      RETURN
```

```
      END
C
C
C
C  SUBROUTINE TO CALCULATE FANNING FRICTION FACTOR
C
      SUBROUTINE FRFACT (REY,ED,FF)
      IMPLICIT REAL*8 (A-H,O-Z)
      FGI=0.0056+0.5/REY**0.32
      I=1
    5 DEN=1.14-2.*DLOG10(ED+9.34/(REY*DSQRT(FGI)))
      FF=(1./DEN)**2
      DIFF=DABS(FGI-FF)
      IF (DIFF.LE.1.D-4) GO TO 8
      FGI=(FGI+FF)/2.
      I=I+1
      IF (I.LT.10) GO TO 5
      WRITE(6,1)
    1 FORMAT(1X,' THE FRICTION FACTOR DOES NOT CONVERGE')
      STOP
    8 FF=FF/4.
      RETURN
      END


C  SUBROUTINE TO CALCULATE Z FACTOR
C
      SUBROUTINE ZFACHY(T,P,SGFG,Z)
      IMPLICIT REAL*8 (A-H,O-Z)
      TC = 169.0 + 314.0 * SGFG
      PC = 708.75 - 57.5 * SGFG
      TR = (T + 459.67) / TC
      PR = ( P + 14.7 ) / PC
      IF(PR.LE.0.0) GOTO 2
      A = 0.06423
      B = 0.5353*TR-0.6123
      C = 0.3151*TR-1.0467-0.5783/(TR*TR)
      D = TR
      E = 0.6816/(TR*TR)
      F = 0.6845
      G = 0.27*PR
      X = G/D
      Z1 = 1.0
      X0 = X
    1 XS = X0*X0
      XC = XS*X0
      FX = A*XC*XC+C*XS+D*X0+XC*(B+E*(1.0+F*XS)/DEXP(F*XS))-G
      FPX = 6.0*A*XC*XS+2.0*C*X0+D+XS*(3.0*B+E*(3.0+
     $ F*XS*(3.0-2.0*F*XS))/DEXP(F*XS))
      X1 = X0 - FX / FPX
      Z2 = X / X1
      X0 = X1
      DIF = DABS(Z2-Z1)
      Z1 = Z2
      IF(DIF.GT.1.D-4) GOTO 1
      Z = Z2
      RETURN
```

```
    2 Z = 1.0
      RETURN
      END

C
      FUNCTION FLAGR (X,Y,XARG,IDEG,NPTS)
      IMPLICIT REAL*8 (A-H,O-Z)
      DIMENSION X(NPTS),Y(NPTS)
      N=IABS(NPTS)
      N1=IDEG+1
      L=1
      IF (X(2).GT.X(1)) GO TO 1
      L=2
    1 GO TO (2,3),L
    2 IF (XARG.LE.X(1)) GO TO 4
      IF (XARG.GE.X(N)) GO TO 5
      GO TO 6
    3 IF (XARG.GE.X(1)) GO TO 4
      IF (XARG.LE.X(N)) GO TO 5
      GO TO 6
    4 FLAGR=Y(1)
      RETURN
    5 FLAGR=Y(N)
      RETURN
    6 GO TO (10,20),L
   10 DO 11 MAX=N1,N
      IF (XARG.LT.X(MAX)) GO TO 12
   11 CONTINUE
   20 DO 21 MAX=N1,N
      IF (XARG.GT.X(MAX)) GO TO 12
   21 CONTINUE
   12 MIN=MAX-IDEG
      FACTOR=1.
      DO 7 I=MIN,MAX
      IF (XARG.NE.X(I)) GO TO 7
      FLAGR=Y(I)
      RETURN
    7 FACTOR=FACTOR*(XARG-X(I))
      YEST=0.
      DO 9 I=MIN,MAX
      TERM=Y(I)*FACTOR/(XARG-X(I))
      DO 8 J=MIN,MAX
      IF (I.NE.J) TERM=TERM/(X(I)-X(J))
    8 CONTINUE
    9 YEST=YEST+TERM
      FLAGR=YEST
      RETURN
      END


      SUBROUTINE FRACTURE(IFR,DTAS,QL,DP,QMIX,V,E,POIS,SIG1,SIG2,SIG3,
     *PL,CN,DM,DEPF,AMVF,TALY,VISC,K,KP,AKLC,AKLCBOT,AKLCTOP,GD,
     *H,COEF,CS,PIC,PO)
      IMPLICIT REAL*8(A-H,O-Z)
      DIMENSION TFR(0:500),PFR(0:500),PANT(0:500),WF(0:30),WFM(0:30),
     *AFANT(0:500),AF1ANT(0:500),AFATM(0:500),AF1ATM(0:500),
     *DANT(0:500),D1ANT(0:500),DANTM(0:500),D1ANTM(0:500),
     *P1ANT(0:500)
```

```
      DIMENSION VSANT(0:500),V1SANT(0:500)
      COMMON/TEMP/GT,SURT,TEMPFR
      COMMON/FRAPAR/PFR,PANT,WF,WFM,AFANT,AF1ANT,AFATM,AF1ATM,DANT,
     *D1ANT,DANTM,D1ANTM,P1ANT,TFR
      COMMON/DIMFRA/AREA1,AREXP1,PER1,AF1,BF1,ARC,XLF,AF2,BF,DELX,
     *ARCEXP,PERC
      COMMON/VOL/VSANT,V1SANT
      K=1
      KP=1
      XLF=IFR*DELX
      PGA=QL
      ITFU=0
   10 NC=IFR
      DO 100 J=1,IFR
      PGAP=DP
   20 PFR(J)=PFR(J-1)+DP
      P1=PFR(J-1)
      P2=PFR(J)
      RHO1=GDEN(P1,TEMPFR,GD)
      RHO2=GDEN(P2,TEMPFR,GD)
      DMIX1=RHO1*(1.-AMVF)/7.48+AMVF*DM
      DMIX2=RHO2*(1.-AMVF)/7.48+AMVF*DM
      IF(J.EQ.1) THEN
      VSANT(1)=0.
      Q1=QL
      AREXP1=ARCEXP
      PER1=PERC
      AREA1=ARC
      END IF
      TFR(IFR)=TFR(IFR-1)+DTAS
      TAL2=TFR(NC-1)
      TAL1=TFR(NC)
      PM=0.5*(P1+P2)
      RHOM=GDEN(PM,TEMPFR,GD)
      DMIXM=RHOM*(1.-AMVF)/7.48+AMVF*DM
      CALL HEIGHT(H,SIG1,SIG2,SIG3,AKLCBOT,AKLCTOP,P2,AF,BF,DELX,
     *AFANT(J-1),PL,J)
      JTM=2*(2*J-1)
      CALL HEIGHT(H,SIG1,SIG2,SIG3,AKLCBOT,AKLCTOP,PM,AFM,BFM,DELX/2.,
     *AFATM(J-1),PL,JTM)
      AF2=2.*AF
      AFMM=2.*AFM
      CALL WIDTH(E,POIS,H,SIG1,SIG2,SIG3,P2,AF,BF,WF,AREA,AREXP,CN,PER)
      CALL WIDTH(E,POIS,H,SIG1,SIG2,SIG3,PM,AFM,BFM,WFM,AREAM,ARPM,CN,
     *PERM)
      PER2=PER
      AREXP2=AREXP
      AREA2=AREA
      IF(J.EQ.1) THEN
      ANT1=H
      ANT2=H
      ANTM=H
      ELSE
      ANT1=2*AFANT(J-2)
      ANT2=2*AFANT(J-1)
      ANTM=2*AFATM(J-1)
      END IF
      CALL RUNGFLOW(DELX,COEF,H,AF1,AF2,P1,P2,Q1,Q2,TAL1,TAL2,TFR(IFR),
```

```
     *PANT(J-1),PANT(J),DTAS,POIS,E,J,V,AFMM,DMIX1,DMIX2,DMIXM,DANT
     *(J-1),DANT(J),DANTM(J),ANT1,ANT2,ANTM,PO,AMVF,IFR)
      CALL RUNGPRES(DELX,P1,P2C,Q1,Q2,AREXP1,AREXP2,CN,ARPM,
     *DP,GD,TEMPFR,AMVF,VISC,TALY,PER1,PER2,PERM,AREA1,AREA2,AREAM)
      DIFFP=P2C-P2
      EPP=0.1
      CALL ITERATION(KP,DIFFP,PCAP,FP,DP,PGPP,PGAP,ITERP,PCPP,CEP,BP,
     *EPP)
      IF(ITERP.EQ.0) GO TO 20
      AREXP1=AREXP2
      PER1=PER2
      AREA1=AREA2
      KP=1
      AF1=AF2
      BF1=BF
      Q1=Q2
      P1ANT(J+1)=P2
      D1ANT(J+1)=DMIX2
      D1ANTM(J+1)=DMIXM
      NC=NC-1
      AF1ANT(J)=AF
      AF1ATM(J)=AFM
  100 CONTINUE
      DIFF=QMIX-Q2
      EPQ=0.1
      CALL ITQ(K,DIFF,PCA,FQ,QL,PGP,ITER,EPQ,PGA,IC,ITFU)
      DPR=PL-PO
      TANT=0.
      TPOS=DTAS
      CALL LECOE(DPR,AMVF,TANT,TPOS,DVCOE,CS)
        TMCELL=0.5*(TANT+TPOS)
        IF(DVCOE.LT.CS) THEN
        COEF=0.
        ELSE
        COEF=(DVCOE-CS)/(2*DSQRT(TMCELL))
        END IF
      AQ1=-2.22144*COEF*(H)**1.5
      AQ2=DSQRT((2.22144*COEF*(H)**1.5)**2+4.*QL*(ARC+2.*CS*H))
      AQ3=(AQ1+AQ2)/(2.*(ARC+2*CS*H))
      DTAS=DELX/(AQ3**2)
      V=DELX/DTAS
      AF1=H
      IF(ITER.EQ.0) GO TO 10
      PIC=PFR(IFR)
      RETURN
      END

      SUBROUTINE WIDTH(E,POIS,H,SIG1,SIG2,SIG3,P,AF,BF,WF,AREA,AREXP,CN,
     *PER)
      IMPLICIT REAL*8(A-H,O-Z)
      DIMENSION WF(0:30)
      E1=E/(1.-POIS**2)
      DY=AF/10.
      Y=-AF
      AREA=0.
      AREXP=0.
      PER=0.
      DO 10 I=1,21
```

```
      IF(I.EQ.1.OR.I.EQ.21) THEN
      W1=0.
      W2=0.
      W3=0.
      GO TO 20
      END IF
      W1=4.*(P-SIG1)*DSQRT(AF**2-Y**2)/E1
      AUX1=4.*(SIG2-SIG1)/(E1*3.1416)
      IF(BF.EQ.AF) THEN
      W2=0.
      ELSE
      Z1=(AF**2-BF*Y)/(AF*DABS(Y-BF))
      AUX2=-(BF-Y)*DLOG(Z1+DSQRT(Z1**2-1.))
      AUX3=DACOS(BF/AF)*DSQRT(AF**2-Y**2)
      W2=AUX1*(AUX2+AUX3)
      END IF
      BF3=H-BF
      IF(BF3.EQ.AF) THEN
      W3=0.
      ELSE
      AUX4=4*(SIG3-SIG1)/(E1*3.1416)
      Z2=(AF**2+BF3*Y)/(AF*DABS(Y+BF3))
      AUX5=-(BF3+Y)*DLOG(Z2+DSQRT(Z2**2-1.))
      AUX6=DACOS(BF3/AF)*DSQRT(AF**2-Y**2)
      W3=AUX4*(AUX5+AUX6)
      END IF
   20 WF(I)=W1-W2-W3
      IF(I.GT.1) THEN
      ARINC=DY*(WF(I)+WF(I-1))/2.
      ARTO=DY*((WF(I)+WF(I-1))/2.)**((2.*CN+1.)/CN)
      WPM=ABS((WF(I)-WF(I-1))/2.)
      PERINC=2.*DSQRT(WPM**2.+DY**2.)
      AREA=AREA+ARINC
      AREXP=AREXP+ARTO
      PER=PERINC+PER
      END IF
      Y=Y+AF/10.
      IF(ABS(Y-AF).LT.0.001) Y=AF
   10   CONTINUE
      AREXP=AREXP**CN
      RETURN
      END

      SUBROUTINE HEIGHT(H,SIG1,SIG2,SIG3,AKLCBOT,AKLCTOP,P,AF,BF,DX,
     *AFANT,P1,J)
      IMPLICIT REAL*8(A-H,O-Z)
      K=1
      ITCOUN=0
      A2=(SIG2-SIG1)
      A3=(SIG3-SIG1)
      AUX1=(A2/A3)**2
      SIGMIN=MIN(SIG2,SIG3)
      SIGMAX=MAX(SIG2,SIG3)
      IF(SIGMIN.EQ.SIGMAX) ITC=1
      CALL LIM1(H,SIGMIN,SIG1,P,AKLCTOP,AFMAX1,DX,AFANT,P1,J)
      CALL LIM1(H,SIGMAX,SIG1,P,AKLCTOP,AFMIN1,DX,AFANT,P1,J)
      CALL LIM(H,SIGMIN,SIG1,P,AKLCTOP,AFMAX,DX,AFANT,P1,J)
      CALL LIM(H,SIGMAX,SIG1,P,AKLCTOP,AFMIN,DX,AFANT,P1,J)
```

```
      IF(ITC.EQ.1.AND.AKLCTOP.EQ.AKLCBOT) THEN
      AASS=AFMAX
      BF=H/2.
      GO TO 50
      END IF
      AFUMIN=MIN(AFMIN1,AFMIN)
      AFUMAX=MAX(AFMAX1,AFMAX)
      AASS=AFANT
      PGA=AASS
10    A1=0.886227*(AKLCBOT-AKLCTOP)*DSQRT(AASS)
      AUX2=DSQRT(4.*H**2-4.*(1.-AUX1)*(AASS**2*
     *(AUX1-1.)+H**2))
      GV=2.*(AASS-AFANT)*(P-P1)/(J*DX**2)
      IF(AUX1.EQ.1.) THEN
      B1=H/2.
      ELSE
      B1=(2.*H+AUX2)/(2.*(1.-AUX1))
      B2=(2.*H-AUX2)/(2.*(1.-AUX1))
      D=ABS(B1)-ABS(B2)
      IF(D.GT.0.) B1=B2
      END IF
      BF=B1
      IF(ABS(B1).GT.AASS) THEN
      BF=AASS
      END IF
      IF(BF.EQ.AASS) GO TO 2
      DO 1 ITER=1,100
      IF((H-BF).GT.AASS) THEN
      BF=H-AASS
      GO TO 2
      ELSE
      DEL1=A2*DSQRT(AASS**2-BF**2)-A3*DSQRT(AASS**2-
     *(H-BF)**2)-A1
      DEL2=-BF*A2/DSQRT(AASS**2-BF**2)-(A3*(H-BF)/
     *DSQRT(AASS**2-(H-BF)**2))
      END IF
      DELTAB=-DEL1/DEL2
      BF=BF+DELTAB
      IF(ABS(DELTAB/BF).LT.0.001) GO TO 2
1     CONTINUE
2     IF(BF.GT.AASS) BF=AASS
      A4=0.886227*(AKLCBOT+AKLCTOP)/DSQRT(AASS)
      A5=A2*DACOS(BF/AASS)
      A6=A3*DACOS((H-BF)/AASS)
      PC=(A5+A6+A4+2.*AASS*GV)/3.1416+SIG1
      DIFF=P-PC
      EPS=0.1
      CALL ITERATION(K,DIFF,PCA,FM,AASS,PGP,PGA,ITER,PCP,CE,B,EPS)
      IF(K.EQ.1.AND.AASS.LT.H/2.)THEN
      AASS=H/2.
      ITCOUN=1
      END IF
      IF(AASS.LT.H/2.) THEN
      ITCOUN=ITCOUN+1
      AASS=H/2.
      END IF
      IF(ITCOUN.EQ.2) GO TO 50
      IF(ITER.EQ.0) GO TO 10
```

```
 50   AF=AASS
      RETURN
      END

      SUBROUTINE LIM(H,SIG,SIG1,P,AKLC,AF,DX,ASANT,P1,J)
      IMPLICIT REAL*8(A-H,O-Z)
      K=1
      AASS=1.001*ASANT
      A1=1.772453*(P-SIG1)
      DO 4 I=1,100
      GV=2.*(AASS-ASANT)*(P-P1)/(J*DX**2)
      F1=A1*DSQRT(AASS)-1.128379*(SIG-SIG1)*DSQRT(AASS)*
     *DACOS(H/(2.*AASS))-AKLC-1.12838*AASS**1.5*GV
      F2=0.886225*(P-SIG1)/(DSQRT(AASS))-0.5641895*(SIG-SIG1)*
     *DACOS(H/(2.*AASS))/DSQRT(AASS)-1.128379*(SIG-SIG1)*
     *DSQRT(AASS)*(H/(AASS*DSQRT(4.*AASS**2-H**2)))-1.6926*GV*AASS**0.5
     *-2.25676*AASS**1.5*(P-P1)/(J*DX**2)
      DELX=-F1/F2
      AASS=AASS+DELX
      IF(AASS.LT.H/2.) AASS=H/2.
      IF(ABS(DELX/AASS).LT.0.001.OR.AASS.EQ.H/2.) THEN
      AF=AASS
      RETURN
      END IF
     4 CONTINUE
      RETURN
      END

      SUBROUTINE LIM1(H,SIG,SIG1,P,AKLC,AF,DX,ASANT,P1,J)
      IMPLICIT REAL*8(A-H,O-Z)
      K=1
      AASS=1.001*ASANT
      A1=1.772453*(P-SIG1)
      DO 4 I=1,100
      GV=2.*(AASS-ASANT)*(P-P1)/(J*DX**2)
      F1=A1*DSQRT(AASS)-0.56419*(SIG-SIG1)*(DSQRT(AASS)*
     *DACOS(1.-H/AASS)+DSQRT((2.*AASS*H-H**2)/AASS))
     *-1.12838*AASS**1.5*GV-AKLC
      F2=0.886227*(P-SIG1)/DSQRT(AASS)-0.5641896*(SIG-SIG1)*
     *(0.5*DACOS(1.-H/AASS)/DSQRT(AASS)-H/(AASS**1.5*
     *DSQRT(1.-(1.-H/AASS)**2))+0.5*H**2/(AASS**2*
     *DSQRT((2*AASS*H-H**2)/AASS)))-1.6926*AASS**0.5*GV
     *-2.25676*AASS**1.5*(P-P1)/(J*DX**2)
      DELX=-F1/F2
      AASS=AASS+DELX
      IF(AASS.LT.H/2.) AASS=H/2.
      IF(ABS(DELX/AASS).LT.0.001.OR.AASS.EQ.H/2.) THEN
      AF=AASS
      RETURN
      END IF
     4 CONTINUE
      RETURN
      END


      SUBROUTINE ITERATION(K,DIFF,PCA,FM,VAR,PGP,PGA,ITER,PCP,CE,B,EPS)
      IMPLICIT REAL*8(A-H,O-Z)
      ITER=0
```

```
      IF(K.GT.2) GO TO 40
      IF(K.EQ.1)THEN
      IF(DABS(DIFF).LT.EPS) THEN
      ITER=1
      RETURN
      END IF
      PCA=DIFF
      FM=VAR/10.
      IF(DIFF.LT.0.) FM=-FM
      PGP=PGA+FM
      VAR=PGP
      K=K+1
      RETURN
      END IF
      IF(DABS(DIFF).LT.EPS) THEN
      ITER=1
      RETURN
      END IF
      IF(DABS(DIFF).GT.DABS(PCA)) THEN
      FM=FM/2.
      PGP=PGA+FM
      VAR=PGP
      RETURN
      END IF
      IF(K.EQ.2) PCP=DIFF
30    A=PGA
      B=PGP
      F=PCA
      C=PCP
      PGA=PGP
      PCA=PCP
      IF(DABS(A-B).LT.1.D-9) THEN
      IF(DIFF.GT.0.) THEN
      VAR=VAR+VAR/10.
      RETURN
      ELSE
      VAR=VAR-VAR/10.
      RETURN
      END IF
      END IF
      E=(F-C)/(A-B)
      CE=C/E
      PGP=B-CE
      VAR=PGP
      K=K+1
      IF(DABS(DIFF).LT.EPS) ITER=1
      RETURN
40    PCP=DIFF
      IF(DABS(DIFF).GT.DABS(PCA))THEN
      CE=CE/2.
      PGP=B-CE
      VAR=PGP
      RETURN
      END IF
      IF(DABS(DIFF).LT.EPS) THEN
      ITER=1
      RETURN
      ELSE
```

```
IF(K.GT.100) STOP 2
GO TO 30
END IF
END


SUBROUTINE ITQ(K,DIFF,PCA,FM,VAR,PGP,ITER,EPS,PGA,IC,ITFU)
IMPLICIT REAL*8(A-H,O-Z)
ITER=0
IF(K.EQ.1)THEN
IF(DABS(DIFF).LT.EPS) THEN
ITER=1
RETURN
END IF
PCA=DIFF
FM=VAR/30.
IF(ITFU.EQ.1) FM=FM/10.
IF(DIFF.LT.0.) FM=-FM
PGP=PGA+FM
VAR=PGP
IC=0
K=K+1
RETURN
END IF
IF(DABS(DIFF).LT.EPS) THEN
ITER=1
RETURN
END IF
IF((PCA*DIFF).LT.0.) THEN
FM=FM/2.
PGP=PGA+FM
VAR=PGP
IF(ABS(VAR-PGA).LT.1.D-9) THEN
VAR=(VAR+PGA)/2.
K=1
ITFU=1
PGA=VAR
ITER=1
RETURN
END IF
IC=1
K=K+1
RETURN
END IF
IF(IC.EQ.0) THEN
PCA=DIFF
PGA=PGP
PGP=PGP+FM
IF(PGP.LE.0.) THEN
FM=FM/2.
PGP=PGP+ABS(FM)
END IF
VAR=PGP
K=K+1
RETURN
ELSE
FM=FM/2.
PGA=PGP
```

```
      PGP=PGP+FM
      PCA=DIFF
      VAR=PGP
      IC=0
      K=K+1
      RETURN
      END IF
      RETURN
      END

      SUBROUTINE RUNGFLOW(DELX,COE,H,AF1,AF2,P1,P2,Q1,Q2,TAL1,TAL2,T,
     *PANT1,PANT2,DT,POIS,E,J,V,AFMM,DMIX1,DMIX2,DMIXM,DANT1,DANT2,
     *DANTM,ANT1,ANT2,ANTM,PO,AMVF,IFR)
      IMPLICIT REAL*8(A-H,O-Z)
      DIMENSION VSANT(0:500),V1SANT(0:500)
      COMMON/VOL/VSANT,V1SANT
      E1=E/(1.-POIS**2)
      AF1M=0.5*(AF1+ANT1)
      AF2M=0.5*(AF2+ANT2)
      AFMMT=0.5*(AFMM+ANTM)
      PM=0.5*(P1+P2)
      DPR=P1-PO
      TANT=T-TAL1
      TPOS=T-TAL2
      CALL LECOE(DPR,AMVF,TANT,TPOS,DVCOE,CS)
      TMCELL=0.5*(TANT+TPOS)
      VOLCOE=VSANT(J)+DVCOE
      IF(VOLCOE.LT.CS) THEN
      COE=0.
      ELSE
      COE=(VOLCOE-CS)/(2*DSQRT(TMCELL))
      END IF
      V1SANT(J+1)=VSANT(J)+DVCOE
      IF(J.EQ.1) THEN
      IF(P1*DMIX1.LT.PANT1*DANT1) THEN
      RK1=0.
      ELSE
      RK1=DELX*(3.1416*AF1M**2*(DMIX1*P1-DANT1*PANT1)/(2.*E1*DT))
      END IF
      ELSE
      IF(P1*DMIX1.LT.PANT1*DANT1) THEN
      RK1=DELX*2.*COE*AF1M*DMIX1/DSQRT(T-TAL1)
      ELSE
      RK1=DELX*(2.*COE*AF1M*DMIX1/(DSQRT(T-TAL1))+3.1416*AF1M**2*
     *(DMIX1*P1-DANT1*PANT1)/(2.*E1*DT))
      END IF
      END IF
      A1=DMIXM*(P1+P2)
      A2=DANTM*(PANT1+PANT2)
      IF(A1.LT.A2) THEN
      RK2=DELX*2.*COE*AFMMT*DMIXM/(DSQRT(T-0.5*(TAL1+TAL2)))
      ELSE
      RK2=DELX*(2.*COE*AFMMT*DMIXM/(DSQRT(T-0.5*(TAL1+TAL2)))+3.1416*
     *AFMMT**2*(DMIXM*(P1+P2)-DANTM*(PANT1+PANT2))/(4.*E1*DT))
      END IF
      IF(P2*DMIX2.LT.PANT2*DANT2) THEN
      RK4=DELX*2.*COE*AF2M*DMIX2/(DSQRT(T-TAL2))
      ELSE
```

```
RK4=DELX*(2.*COE*AF2M*DMIX2/(DSQRT(T-TAL2))+3.1416*AF2M**2*
*(DMIX2*P2-DANT2*PANT2)/(2.*E1*DT))
END IF
Q2=((RK1+4.*RK2+RK4)/6.+DMIX1*Q1)/DMIX2
RETURN
END


SUBROUTINE RUNGPRES(DELX,P1,P2,Q1,Q2,AREXP1,AREXP2,CN,ARPM,
*DP,GD,T,AMVF,VISC,TALY,PER1,PER2,PERM,AREA1,AREA2,AREAM)
IMPLICIT REAL*8(A-H,O-Z)
PI=P1
CALL GASVIS (T,GD,PI,GVIS)
VISCAPL=VISC+260.539*TALY*AREA1**2/(PER1*Q1)
VISM=AMVF*VISCAPL+GVIS*(1-AMVF)
CKM=VISM/6894757
CIK=CKM*2.**(CN+1.)*(2.+(1./CN))**CN
RK1=DELX*(CIK*(Q1**CN))/AREXP1
PI=P1+DP/2.
CALL GASVIS (T,GD,PI,GVIS)
VISCAPL=VISC+260.539*TALY*AREAM**2/(PERM*.5*(Q1+Q2))
VISM=AMVF*VISCAPL+GVIS*(1-AMVF)
CKM=VISM/6894757.
CIK=CKM*2.**(CN+1.)*(2.+(1./CN))**CN
RK2=DELX*(CIK*((0.5*(Q1+Q2))**CN))/ARPM
PI=P1+DP
CALL GASVIS (T,GD,PI,GVIS)
VISCAPL=VISC+260.539*TALY*AREA2**2/(PER2*Q2)
VISM=AMVF*VISCAPL+GVIS*(1-AMVF)
CKM=VISM/6894757
CIK=CKM*2.**(CN+1.)*(2.+(1./CN))**CN
RK4=DELX*(CIK*(Q2**CN))/AREXP2
P2=(RK1+4.*RK2+RK4)/6.+P1
RETURN
END

SUBROUTINE LECOE(DPR,AMVF,TANT,TPOS,DVCOE,VSP)
IMPLICIT REAL*8 (A-H,O-Z)
DIMENSION CBUILD(5),CMVEL(5),DP(5),VSPLO(5)
DATA CBUILD/.03197,.02895,.02662,.02683,.02423/
DATA CMVEL/1.7935E-5,2.3458E-5,2.5426E-5,2.5263E-5,1.7717E-5/
DATA DP/200.,400.,600.,800.,1000./
CB=FLAGR(DP,CBUILD,DPR,1,5)
CMV=FLAGR(DP,CMVEL,DPR,1,5)
IF(AMVF.LT..07) THEN
VSPLO(1)=0.03684
VSPLO(2)=0.04163
VSPLO(3)=0.04295
VSPLO(4)=0.04557
VSPLO(5)=0.05272
ELSE
IF(AMVF.GE..07.AND.AMVF.LT..08) THEN
VSPLO(1)=0.03684
VSPLO(2)=0.04163
VSPLO(3)=(4.47*AMVF+1.002)/30.48
VSPLO(4)=0.04557
VSPLO(5)=0.05272
ELSE
```

```
IF(AMVF.GE..08.AND.AMVF.LT..09) THEN
VSPLO(1)=0.03684
VSPLO(2)=0.04163
VSPLO(3)=(4.47*AMVF+1.002)/30.48
VSPLO(4)=0.04557
VSPLO(5)=(5.07*AMVF+1.215)/30.48
ELSE
IF(AMVF.GE..09.AND.AMVF.LT..14) THEN
VSPLO(1)=0.03684
VSPLO(2)=0.04163
VSPLO(3)=(4.47*AMVF+1.002)/30.48
VSPLO(4)=(5.12*AMVF+0.899)/30.48
VSPLO(5)=(5.07*AMVF+1.215)/30.48
ELSE
VSPLO(1)=(4.29*AMVF+0.502)/30.48
VSPLO(2)=(4.04*AMVF+0.704)/30.48
VSPLO(3)=(4.47*AMVF+1.002)/30.48
VSPLO(4)=(5.12*AMVF+0.899)/30.48
VSPLO(5)=(5.07*AMVF+1.215)/30.48
END IF
END IF
END IF
END IF
VSP=FLAGR(DP,VSPLO,DPR,1,5)
VANT=VSP*(1.-DEXP(-CB*TANT))+CMV*TANT
VPOS=VSP*(1.-DEXP(-CB*TPOS))+CMV*TPOS
DVCOE=VPOS-VANT
RETURN
END
```

Appendix

B

Steady-State Dynamic Kill Spreadsheet for Surface Blowouts

This appendix is for a separate MS Excel ™ spreadsheet set up for design and analysis of a dynamic kill of a surface blowout. The spreadsheet name is FINAL- Surface Dynamic Kill (Arun).xls. The spreadsheet contains the input data and results for the actual Arun blowout described in Chapter 5.

Appendix

C

Steady-State Dynamic Kill Spreadsheet for Underground Blowouts

This appendix is for a separate MS Excel ™ spreadsheet set up for design and analysis of a dynamic kill of an underground blowout. The spreadsheet name is Underground Dynamic Kill-FINAL.xls. The file contains the input data and results for the actual dynamic kill described in Chapter 5.